การจำลองการผลิตเอทิลีนโดยปฏิกิริยาคู่ควบแบบออกซิไดซ์ของมีเทนด้วยสมดุลเคมี

นายกริชชาติ ว่องไวลิขิต

วิทยานิพนธ์นี้เป็นส่วนหนึ่งของการศึกษาตามหลักสูตรปริญญาวิศวกรรมศาสตรมหาบัณฑิต
สาขาวิชาวิศวกรรมเคมี ภาควิชาวิศวกรรมเคมี
คณะวิศวกรรมศาสตร์ จุฬาลงกรณ์มหาวิทยาลัย
ปีการศึกษา 2556

MODELING OF OXIDATIVE COUPLING OF METHANE TO ETHYLENE WITH CHEMICAL EQUILIBRIA

Mr. Kritchart Wongwailikhit

A Thesis Submitted in Partial Fulfillment of the Requirements
for the Degree of Master of Engineering Program in Chemical Engineering
Department of Chemical Engineering
Faculty of Engineering
Chulalongkorn University
Academic Year 2013

Thesis Title	MODELING OF OXIDATIVE COUPLING OF METHANE TO ETHYLENE WITH CHEMICAL EQUILIBRIA
By	Mr. Kritchart Wongwailikhit
Field of Study	Chemical Engineering
Thesis Advisor	Associate Professor Deacha Chatsiriwech

Accepted by the Faculty of Engineering, Chulalongkorn University in Partial Fulfillment of the Requirements for the Master's Degree

.....Dean of the Faculty of Engineering

(Professor Bundhit Eua-arporn, Ph.D.)

THESIS COMMITTEE

.....Chairman

(Professor Suttichai Assabumrungrat)

.....Thesis Advisor

(Associate Professor Deacha Chatsiriwech)

.....Examiner

(Assistant Professor Amornchai Arpornwichanop)

.....External Examiner

(Associate Professor Phungphai Phanawadee)

กริชชาติ ว่องไวลิขิต : การจำลองการผลิตเอทิลีนโดยปฏิกิริยาคู่ควบแบบออกซิไดซ์ของมีเทนด้วยสมดุลเคมี. (MODELING OF OXIDATIVE COUPLING OF METHANE TO ETHYLENE WITH CHEMICAL EQUILIBRIA) อ.ที่ปรึกษาวิทยานิพนธ์หลัก: รศ. ดร. เดชา ฉัตรศิริเวช, 157 หน้า.

ในงานวิจัยนี้ได้สร้างแบบจำลองทางคณิตศาสตร์เพื่อการคำนวณสารในระบบปฏิกิริยาคู่ควบแบบออกซิไดซ์ของมีเทน (Oxidative Coupling of Methane) ที่สภาวะสมดุลของปฏิกิริยา โดยใช้ตัวเร่งปฏิกิริยา 3 ชนิด ได้แก่ $Mn/Na_2WO_4/SiO_2$ La_2O_3/CaO และ PbO/Al_2O_3 โดยทำการตรวจสอบความแม่นยำด้วยการเปรียบเทียบข้อมูลที่คำนวณได้จากแบบจำลองกับค่าที่ได้จากผลการทดลอง ณ สภาวะที่ปฏิกิริยาเข้าสมดุลแล้ว ซึ่งช่วงอุณหภูมิที่ทำการศึกษาจะอยู่ในช่วง 650-900 องศาเซลเซียสและอัตราส่วนการป้อนมีเทนต่อออกซิเจนที่ 3 ถึง 10 ผลการศึกษาพบว่าแบบจำลองทางคณิตศาสตร์ที่เหมาะสมจะขึ้นกับชนิดของตัวเร่งปฏิกิริยาที่ใช้ในระบบ เช่น สำหรับ $Mn/Na_2WO_4/SiO_2$ และ PbO/Al_2O_3 ได้แบบจำลองที่เหมาะสมคือ แบบที่เป็นการแยกคำนวณตามชนิดของปฏิกิริยา (ปฏิกิริยาบนผิวของตัวเร่งปฏิกิริยาและปฏิกิริยาระบบแก๊ส) แล้วคำนวณต่อด้วยปฏิกิริยาการแตกตัวแบบใช้ไฮโดรเจน ในขณะที่แบบจำลองที่เป็นแบบคู่ขนาน จะเหมาะสมกับตัวเร่งปฏิกิริยาที่เป็น La_2O_3/CaO โดยแบบจำลองทางสมดุลปฏิกิริยานี้จะสามารถเพิ่มความแม่นยำได้มากขึ้นหากทำการกำหนดผลได้ของอีเทนเข้าไปในระบบ ซึ่งหากทำการเปรียบเทียบตัวแปรที่ใช้บอกความสามารถของเครื่องปฏิกรณ์ เช่น การเปลี่ยนแปลงสารตั้งต้น (Conversion) และ ผลได้จากปฏิกิริยา (yield) จะพบว่า แบบจำลองทางสมดุลจะสามารถใช้ได้ในช่วงอุณหภูมิและอัตราการป้อนมีเทนต่อออกซิเจนที่ได้กล่าวข้างต้น นอกจากนี้ แบบจำลองทางสมดุลยังสามารถใช้ในการทำนายผลของตัวเร่งปฏิกิริยาชนิดอื่นได้

ภาควิชา วิศวกรรมเคมี ลายมือชื่อนิสิต .....

สาขาวิชา วิศวกรรมเคมี ลายมือชื่อ อ.ที่ปรึกษาวิทยานิพนธ์หลัก .....

ปีการศึกษา 2556

5570520321 : MAJOR CHEMICAL ENGINEERING
KEYWORDS: CHEMICAL EQUILIBRIUM; OXIDATIVE COUPLING OF METHANE (OCM); MODELING

KRITCHART WONGWAILIKHIT: MODELING OF OXIDATIVE COUPLING OF METHANE TO ETHYLENE WITH CHEMICAL EQUILIBRIA. ADVISOR: ASSOC. PROF. DEACHA CHATSIRIWECH, 157 pp.

Chemical Equilibrium models were constructed for Oxidative Coupling of Methane reaction (OCM) with three catalysts, i.e. Mn/Na2WO4/SiO2, La2O3/CaO and PbO/Al2O3. The models were verified under operating temperatures of 650-900oC and methane to oxygen feed ratio 3-10. The compositions of methane, ethane, ethylene, hydrogen, water and carbon oxides in the effluent of each model were compared with the corresponding experiments. The suitable equilibrium model for both Mn/Na2WO4/SiO2 and PbO/Al2O3 was the trio-equilibrium reaction model, consisting of OCM and oxidative dehydrogenation model, combustion model, and hydrocracking model. While, the duo-equilibrium reaction model, containing OCM and oxidative dehydrogenation model, and combustion model, was appropriate for La2O3/CaO catalyst. The accuracy of all equilibrium models could be improved by specifying the desired ethane yield. In addition, based on the reactor performance, i.e. conversion, and yields, the limitation of the manipulated equilibrium models was evaluated within the operating temperatures and the methane to oxygen ratio above. Finally, the equilibrium models, especially the duo-equilibrium model, could be employed to predict the reactor performance containing other OCM catalysts.

Department: Chemical Engineering Student's Signature .....
Field of Study: Chemical Engineering Advisor's Signature .....
Academic Year: 2013

ACKNOWLEDGEMENTS

I would like to express my sincere gratitude to my advisor Associate Professor Deacha Chatsiriwech for the support of my master degree study and research, for his patience, motivation, enthusiasm, and immense knowledge. His guidance helped me in all the time of research and writing of this thesis.

Besides my advisor, I would like to thank of my thesis committee: Professor Sutthichai Assabumrungrat, Assistant Professor Amornchai Arpornwichanop, and Associate Professor Phungphai Phanawadee, for their recommendation and insightful comments.

Last but not the least, I would like to thank my family: my parents Kanda and Somyos Wongwailikhit and my brother Kosawat Wongwailikhit for supporting me spiritually throughout my life.

CONTENTS

Page

Page

Page

Page

LIST OF TABLES

LIST OF FIGURES

Page

Page

Page

CHAPTER 1

INTRODUCTION

1.1 Introduction

Natural gas is an energy source often used for heating, transportation, and electricity generation. The reservoir of natural gas increases rapidly higher than that of crude oil and expected to ahead of by the 21st century [1]. The conversion of methane, the main component of natural gas, into higher economic products is now being interested in many industries. Most processes convert of methane into syngas via steam reforming [2] and then consecutively convert to methanol, ammonia [3] and also hydrocarbons [4]. However, the production are the indirect method consuming more energy than direct method [3].

Directly converting methane into value added C_2 hydrocarbon products had been developed since 1980s via oxidative coupling of methane (OCM) process[5]. The oxidative coupling of methane is exothermic reaction that coupling two methanes into ethane by oxidizing agent as oxygen (Eq. 1.1). As OCM is operated at high temperature (600-1000°C) and simultaneously fed methane with oxygen as raw material, side reactions such as combustion, shown in equation (1.2-1.3), could not be avoided. Therefore, methane to oxygen feed ratio should be as high as possible for promoting equation (1.1) rather than equation (1.2) and (1.3).

$$CH_4 + 0.5\ O_2 \longrightarrow C_2H_6 + H_2O \quad (1.1)$$

$$CH_4 + 1.5\ O_2 \longrightarrow CO + 2\ H_2O \quad (1.2)$$

$$CH_4 + 2\ O_2 \longrightarrow CO_2 + 2\ H_2O \quad (1.3)$$

Many catalysts had been developed to achieve higher yield of C_2. Example of some catalysts performance was showed in table 1.1. It showed performance of each catalyst with reactor performances. Methane conversion (X_{CH4}), C_2 hydrocarbon selectivity (S_{C2}) and C_2 hydrocarbon yield (Y_{C2}) were detailed in the table at various feed ratio of CH_4/O_2 and temperature.

Table 1.1 Example of OCM Catalyst and their performance [6]

Catalyst	CH_4/O_2	T(^{o}C)	X_{CH4}	S_{C2}	Y_{C2}
La/CaO	4	800	28	56	16
Ce/MgO	4	800	28	50	14
Sr/La_2O_3	4	800	29	59	17
La_2O_3	5.4	800	24	65	15.6
Li/MgO	2	750	37.8	50.3	19
Pb/SiO_2	6	750	13	58.2	7.6
$Mn/Na_2WO_4/MgO$	7.4	800	20	80	16
Li/Sn/MgO	9.6	680	14.3	84	12
$Mn/Na_2WO_4/SiO_2$	4	820	30	68	21

** X_{CH4} = Methane Conversion ** S_{C2} = C_2 Selectivity ** Y_{C2} = C_2 Yield

In the table, $Mn/Na_2WO_4/SiO_2$ was one of the best catalysts[7] in OCM reaction. Not only its performance in selectivity (S_{C2}) and methane conversion (X_{CH4}) but also its stability at high temperature was proven [8, 9]. So this catalyst was one of the future catalysts in OCM reaction.

Because OCM was operated at high temperature (600-1000^{o}C), many competitive side reactions, mainly combustion reaction, made OCM system very complex. Many literatures had studied kinetic of OCM reaction over a variety of types of catalyst and proposed their reaction networks as shown in table 1.2. The most acceptable and reliable was the reaction network proposed by Stranch et al [10]. The reaction network comprises of 9 reactions consisting of oxidative dehydrogenation, water-gas shift and combustion reactions. The kinetic study of this reaction network was further studied by Daneshpayeh et al [11] over $Mn/Na_2WO_4/SiO_2$. The results indicated that OCM reaction requires very short

residence time to complete conversion of oxygen. After oxygen conversion reached almost 100%, methane conversion, selectivity and yield were stable.

Table 1.2 Example of reported reaction network models

No.	Reaction	Stransch et al [10]	Hinsen et al [12]	Olsbye et al [13]
1	CH_4+2O_2 -> $CO_2 + H_2O$	✓	✓	
2	$2CH_4 + 0.5O_2$ -> $C_2H_6 + H_2O$	✓	✓	✓
3	$CH_4 + O_2$ -> $CO + H_2O + H_2$	✓		
4	$CO + 0.5O_2$ -> CO_2	✓		
5	$C_2H_6 + 0.5O_2$ -> $C_2H_4 + H_2O$	✓	✓	✓
6	$C_2H_4 + 2O_2$ -> $2CO + 2H_2O$	✓		
7	C_2H_6 -> $C_2H_4 + H_2$	✓		✓
8	$C_2H_4 + 2H_2O$ -> $2CO + 4H_4$	✓		
9	$CO + H_2O$ -> $CO_2 + H_2$	✓		✓
10	$C_2H_4 + 3O_2$ -> $2CO_2 + 2H_2O$		✓	
11	$CH_4 + 1.5\ O_2$ -> $CO + 2H_2O$			✓

In general, the kinetic studies of chemical reaction provide the time dependent results describing the concentration of components in reactor. However, those attempts required a set of repeating laboratory experiments for the mathematic regression processes. This research was aimed to simplify the method predicting the effluence of OCM instead of kinetic approach.

The chemical equilibrium concept determines the composition of components which were constant at the equilibration time which is a point of the lowest Gibbs free energy of the system [14]. In OCM system, after the oxygen was consumed in reactor and concentration of oxygen was very low, concentration of others components were also stable. It could be compiled that this state was the equilibrium of OCM reaction. Thus, concentration of components should be explained by chemical equilibrium theory.

Then In this study, it is curious to use chemical equilibrium concept for describing the fraction of components and determining the reaction performance of

OCM reaction with the assistance of computer simulation. This research may extend the feasibility of the chemical equilibrium concept.

1.2 Objective

To develop an appropriate equilibrium model for production of olefin from methane with oxidative coupling of methane.

1.3 Scope of work

- Kinetic simulation for consideration of residence time and determine the mole fraction of product at the chemical equilibrium state.
- OCM reaction was run over the three catalysts, $Mn/Na_2WO_4/SiO_2$, La_2O_3/CaO and PbO/Al_2O_3.
- Develop the equilibrium model of OCM with the information of operating condition and mole fraction of effluents from Literatures
- Studied OCM reaction at temperature 650-900°C and methane to oxygen feed ratio at 3-10.
- Verify the precision of the developed model by comparing the studied factors to that of equilibrium composition calculated by kinetic model at the equilibration time
- Determine the error using RSS and AARD statistic
- Determine the validity region of the developed model
- Testing the extrapolated prediction of the developed model

1.4 Expected Outputs

The appropriate simulation model for the reaction network of oxidative coupling of methane reaction.

CHAPTER 2

THEORY

2.1 Oxidative Coupling of methane

Oxidative coupling of methane (OCM) was the value added reaction, Eq. 2.1, which converted methane into ethane. The ethane formed by OCM could further oxidize to form ethylene by oxidative dehydrogenation (ODH), Eq.2.2. However, there were others competitive reactions that converted methane into carbon oxide (CO and CO_2) i.e. combustion reaction (Eq. 2.3-2.4). This competitive regime decreased the selectivity of C_2 hydrocarbon in product stream.

$$CH_4 + 0.5\ O_2 \rightarrow C_2H_6 + H_2O \quad (2.1)$$

$$C_2H_6 + 0.5\ O_2 \rightarrow C_2H_4 + H_2O \quad (2.2)$$

$$CH_4 + 1.5\ O_2 \rightarrow CO + 2\ H_2O \quad (2.3)$$

$$CH_4 + 2\ O_2 \rightarrow CO_2 + 2\ H_2O \quad (2.4)$$

2.1.1 Catalyst for Oxidative Coupling of methane reaction

Since Keller and Bhasin [15] had pioneered oxidative coupling of methane reaction in 1982, there were many researchers paid their attention to this reaction. Most of literatures focused in catalytic development to raise C_2 selectivity and methane conversion as high as possible. Until now, there were various types of catalysts for OCM reaction that had been studied. Example of these catalysts and their performances were presented in table 2.1.

Table 2.1 Example of OCM Catalyst and their performance [6]

Catalyst	CH_4/O_2	T ($^{\circ}C$)	Methane Conversion	C_2 Selectivity	C_2 Yield
La/CaO	4	800	28	56	16
Ce/MgO	4	800	28	50	14
Sr/La_2O_3	4	800	29	59	17
La_2O_3	5.4	800	24.0	65	15.6
Li/MgO	2	750	37.8	50.3	19.0
Pb/SiO_2	6	750	13.0	58.2	7.6
$Mn/Na_2WO_4/MgO$	7.4	800	20.0	80	16.0
Li/Sn/MgO	9.6	680	14.3	84	12.0
$Mn/Na_2WO_4/SiO_2$	4	820	30	68	21

Table 2.1 showed performance of each catalyst including the reactor performances. Methane conversion (X_{CH4}), C_2 hydrocarbon selectivity (S_{C2}) and C_2 hydrocarbon yield (Y_{C2}) were detailed in the table at various feed ratio of CH_4/O_2 and temperature. In the table, methane conversions of all catalysts were around 13-40 % with their selectivity in range of 50-85%. $Mn/Na_2WO_4/SiO_2$ was one of the suitable catalyst for practical application. Methane conversion was reasonably high at 30% with 80% C_2 selectivity.

2.1.2 Reactor for Oxidative Coupling of methane reaction

As OCM was the heterogeneous reaction, the reactor should appropriate with the fluid-solid application such as the fixed bed reactors and fluidized bed reactors. To determine the appropriate type, their performance in products yield and heat distribution in the reactor should be considered. The heat distribution was one of the concern issues for OCM because it was the highly exothermic reaction. Thus, the reactor should have capability to transfer heat out of reactor to avoid hot spot in reactor.

2.1.2.1 Fixed Bed Reactor (FBR)

The common configuration of fixed bed reactor (FBR) led researchers to apply it in many developments. However, there was a problem for scaling up fixed bed reactor due to hot spot in reactor.

Most of the researches experimented OCM in micro reactor which provided enough heat transfer. However, J.Y. Lee et al [16] studied OCM reaction in different size of fixed bed reactor and observed the hot spot in reactor that impact C_2 selectivity. Hot spot in reactor led the gas phase combustion to react faster. Thus, methane would convert into carbon oxide rather than C_2 hydrocarbon. In addition, Lee as well as S. Jaso et al [17] suggested using dilution of feed by heat carrier inert or added more methane to oxygen feed ratio to reduce the hot spot phenomena. Except the heat transfer problem, FBR will beyond reasonable doubt for practical application [18].

2.1.2.2 Fluidized Bed Reactor

Heat dispersion ability of fluidized bed reactor was interested by many OCM researchers. In this reactor, isothermal operation could be obtained without any dilute addition. Moreover, equal or higher yield of C_2 in fluidized bed reactor has been investigated by S. Jaso et al [19]. Their experimental gave 19% yield of C_2 without any hot spot observed.

2.2 Chemical Reaction Equilibrium

2.2.1 Reaction Equilibrium Calculation with specifying reactions.

Gibbs free energy minimization method for calculation of reaction equilibrium is proved and expressed in Eq. 2.5. Equilibrium constant (K) can be calculated from Gibbs free energy of chemical reaction divided by reference temperature (T) and gas constant (R). Equilibrium constant (K) from this equation will be used to specify equilibrium composition by Eq. 2.6. With assumption of ideal gas, equation 2.6 turns into equation 2.7. Equation 2.7 can predict equilibrium mole fraction of each component (y_i) at specific pressure (P). The mole fraction (y_i) in equation 2.7 could be calculated with equation 2.8. For the abbreviation, v_i is summarization of reaction coefficient of each components in the reaction, ε is the molar extension in reaction, n_i is the i component effluent mole flow, n_{i0} is the initial mole flow and n and n_{i0} is the sum total of n_i and n_{i0} respectively [14].

$$K = \exp(\frac{-\Delta G^0}{RT}) \tag{2.5}$$

$$K = \prod(\frac{\hat{f}_i}{f_i^o})^{v_i} \tag{2.6}$$

$$K\left(\frac{P}{P^o}\right)^{v_i} = \prod(y_i)^{v_i} \tag{2.7}$$

$$y_i = \frac{n_i}{n} = \frac{n_{i0} + v_i\varepsilon}{n_{i0} + v\varepsilon} \tag{2.8}$$

However, K value obtain from Eq. 2.5 was the value at standard temperature and pressure. The real K value had to adjust to the operating condition by Eq. 2.8-2.11 before calculate equilibrium compositions with Eq. 2.6 or Eq. 2.7.

$$K = K_o K_1 K_2 \tag{2.9}$$

$$K_1 = \exp\left[\frac{\Delta H_0^o}{RT_0}(1 - \frac{T_o}{T})\right] \tag{2.10}$$

$$K_2 = \exp\left(-\frac{1}{T}\int_{T_o}^{T}\frac{\Delta C_p^0}{R}dT + \int_{T_o}^{T}\frac{\Delta C_p^0}{RT}dT \right) \qquad (2.11)$$

In this research, Aspen Plus simulator will be used for equilibrium calculation. All equations mentioned above can be calculated with REquil model in Aspen plus Program.

2.2.2 Reaction Equilibrium Reaction with specifying effluent components.

This model predicts the equilibrium conversion by defining components in the reaction model instead of reaction involved. By specified what component could be in product stream and combination with Gibbs free energy minimization, results of equilibrium composition can be calculated by equation 2.12. In the equation, a_{ik} is numbers of atoms element j in component i, y_i is mole fraction of component i. Solving Eq. 2.12 together with 2.13 yields the equilibrium composition of each component.

$$\Delta G_{f_i}^{o} + RT\ln(y_i\hat{\phi}P / P^0) + \sum_k \lambda_k a_{ik} = 0 \qquad (2.12)$$

$$\sum_i n_i a_{ik} = A_k \qquad (2.13)$$

As well as calculation in previous section, this calculation procedure will use Aspen plus program with RGibbs Model.

CHAPTER 3

LITERATURE REVIEWS

Methane is the major component in natural gas and landfill gas [20]. It was expected to be both clean energy and chemical raw material instead of crude oil in future [1, 21]. Nowadays besides the utilization of methane as green energy, methane converting into value-added products was also practical. Figure 3.1 represent these days industrial application.

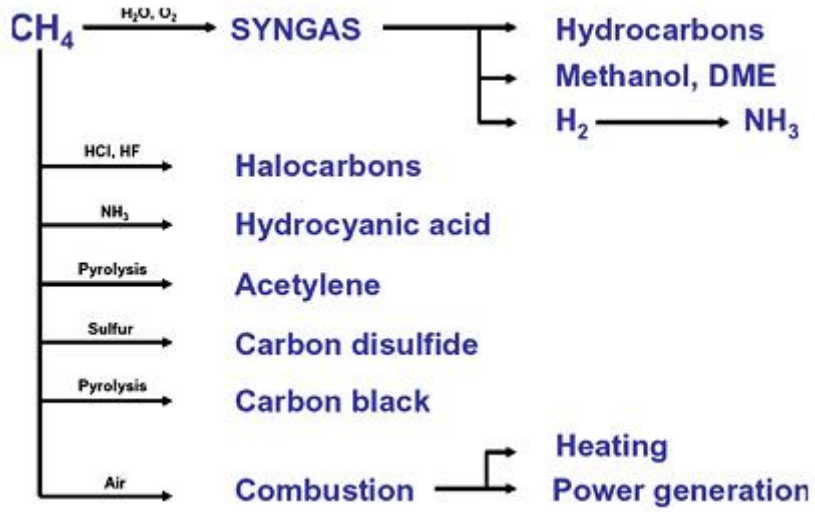

Fig 3.1 Industrial Methane Utilization [3]

In the figure 3.1, methane could convert into syngas by reacting with H_2O called "reforming reaction" or reacting with O_2 called "partial oxidation reaction". Moreover, methane could react with other reactants to form halocarbons, hydrocyanic acid, acetylene, carbon disulfide and carbon black. Beside, methane could be used as power generating agent or heating substance by using it as raw material of combustion.

At this day, mostly deal of methane is reforming process to form syngas (both steam reforming and partial oxidation [2, 22]). Only less of methane convert into hydrocyanic via Andrussow or Degussa processes[23]. In consecutively, most of

syngas nowadays apply to produce methanol, ammonia [3] and also hydrocarbons via Fischer–Tropsch synthetic [24].

Nevertheless, the methane reforming process, which nowadays dominating utilization of methane, is 2 steps method. This process have to convert methane into intermediate syngas and then others products. This two steps demand more energy than direct converted method [3]. Oxidative coupling of methane (OCM) reaction is one of the processes answer the issue because this reaction directly combines methane into C_2 hydrocarbon (i.e. ethane and ethylene).

OCM intended to produce higher hydrocarbons from C_1 hydrocarbon as well as Fischer–Tropsch process. However, there were many differences of both processes as summary in table 3.1

Table 3.1 Comparison of Fischer–Tropsch process and oxidative coupling of methane

Issue	Partial Oxidation of Methane[25]	Fischer–Tropsch Process [26]	Oxidative Coupling of Methane [5]
Raw Material	Methane	Syngas	Methane
Temperature (^{0}C)	800-1200	300-350	600-1000
Pressure (bar)	1	10-40	1
Conversion (%)	$\geq$ 90 %	50-90%	10-40%
Selectivity			
Gas			
Methane	**	11	**
Ethylene	-	4	7 to 43
Ethane	-	6	10 to 55
Propylene	-	11	Small
Propane	-	2	Small
Butene	-	8	-
Carbon Oxide	$\geq$ 99	**	27 to 60
Liquid			
C_5-C_7	-	8	-
Light Oils	-	33	-
Heavy oils	-	6	-
Alcohols	-	9	-
Acids	-	2	-

** indicate the raw material of the process

In table 3.1, oxidative coupling of methane was the reaction that converting methane into C_2-C_3 hydrocarbon directly with operating temperature 600-1000°C at ambient pressure. But for Fischer–Tropsch process, methane had to initially convert into syngas (CO and H_2) via partial oxidation reaction. This reaction was operating at high temperature as well as OCM. After obtained syngas, it was fed into Fischer–Tropsch reactor. The reaction required mild temperature (300-350°C) but high pressure (10-40 bar). The products obtained from this process were various from C_1 hydrocarbon to heavy liquid oil. Moreover, alcohol and carboxylic acid were also obtained in at the products. The difference of product distribution between OCM and Fischer–Tropsch process was come from their dissimilarity in their mechanisms which reviewed in latter section.

Since 1980s that Keller and Bhasin et al [15] pioneered oxidative coupling of methane reaction, many researches were interested in this reaction. Most of them were in catalytic development [3] because the selectivity of C_2 were low. So most of the researches since then concentrated at increasing the C_2 selectivity by both development of common catalysts and synthesis the new one [6]. But at this present time, not only the catalysts development was now studied but also stability of catalyst [8, 9]. In addition, there were various studies in kinetic modeling, reactor configuration and process simulation as well.

Even many literatures attended the OCM, chemical equilibrium of this reaction was not covered. This fact had motivated this research to analyze the OCM reaction is aspect of chemical equilibrium. Literature in catalyst, kinetic, reactor configuration and operating condition should be reviewed to analyze the equilibrium of OCM.

3.1 Reaction mechanism and kinetics

3.2.1 Reaction Mechanism

Initiation of OCM reaction was the activation of methane into methyl radical on catalytic surface. Electron Spin Resonance (ESR) detected methyl radical formation in reactor [27, 28]. Buyevskaya et al. [29] suggested the formation of methyl radical were both on catalytic surface (Eq. 3.1-3.2) and gas phase. For the gas phase mechanism, gas phase methane reacted with adsorbed oxygen on surface (Eq. 3.3). This gas phase mechanism was now more frequently accepted in scientific view.

$$CH_4 + M^{n+}O^{-2} \rightarrow M^{n+}CH_3^- + O^{2-}H^+ \quad (3.1)$$

$$M^{n+}CH_3^- \xrightarrow{e} CH_3^{\bullet} \quad (3.2)$$

$$CH_4 + (O)_s \rightarrow CH_3^{\bullet} + (OH)_s \quad (3.3)$$

Subsequently, formed methyl radical could either coupling into ethane (Eq.3.4) or react with gas phase oxygen (Eq. 3.5) to form CH_3O_2• radical (detected by ESR [30]). CH_3O_2• was consecutively converted into carbon oxide (CO_x) via whether gas phase [31] or heterogeneous [32]. Since methyl radical could convert in many routes, the competition of these reactions determined selectivity of the OCM.

$$CH_3^{\bullet} + CH_3^{\bullet} \rightarrow C_2H_6 \quad (3.4)$$

$$CH_3^{\bullet} + O_2 \rightarrow CH_3O_2^{\bullet} \quad (3.5)$$

$$C_2H_6 \rightarrow C_2H_4 + H_2 \quad (3.6)$$

Ethane also had two consecutively routes in further conversion. First route was the gas phase dehydrogenation (Eq. 3.6) and another was activated into ethyl radical (C_2H_5•) on catalytic surface. Ethyl radical, which was also proved by ESR [33, 34], could afterward convert into ethylene or reacted with gas phase oxygen to form $C_2H_5O_2$• radical which latter go into both CO_x or ethylene.

In order to brief the formation of ethane and ethylene on catalytic surface, The scheme mechanism of Lunsford et al [1] was depicted in figure 3.2.

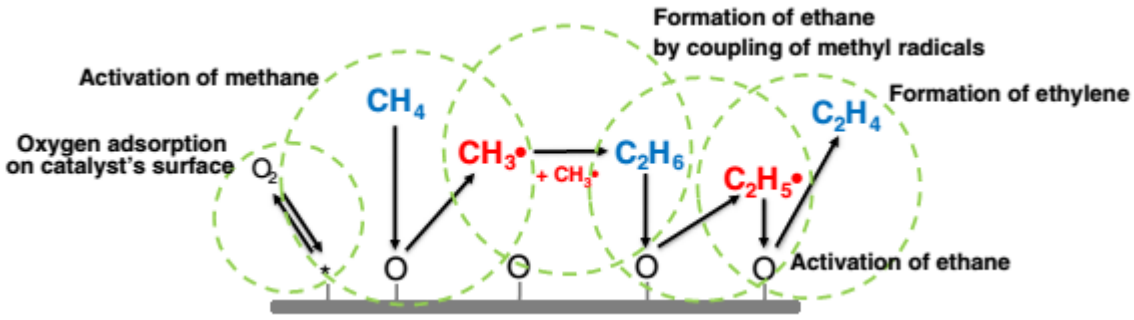

Fig 3.2 Reaction mechanism for oxidative coupling of methane on catalytic surface [1]

Gas phase oxygen that fed into reactor was adsorbed on catalytic surface. Afterward, methane was oxidized by adsorbed oxygen and form methyl radical. After two methyl radicals were combined to form ethane, ethane component could further activated by other adsorbed oxygen site to from ethyl radical. Then, ethylene was produced by oxidized of ethyl radical on adsorbed oxygen site. Sun et al [35] summarized all of reactions above into figure 3.3.

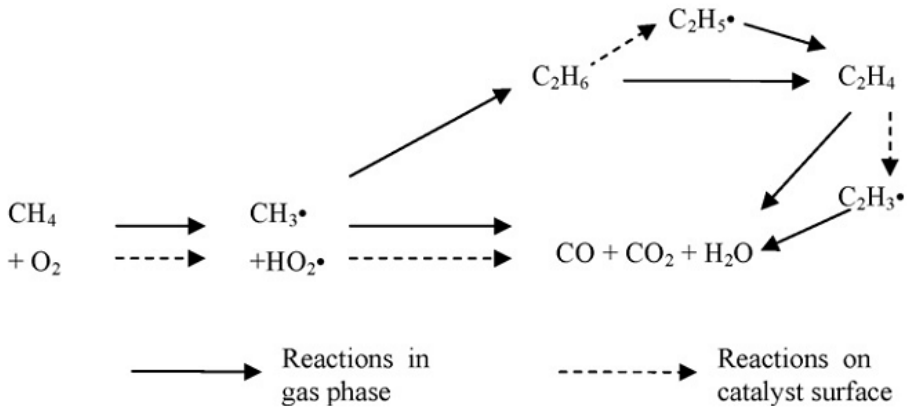

Fig 3.3 Oxidative Coupling of methane mechanism [35]

In the figure, dash line in the figure represented catalytic reaction while solid line represented gas phase. The main substance of the reaction was the same as mentioned above. But Sun added ethene activation into C_2H_3• radical and later to CO_x into mechanism.

As describe above, OCM converted C_1 hydrocarbon into higher order via oxidative active of methane via adsorbed oxygen on catalytic surface. The small amount of oxygen feed into reactor limited the growth of higher hydrocarbon to more than C_2. Unlike the Fischer–Tropsch synthetic, which its mechanism showed in figure 3.4, CO adsorption on catalytic surface could itself grow into higher hydrocarbons without any limitation until lack of raw material. Thus, these mechanisms indicated that OCM reaction was suitable for C_2 production due to high selectivity of the components.

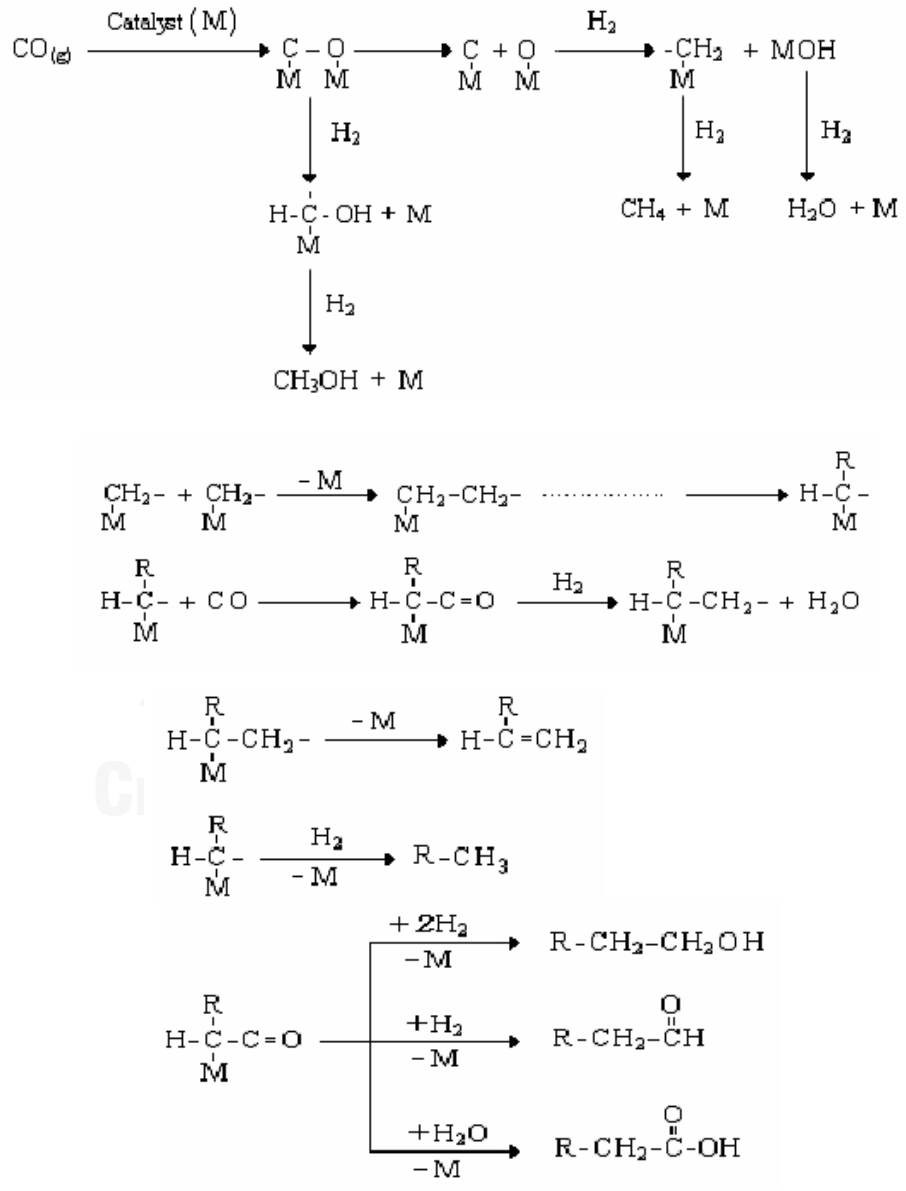

Fig 3.4 Mechanism of Fischer–Tropsch synthetic [4]

3.2.2 Reaction Kinetics

There were many literatures studied about kinetic of OCM reaction. Miro et al [36] was studied OCM reaction and suggested basic power law for this reaction. After that, Sohrabi et al [37] studied OCM with differential tubular reactor and defined methyl radical as intermediate and suggested reaction network model for OCM.

In 1990s, Olsbye et al.[13], Lacombe et al.[38], Stansch et al [10] Hinsen et al [12] and Traykova et al [39] were also studied OCM reaction mostly in micro reactor and suggested their reaction networks which were also summarized in table 3.3. Rate equation of Hinsen was shown in table 3.2.

Table 3.2 Rate equations over PbO/Al_2O_3 catalyst suggested by Hinsen et al [12]

Reaction	Rate Law (mol/g s)
$2CH_4+0.5O_2 \rightarrow C_2H_6+H_2O$	$r = 1.2e^{-99,000/RT} p_{CH_4}^{0.8} p_{O_2}^{1.1}$
$C_2H_6 + 0.5O_2 \rightarrow C_2H_4 + H_2O$	$r = 2.0x10^{-4} e^{-6,000/RT} p_{CH_4}^{0.8} p_{O_2}^{1.0}$
$CH_4+2O_2 \rightarrow CO_2 + H_2O$	$r = 1.5x10^{-2} e^{-51,000/RT} p_{CH_4}^{0.4} p_{O_2}^{1.5}$
$C_2H_4+3O_2 \rightarrow 2CO_2+2H_2O$	$r = 2.0x10^{-16} e^{-220,000/RT} p_{CH_4}^{0.8} p_{O_2}^{1.6}$

Stransch et al [10] studied kinetic of OCM over La_2O_3 catalytic and suggested 10-reaction network which expressed in table 3.4. The rate equation of each reaction in table 3.4 was showed in equation 3.7-3.12.

$$r_2 = \frac{k_{02} e^{-E_2/RT} (0.23x10^{-11} e^{124,000/RT} p_{O_2})^{n_1} p_{CH_4}^{m_j}}{\left[1 + (0.23x10^{-11} e^{124,000/RT} p_{O_2})^{n_1} + K_{0CO_2} e^{-\Delta H_{ad,CO_{2,j}}/RT} p_{O_2}\right]^2} \qquad (3.7)$$

$$r_j = \frac{k_{0j} e^{-E_j/RT} p_{CH_4}^{m_j} p_{O_2}^{n_1}}{\left[1 + K_{0CO_2} e^{-\Delta H_{ad,CO_{2,j}}/RT} p_{CO_2}\right]^n} \qquad j = 1, 3\text{-}6 \qquad (3.8)$$

$$r_7 = k_{0,7} e^{-E_7/RT} p_{C_2H_6} \qquad (3.9)$$

$$r_8 = k_{0,8} e^{-E_8/RT} p_{C_2H_4}^{m_8} p_{H_2O}^{n_8} \qquad (3.10)$$

$$r_9 = k_{016} e^{-E_9/RT} p_{CO_2}^{m_9} p_{H_2}^{n_9} \qquad (3.11)$$

$$r_{10} = k_{0,10} e^{-E_{10}/RT} p_{CO}^{m_{10}} p_{H_2O}^{n_{10}} \quad (3.12)$$

Later in 2009, Daneshpayeh et al [11] developed kinetic model for $Mn/Na_2WO_4/SiO_2$ catalyst by regression their experimental data with previous suggested reaction networks. 10-Step reaction network model of Stansch yielded the least relative deviation at ±9.1 % and were indicated as most suitable reaction network for $Mn/Na_2WO_4/SiO_2$ catalyst. Daneshpayeh's kinetic parameter, rate equations were outlined in table 3.5 and Eq. 3.13 to 3.14 with Eq 3.9-1.12 which the same equations as Stransch.

$$r_1 = \frac{k_{01} e^{-E_1/RT} (K_{0O_2} e^{-\Delta H_{ad,O_2,j}/RT} p_{O_2})^{n_1} p_{CH_4}^{m_j}}{\left[1 + (K_{0O_2} e^{-\Delta H_{ad,O_2,j}/RT} p_{O_2})^{n_1}\right]^2} \quad (3.13)$$

$$r_j = k_{0j} e^{-E_j/RT} p_C^{m_j} p_{O_2}^{n_j} \qquad j = 2\text{-}6 \quad (3.14)$$

In the same year, Shahri et al [40] experimented and suggested their 7-heterogeneous reaction network for the same catalyst , $Mn/Na_2WO_4/SiO_2$, with accuracy of ±15 %. Shahri reaction network, rate equations and kinetic parameters were also shown in table 3.3, Eq. 3.15-3.18 and table 3.6 respectively.

$$r_1 = \frac{k_{0,1} e^{-E_{a,1}/RT} p_{CH_4}^{m_1} p_{O_2}^{n_1}}{[1 + K_{1,CH_4} e^{-\Delta H_{ad,1,CH_4}/RT} p_{CH_4} + K_{1,O_2} e^{-\Delta H_{ad,1,O_{2,j}}/RT} p_{O_2}]^2} \quad (3.15)$$

$$r_j = \frac{k_{0,j} e^{-E_{a,j}/RT} p_C^{m_j} p_{O_2}^{n_j}}{[1 + K_{1,C} e^{-\Delta H_{ad,j,C}/RT} p_C^{m_j} + K_{j,O_2} e^{-\Delta H_{ad,j,O_{2,j}}/RT} p_{O_2}^{n_j}]^2} \qquad j = 2\text{-}5 \quad (3.16)$$

$$r_6 = k_{0,6} e^{-E_{a,6}/RT} p_{CO}^{m_6} p_{H_2O}^{n_6} \quad (3.17)$$

$$r_7 = k_{0,7} e^{-E_{a,7}/RT} p_{CO_2}^{m_7} p_{H_2}^{n_7} \quad (3.18)$$

Table 3.3 Stoichiometric equation of reaction network models

No.	Reaction	Stansch (La_2O_3/CaO)	Sohrabi ($CaTiO_3$)	Lacombe (La_2O_3)	Olsbye ($BaCO_3$)/LaOn$(CO_3)_{3-n}$	Traykova (La_2O_3/MgO)	Shahri (Mn/Na_2WO_4/SiO_2)	Hinsen (Pb_2O_3)
Catalytic Reaction								
	Oxidative Coupling							
1	$2CH_4+0.5O_2 \rightarrow C_2H_6+H_2O$	✓	✓	✓	✓	✓	✓	✓
2	$2CH_4+O_2 \rightarrow C_2H_4+2H_2O$		✓					
	Partial Oxidation							
3	$CH_4+ 0.5O_2 \rightarrow CO + 2H_2$							
4	$C_2H_6+O_2 \rightarrow 2CO+3H_2$			✓				
5	$C_2H_4+O_2 \rightarrow 2CO+2H_2$			✓				
	Steam Reforming							
6	$CH_4+H_2O \rightarrow CO + 3H_2$							
7	$C_2H_6 + 2H_2O \rightarrow 2CO + 5H_2$							
8	$C_2H_4 + 2H_2O \rightarrow 2CO + 4H_2$	✓						
	Carbon Dioxide Reforming							
9	$CH_4 + CO_2 \rightarrow 2CO + 2H_2$							
10	$C_2H_6+ 2CO_2 \rightarrow 4CO + 3H_2$							
11	$C_2H_4+2CO_2 \rightarrow 4CO + 2H_2$							
	Oxidative Dehydrogenation							
12	$C_2H_6 + 0.5O_2 \rightarrow C_2H_4 + H_2O$	✓		✓		✓	✓	✓
	Dehydrogenation							
13	$C_2H_6 \rightarrow C_2H_4 + H_2$	✓			✓	✓		
	Water-Gas Shift							
14	$CO_2 + H_2 = CO + H_2O$	✓				✓	✓	

Table 3.3 Stoichiometric equation of reaction network models (Con't)

No.	Reaction	Stansch (La_2O_3/CaO)	Sohrabi ($CaTiO_3$)	Lacombe (La_2O_3)	Olsbye ($BaCO_3$)/LaOn$(CO_3)_{3-n}$	Traykova (La_2O_3/MgO)	Shahri (Mn/Na_2WO_4/SiO_2)	Hinsen (Pb_2O_3)
Non-Catalytic Reaction								
	Combustion							
15	$CH_4 + O_2 \rightarrow CO + H_2O + H_2$	✓			✓			
16	$CH_4+1.5O_2 \rightarrow CO + 2H_2O$		✓			✓	✓	
17	$CH_4+2O_2 \rightarrow CO_2 + H_2O$	✓	✓	✓	✓		✓	✓
18	$CO + 0.5O_2 \rightarrow CO_2$	✓		✓				
19	$C_2H_6+2.5O_2 \rightarrow 2CO+3H_2O$				✓			
20	$C_2H_6+3.5O_2 \rightarrow 2CO_2+H_2O$			✓	✓			
21	$C_2H_4 + 2O_2 \rightarrow 2CO + 2H_2O$	✓			✓		✓	
22	$C_2H_4+3O_2 \rightarrow 2CO_2+2H_2O$				✓			✓

Table 3.4 Kinetic parameter of La_2O_3/CaO by Stransch et al [10]

Step	Reaction	k_{0j} mol g^{-1} s^{-1} $Pa^{-(m+n)}$	$E_{a,j}$ kJ/mol	K_{CO2} Pa^{-1}	$\Delta H_{ad,CO2}$ kJ/mol	m_j	n_j
1	CH_4+2O_2 -> $CO_2 + H_2O$	0.2×10^{-5}	48	0.25×10^{-12}	-175	0.24	0.76
2	$2CH_4 + 0.5O_2$ -> $C_2H_6 + H_2O$	23.2	182	0.82×10^{-13}	-186	1.0	0.40
3	$CH_4 + O_2$ -> $CO + H_2O + H_2$	0.52×10^{-6}	68	0.36×10^{-13}	187	0.57	0.85
4	$CO + 0.5O_2$ -> CO_2	0.11×10^{-3}	104	0.40×10^{-12}	-168	1.0	0.55
5	$C_2H_6 + 0.5O_2$ -> $C_2H_4 + H_2O$	0.17	157	0.45×10^{-12}	-166	0.95	0.37
6	$C_2H_4 + 2O_2$ -> $2CO + 2H_2O$	0.06	166	0.16×10^{-12}	-211	1.0	0.96
7	C_2H_6 -> $C_2H_4 + H_2$	1.2×10^{7} [a]	226				
8	$C_2H_4 + 2H_2O$ -> $2CO + 4H_4$	9.3×10^{3}	300			0.97	0
9	$CO + H_2O$ -> $CO_2 + H_2$	0.19×10^{-3}	173			1.0	1.0
10	$CO_2 + H_2$ -> $CO + H_2O$	0.26×10^{-1}	220			1.0	1.0

[a] Units are mol s^{-1} m^{-3} Pa^{-1}

Table 3.5 Kinetic parameter of $Mn/Na_2WO_4/SiO_2$ by Daneshpayeh et al [11]

Step	Reaction	k_{0j} mol g^{-1} s^{-1} $Pa^{-(m+n)}$	$E_{a,j}$ kJ/mol	K_{O2} Pa^{-1}	$\Delta H_{ad,O2}$ kJ/mol	m_j	n_j
1	CH_4+2O_2 -> $CO_2 + H_2O$	29.4	212.6	4.39×10^{-11}	-121.9	1	0.75
2	$2CH_4 + 0.5O_2$ -> $C_2H_6 + H_2O$	3.07×10^{-7}	98.54			0.85	0.5
3	$CH_4 + O_2$ -> $CO + H_2O + H_2$	6.65×10^{-8}	146.8			0.5	1.57
4	$CO + 0.5O_2$ -> CO_2	5.26×10^{-4}	114.6			0.5	0.5
5	$C_2H_6 + 0.5O_2$ -> $C_2H_4 + H_2O$	2.70×10^{-3}	153.5			0.91	0.5
6	$C_2H_4 + 2O_2$ -> $2CO + 2H_2O$	1.81×10^{-1}	174.4			0.72	0.40
7	C_2H_6 -> $C_2H_4 + H_2$	4.61×10^{2}	394.2			1.62	0.71
8	$C_2H_4 + 2H_2O$ -> $2CO + 4H_4$	1.08×10^{7} [a]	291.9			0.88	0
9	$CO + H_2O$ -> $CO_2 + H_2$	5.77×10^{-3}	158.0			1	1
10	$CO_2 + H_2$ -> $CO + H_2O$	5.24×10^{-6}	131.3			1	1

[a] Units are mol s^{-1} m^{-3} Pa^{-1}

Table 3.6 Kinetic parameter of $Mn/Na_2WO_4/SiO_2$ by Shahri et al [40]

Step	No. of Reaction in table 3.3	k_{0j} mol g^{-1} s^{-1} $Pa^{-(m+n)}$	$E_{a,j}$ kJ/mol	$K_{j,C}$ (Pa^{-1})	$\Delta H_{ad,C}$ kJ/mol	K_{O2} Pa^{-1}	$\Delta H_{ad,O2}$ kJ/mol	m_j	n_j
1	1	1.07×10^{-3}	133	5.50×10^{-14}	-126	1.96×10^{-13}	-125	0.501	0.504
2	16	6.82×10^{-9}	30	7.60×10^{-14}	-93	1.10×10^{-14}	-156	0.604	0.297
3	17	1.36×10^{-9}	24.5	2.54×10^{-14}	-99.8	3.79×10^{-11}	-175	0.875	0.047
4	12	1.26×10^{-5}	23.	1.98×10^{-13}	-147	7.86×10^{-14}	-99	1.295	1.22
5	21	4.78×10^{-4}	110	3.46×10^{-13}	-167	6.87×10^{-9}	-135	0.42	0.31
6	14	5.27×10^{-7}	53.8					0.5	0.5
7	14	3.9×10^{-4}	99					0.5	0.5

Later, Mi Ran Lee et al [41] developed kinetic model for $Mn/Na_2WO_4/SiO_2$ catalyst but in elementary reaction of gas phase radicals. The reaction network divided into 7 surface reactions and 7 gas phase reactions with 2 adsorption reactions. Table 3.7 showed details of those described reaction above. Simulation result for this reaction network gave accuracy within ±31%. This model were further developed by Ahari et al [42] by adding more reactions. 11 surface reactions and 39 gas phase reactions were concluded with more accuracy at ±13.6 %.

Table 3.7 OCM mechanism of Mi Ran Lee

Reaction Type			Reaction
Adsorption	A_1	:	$O_2 + 2S \leftrightarrow 2O(s)$
	A_2	:	$2OH(s) \leftrightarrow H_2O + O(s) + s$
Catalytic Surface Reaction	R_1	:	$CH_4 + O(s) \rightarrow CH_3\bullet + OH(s)$
	R_2	:	$C_2H_6 + O(s) \rightarrow C_2H_5\bullet + OH(s)$
	R_3	:	$C_2H_5\bullet + O(s) \rightarrow C_2H_4 + OH(s)$
	R_4	:	$CH_3\bullet + 3O(s) \rightarrow CHO(s) + 2OH(s)$
	R_5	:	$CHO(s) + O(s) \rightarrow CO + OH(s) + s$
	R_6	:	$CO + O(s) \rightarrow CO_2 + s$
	R_7	:	$C_2H_4 + O(s) \rightarrow C_2H_3\bullet + OH(s)$
Gas-Phase Reaction	R_8	:	$2CH_3\bullet \rightarrow C_2H_6$
	R_9	:	$CH_3\bullet + O_2 \rightarrow CHO\bullet + H_2O$
	R_{10}	:	$C_2H_3\bullet + O_2 + OH\bullet \rightarrow 2CHO\bullet + H_2O$
	R_{11}	:	$CHO\bullet + O_2 \rightarrow CO + HO_2\bullet$
	R_{12}	:	$CO + HO_2\bullet \rightarrow CO_2 + OH\bullet$
	R_{13}	:	$C_2H_6 \rightarrow C_2H_5\bullet + H\bullet$
	R_{14}	:	$C_2H_5\bullet + H\bullet \rightarrow C_2H_4 + H_2$

3.2 Analytical study of OCM in various aspect

3.2.1 Oxidative Coupling of Methane Process Variables Effect

Effect of process variables in OCM were consisted of temperature, pressure, contact time, feed composition and also dilute addition.

3.2.1.1 Effect of Temperature

Deneshpayeh et al [11] studied effect of reactor temperature on OCM by increasing reactor temperature at constant contact time and feed ratio. The results of experiment were depicted in figure 3.5.

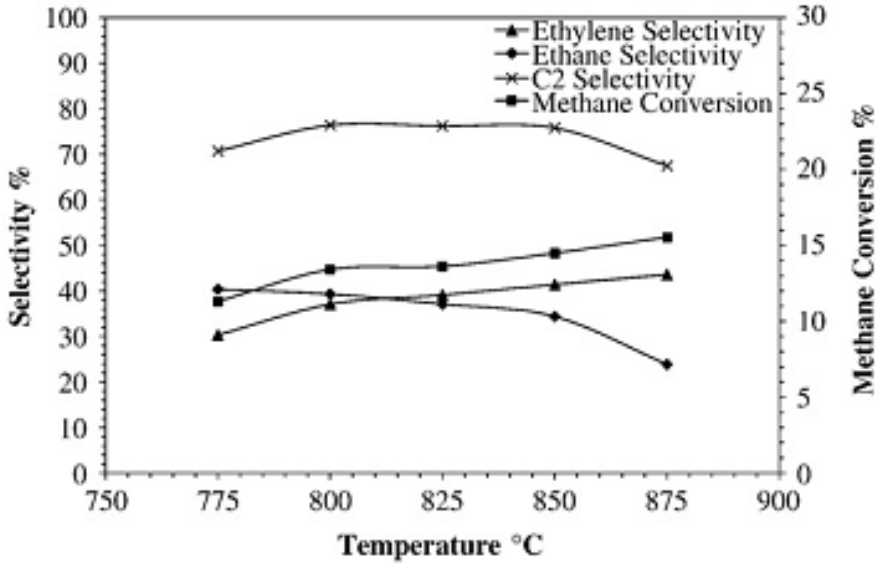

Fig 3.5 Effect of Temperature on conversion and selectivity of Daneshpayeh et al [11]

It was found that increasing reactor temperature was also raised methane conversion. Moreover, increased in temperature would raise C_2 selectivity. However, if the temperature was too high, the selectivity of C_2 was dropped because combustion dominated system at high temperature.

3.2.1.2 Effect of Pressure

Pressure effect of OCM was studied by Ahari et al [43] which vary operating pressure from 0.2 MPa – 0.4 MPa as shown in figure 3.6.

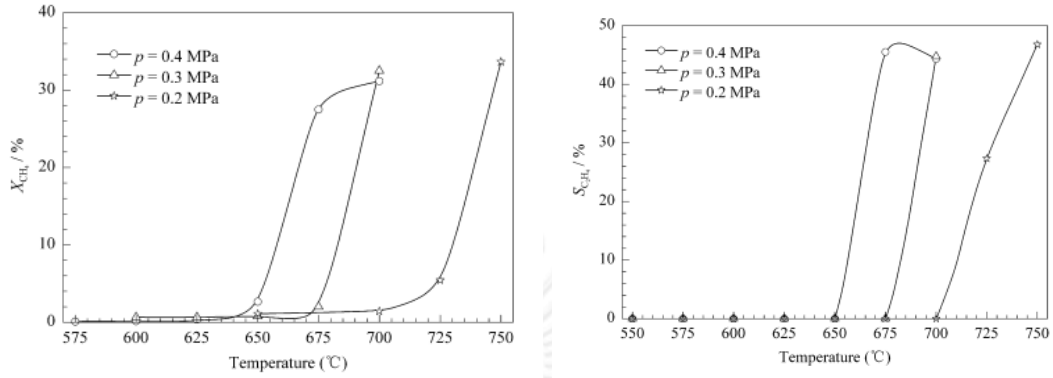

Fig 3.6 Effect of operating pressure on conversion and selectivity
Methane Conversion (Left) and Ethylene Selectivity (Right)

In the figure, it required temperature of 750°C to acquire 30 % conversion and 48 % selectivity of ethane at 0.2 MPa. But at 0.4 MPa, It required only 670°C. Thus, it could be concluded that increasing in pressure reduced temperature required to reach the same conversion or selectivity compared to lower pressure.

3.2.1.3 Effect of Methane to Oxygen Feed Ratio

Effect of variation of methane to oxygen feed ratio displayed in figure 3.7 which from various researches [11, 18, 44].

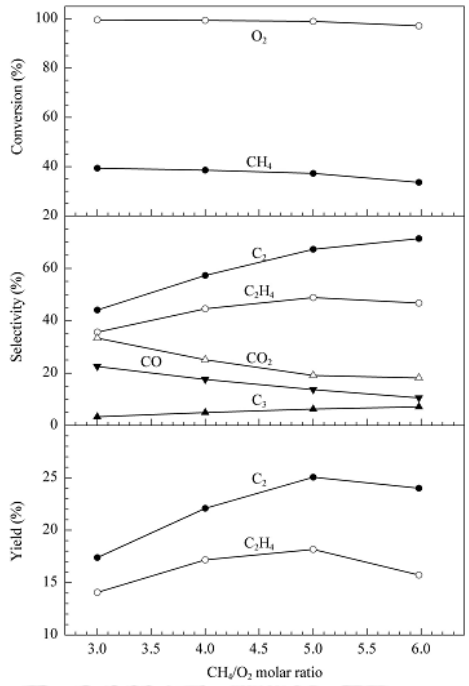

Fig 3.7 Effect of Methane to Oxygen Feed ratio on conversion and selectivity by Liu et al [17]

Increasing in CH_4/O_2 ratio reduced methane conversion due to lower amount of oxygen but selectivity of C_2 would increase. These results were also consisted with experiment of Ahari et al [43].

3.2.1.4 Effect of Contact Time

Effect of contact time experimented by Daneshpayeh et al [9] was depicted in figure 3.8. In the figure, conversion of methane and C_2 selectivity were plot as a function of space time.

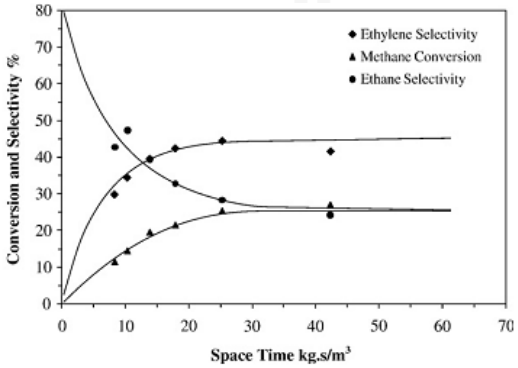

Fig 3.8 Effect of Contact Time on conversion and selectivity by Deneshpayeh et al [9]

Reducing contact time (Increase GHSV) would reduce gas phase oxidation in reactor which converted hydrocarbon in to CO_x. So C_2 selectivity should be higher than larger contact time but also reduced in methane conversion. This result was also confirmed by many researches [9, 12, 48, 51].

3.2.1.5 Effect of inert addition

Dilute addition stimulated selectivity for C_2 due to reduce combustion reaction in gas phase. However, adding too much inert also slow down OCM reaction. Ahari et al [43] used Nitrogen as inert at 0-20% mole at feed and found that in this range of inert addition raised selectivity of C_2 but also decreased in methane conversion. As well as Liu et al [18] experiment which utilized steam as inert and found the result consisted with Ahari.

3.2.2 Simulation of OCM

3.2.2.1 Simulation of Fixed bed Reactor

Except heat transfer problem in fixed bed reactor (FBR), Yan San Su [45] simulated oxidative coupling of methane reaction in many conditions and indicated that the highest yield for C_2 in fixed bed reactor were 28 %. Although this yield may be enough for industrial application, a lot of literature still worked for raise these yield up as high as possible. Y. Lu et al [46] simulated feed policy of OCM and found that distribution of oxygen into series of reactors slightly improve selectivity of C_2 hydrocarbon. As well as Ioannis et al [47] simulated OCM in the same configuration but also separate product out of unreacted reagent in each stage. Outcome of this procedure yielded 87 % of C_2 in 20 stage of FBR. From the concepts mentioned above, concept of membrane reactor and counter current moving bed reactor were generated. Membrane reactor which was suggested as the suitable configuration for OCM [46, 48] . Not only its methane conversion and C_2 selectivity that were higher than FBR but also their feed policy that fed CH_4/O_2 at very low ratio led the heat generation in reactor very less than FBR.

Separation of products in each stage of reactor motivated the idea of Counter-Current Moving Bed Reactor (CCMBR) [49] as well. Its performance was very good at 75 % methane conversion with 55 % C_2 yield. However, using this reactor

type in industrial application still too far out because it effected the economic viable of the process[5].

3.2.2.2 Simulation of Fluidized Bed Reactor

Simulation of fluidized bed reactor initiated by Pannek and Mleczko [50] using bubble assemblage model in fluidized bed. Their result fitted the lab scale reactor within 20 % accuracy but did not fit industrial scale because the industrial scale mass transfer coefficient was lower than in lab scale. Extra contact time had to be added in industrial application allow more gas phase oxidation reaction to more active. So Pennek and Mleczko indicated the flow pattern in reactor was important for the complex reaction like OCM [51].

3.3 Equilibrium Modeling

In process simulation literatures, computer aid simulations were viral to use as representative of real process. Simulation could predict outcome of the process with reliable results. The simulation for chemical reactor was divided into two categories; kinetic model and chemical equilibrium model.

Generally, kinetic model was commonly used in process simulation due to its reliability in prediction. However, equilibrium model was also used in many process simulation. Most of the processes were equilibrium limit reactions or reaction with easily reached equilibrium.

Process literature which used equilibrium model to represent reactor were summarized in table 3.7. In table, there were gasification, pyrolysis, reforming and others reactions. One of advantages for simulation with equilibrium model was ease in utilization. It did not require much parameter as kinetic to represent the model.

Table 3.8 Equilibrium model in process simulation

System	Reactions	Reference
Gasification	RGibbs	[52, 53]
Partial Oxidation	$CH_4 + 1.5O_2 \longrightarrow CO + 2H_2O$	[54]
Reforming	$CH_4 + H_2O \longrightarrow CO + 3H_2O$	[55-57]
Fischer–Tropsch	$nCO + (2n + 1)H_2 \leftrightarrow C_nH_{2n+2} + nH_2O$ $nCO + 2nH_2 \leftrightarrow C_nH_{2n} + nH_2O$	[58-60]
DME Synthesis	$3CO + 3H_2 \leftrightarrow CH_3OCH_3 + CO_2$	[58, 61, 62]
Water Gas Shift	$CO + H_2O \longrightarrow CO_2 + H_2$	[52]
Methanol Synthesis	$CO + 2H_2 \leftrightarrow CH_3OH$ $CO_2 + 3H_2 \leftrightarrow CH_3OH + H_2O$	[52]

However, there was a limitation for equilibrium model. This model could not predict outcome of reactor that did not reach equilibrium. However, OCM reaction reached equilibrium very fast within milliseconds (Described in section 3.4) It would not be impossible to predict OCM effluent with equilibrium model.

3.4 Extension from literature

Adding residence time in reactor led compositions in reactor more approached to almost 100% conversion of oxygen. After the oxygen concentration was very low, concentration of others components were also stable. The stable concentration of each component compiled that the OCM reaction was reach equilibrium state. Moreover, the simulation result of $Mn/Na_2WO_4/SiO_2$ by kinetic of Daneshpayeh et al [11] indicated that OCM reaction needs only short residence time (19-123 millisecond) in reactor to reach equilibrium.

As OCM reaction simply reached equilibrium, it fulfilled concept of chemical equilibrium that could predict reactor effluence composition at equilibrium time. So this research intended to model the OCM reaction in chemical equilibrium aspect which expected to give the same result as experiment at complete conversion of oxygen as show in figure 3.9.

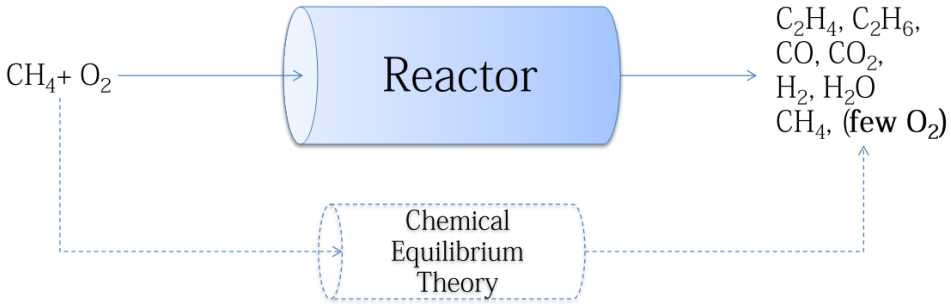

Fig 3.9 Concept of OCM modeling by chemical equilibrium

However, competitive of gas phase reaction and catalytic reaction in OCM led modeling for equilibrium very complex. Integration chemical equilibrium with reactor configuration in modeling such as catalytic density, void fraction etc. was an idea for this modeling which shall be verified the result of developed model with experiment.

CHAPTER 4

SIMULATION

This chapter described methodology to develop appropriate equilibrium model of OCM reaction starting with specifying elementary inputs of model. Then, the equilibrium models were explained. After that the validation methodology were discussed and followed by utilization of the models.

4.1 Concept of Chemical Equilibrium Modeling

Oxidative Coupling of Methane (OCM) was the reaction that co-feed methane and oxygen into reactor to form C_2 hydrocarbon product (Eq.4.1). With the operating condition at very high temperature (650-1000^{o}C), the reaction rate was very fast. Therefore, the concentration of reactant i.e. oxygen in reactor decreased very rapidly and remained only small amount. After the concentration of oxygen was very low, the concentrations of all components were stable. It could be compiled that the very small amount of oxygen left in effluence was in equilibrium with concentration of others products i.e. CH_4, C_2H_6, C_2H_4, CO, CO_2, H_2 and H_2O. Thus, concentration of components should be explained by chemical equilibrium theory.

Therefore, this research intended to simulate and predict the OCM reaction results with chemical equilibrium theory. The simulation results were then compared to the previous literatures.

4.2 Elementary parameters for beginning of simulation

Simulations of OCM in this research were done with Aspen Plus program. In order to start simulation, there were many elementary parameters were required before calculation.

4.2.1 Influent components

Components that fed into reactor were consisted of methane (CH_4) and oxygen (O_2). Purity of both methane and oxygen were at ultrapure condition because it would be easy to analyze the effluence of reactor. The ultrapure feed condition was taken from the laboratory literatures [6, 10, 11, 41].

4.2.2 Reactions in OCM

Specifying the reactions available for the system was one of the important input parameters for simulation. The available reactions were depending on type of catalyst used in reactor. In this research, there were three types of catalysts $Mn/Na_2WO_4/SiO_2$, La_2O_3/CaO and PbO/Al_2O_3. The properties of each catalyst were shown in table 4.1.

Table 4.1 Some properties of catalysts studied in this research.

Model	Catalyst	Catalyst Properties		Operating Condition	
		Density	Void fraction	Temp (^{0}C)	CH_4/O_2
Danashpayeh et al **[11]**	$Mn/Na_2WO_4/SiO_2$	1,100	0.4	700-875	3-10
Stransch et al **[10]**	La_2O_3/CaO	3,600	0.8	700-875	3-10
Hinsen et al **[12]**	PbO/Al_2O_3	2,000	0.7	650-750	5-10

From the various literatures [6, 10-13, 38, 40, 44], there were many proposed reactions in the system which was shown in table 4.1. They were classified into three groups; catalytic reactions, non-catalytic reactions and both of them.

Catalytic reactions were the heterogeneous reaction reacted at the surface of catalyst i.e. OCM, oxidative dehydrogenation (ODH), partial oxidation, steam reforming, carbon dioxide reforming and hydrocracking. Non-catalytic reaction was spontaneous reaction reacted in gas phase i.e. combustion. Some reactions i.e. ethane dehydrogenation and water-gas shift reaction could be functioned as both catalytic and non-catalytic.

Table 4.2 All Possible reactions in OCM from literatures

No.	Reaction	K equilibrium 600 C	K equilibrium 700 C	K equilibrium 800 C
Catalytic Reaction				
	Oxidative Coupling			
1	$2CH_4+0.5O_2 \longrightarrow C_2H_6+H_2O$	$4.41x10^{7}$	$3.73 x10^{6}$	$5.00 x10^{5}$
	Oxidative Dehydrogenation			
2	$C_2H_6 + 0.5O_2 \longrightarrow C_2H_4 + H_2O$	$2.60 x10^{10}$	$5.97 x10^{9}$	$1.79 x10^{9}$
	Partial Oxidation			
3	$CH_4+ 0.5O_2 \longrightarrow CO + 2H_2$	$4.49 x10^{11}$	$3.23 x10^{11}$	$2.49 x10^{11}$
4	$C_2H_6+O_2 \longrightarrow 2CO+3H_2$	$3.98 x10^{27}$	$7.36 x10^{26}$	$1.87 x10^{26}$
5	$C_2H_4+O_2 \longrightarrow 2CO+2H_2$	$1.33 x10^{29}$	$3.24 x10^{27}$	$1.58 x10^{26}$
	Steam Reforming			
6	$CH_4+H_2O \leftrightarrow CO + 3H_2$	$5.15 x10^{-1}$	$1.23 x10^{1}$	$1.64 x10^{2}$
7	$C_2H_6 + 2H_2O \longrightarrow 2CO + 5H_2$	$5.25 x10^{3}$	$1.07 x10^{6}$	$8.19 x10^{7}$
8	$C_2H_4 + 2H_2O \longrightarrow 2CO + 4H_2$	$1.75 x10^{5}$	$4.69 x10^{6}$	$6.89 x10^{7}$
	Carbon Dioxide Reforming			
9	$CH_4 + CO_2 \leftrightarrow 2CO + 2H_2$	$1.92 x10^{-1}$	7.59	$1.51 x10^{2}$
10	$C_2H_6+ 2CO_2 \longrightarrow 4CO + 3H_2$	$7.29 x10^{2}$	$4.06 x10^{5}$	$6.92 x10^{7}$
11	$C_2H_4+2CO_2 \longrightarrow 4CO + 2H_2$	$2.44 x10^{4}$	$1.79 x10^{6}$	$5.84 x10^{7}$
	Hydrocracking			
12	$C_2H_6 + H_2 \longrightarrow 2CH_4$	$1.98 x10^{4}$	$7.05 x10^{3}$	$3.02 x10^{3}$
13	$C_2H_4 + 2H2 \longrightarrow 2CH_4$	$6.61 x10^{5}$	$3.11 x10^{4}$	$2.55 x10^{3}$
Non-Catalytic Reaction				
	Combustion			
14	$CH_4+1.5O_2 \longrightarrow CO + 2H_2O$	$3.41 x10^{35}$	$2.23 x10^{32}$	$5.69 x10^{29}$
15	$CH_4+2O_2 \longrightarrow CO_2 + H_2O$	$7.95 x10^{47}$	$9.51 x10^{42}$	$9.35 x10^{38}$
16	$CO + 0.5O_2 \longrightarrow CO_2$	$2.34 x10^{12}$	$4.26 x10^{10}$	$1.64 x10^{9}$
17	$C_2H_6+2.5O_2 \longrightarrow 2CO+3H_2O$	$2.63 x10^{63}$	$1.34 x10^{58}$	$6.47 x10^{53}$
18	$C_2H_6+3.5O_2 \longrightarrow 2CO_2+H_2O$	$1.43 x10^{88}$	$2.43 x10^{79}$	$1.75 x10^{72}$
19	$C_2H_4 + 2O_2 \longrightarrow 2CO + 2H_2O$	$1.01 x10^{53}$	$2.24 x10^{48}$	$3.60 x10^{44}$
20	$C_2H_4+3O_2 \longrightarrow 2CO_2+2H_2O$	$5.51 x10^{77}$	$4.06 x10^{69}$	$9.73 x10^{62}$
Both Catalytic and Non-Catalytic Reaction				
	Dehydrogenation			
21	$C_2H_6 \leftrightarrow C_2H_4 + H_2$	$2.99 x10^{-2}$	$2.27 x10^{-1}$	1.19
	Water-Gas Shift			
22	$CO + H_2O \leftrightarrow CO_2 + H_2$	2.68	1.62	1.09

Note: Reaction 1-11 and 14-21 were referenced from literatures [6, 10-13, 38, 40, 44] , reaction 12-13 were new proposed in our work. Equilibrium Constants (K) were simulated with Aspen Plus.

Table 4.2 showed the possible reactions in OCM summarized from many published literatures. The Eq. 1 and 2 were the main catalytic reactions of OCM and oxidative dehydrogenation of ethane (ODH) [35, 41], respectively. The partial oxidations (Eq. 3-5) were the oxygen consumed reactions which performed as the side reactions in the process. The stream and carbon dioxide reforming (Eq. 6-11) functioned as the side reactions which consumed water and carbon dioxide

respectively. For Non-catalytic reactions which were the homogeneous reaction, there were many oxygen consumptions of combustion reactions (Eq.14-20) which must be avoided in OCM. Dehydrogenation and water gas (Eq.21-22) shift were able to react in both the catalytic and non-catalytic process.

To complete the reaction in OCM, this research proposed the hydrocracking reaction (Eq.12-13) into possible reactions because some metal in OCM catalyst was used in hydrocracking reaction i.e. Lead (Pb) and Tungsten (W) [63, 64].

4.2.3 Effluent Components

From various OCM literatures [1, 10, 42, 65], the effluence of reactors were consisted of hydrogen (H_2), carbon oxide (CO and CO_2), ethane (C_2H_6), ethylene (C_2H_4), water vapor (H_2O) and also unreacted methane (CH_4) and oxygen (O_2). These components were the same as the products from the possible reactions mentioned in previous section.

4.2.4 Operating Conditions

Temperature reactor and amount of feed were the important input parameters. From OCM experiments, most OCM reactors were operating isothermally in the range of 650-900°C while the feed of methane to oxygen ratio was around 3-10 [10-12].

4.2.5 Thermodynamic property calculation method

Thermodynamic property calculation method was one of input factors in calculation. This method calculated the component properties and their interaction with each other at given temperature and pressure. The selection of thermodynamic property calculation method was based on two guidelines, Aspen plus components guideline [66] shown in figure 4.1 and industrial guideline.

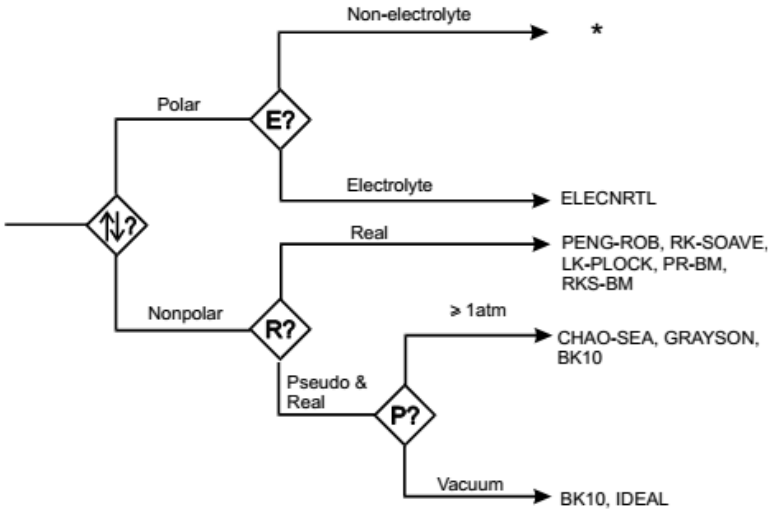

Fig 4.1 Selection guideline of the thermodynamic property calculation method [66]

Most components in both influence and effluence of this simulation were non-polar hydrocarbon except water. However, operating temperature in the simulation was more than 650°C and all components were in gas state including water. So, the polarity of water had no effect for the calculations since it was not in liquid state. Then, the system was nonpolar. Moreover, because all products were known, pathway for real components was selected. Therefore, with respect to the Aspen plus guideline, the suggestions for suitable thermodynamic properties were PENG-ROB, RK-Soave, PR-BM, LK-PLOCK and RKS-BM.

The others industrial guideline [66] for petrochemical process recommended CHAO-SEA, Grayson, PENG-ROB, RK-Soave, NRTL, UNIQUAC and REFPROP. It should be noticed that NRTL and UNIQUAC were liquid activity prediction which were not suitable in this research because all components state were gas phase.

From the two guidelines, the coincident suggestion methods were PENG-ROB and RK-Soave. To select the appropriate method, the simulation at temperature 800°C and pressure 1 atm of mixture of H_2, CH_4, C_2H_6, C_2H_4, CO, CO_2 and H_2O were simulated and expressed in table 4.3. In the table, volume, enthalpy and other properties were calculated with RK-Soave and PENG-ROB and compared the results. It could be clearly seen that difference between the calculation methods was less than 0.01%. Thus, both methods could be used in this work without any insignificant difference. For the simulation in this work, RK-Soave was selected.

Table 4.3 Difference of property calculation using RK-Soave and PENG-ROB*

Property	RK-Soave	PENG-ROB	Difference (%)
Vapor Frac	1.00	1.00	0.000
Total Flow l/hr	11473900.00	11472900.00	0.009
Enthalpy cal/mol	-23674.02	-23674.31	-0.001
Entropy cal/mol-K	2.86	2.85	0.004
Density gm/cc	0.00	0.00	-0.008
Average MW	19.76	19.76	0.000
Liq Vol 60F l/hr	5858.44	5858.44	0.000

*Calculation with Aspen Plus program

4.3 Proposed models

After the elementary parameters were selected, the construction of simulation model was then figured out. For mathematic calculation, it could split calculation in the reactor into many sections. For example in figure 4.2, one real reactor could be split into three sub-reactors and calculated the efflux result.

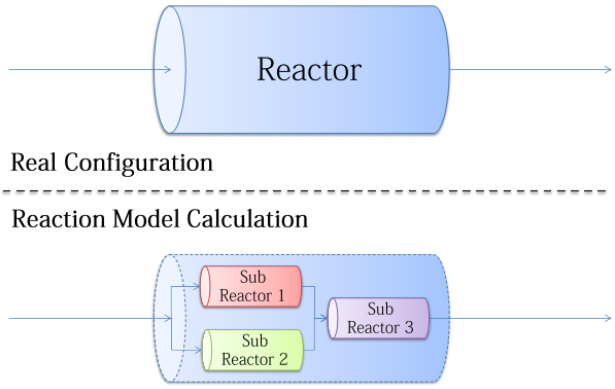

Fig 4.2 Reaction model calculation scheme

In this work, there were three models to be proposed; uni-equilibrium reaction model, duo-equilibrium reaction model and trio-equilibrium reaction model.

4.3.1 Uni-equilibrium reaction model

Uni-equilibrium reaction model, figure 4.3, was the simplest model imitated real configuration of reactor. Simulation was run under the assumption that all

reactions were reacted in the same phase and the equilibrium of every reaction was reached.

In this model, there were three trials to be simulated. First, all possible 22 reactions in table 4.2 were available. Second, some reactions were selective with respected to the literature corresponding to type of catalysts. Finally, the reactions selective to catalysts were chosen by researcher.

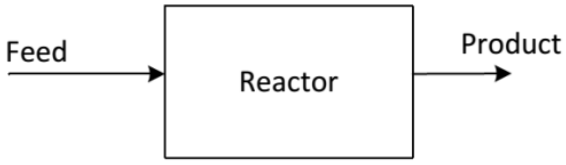

Fig 4.3 Single Equilibirum Reactor model

4.3.2 Duo-equilibrium reaction model

Duo-equilibrium reaction model was developed under the assumption that catalytic reaction (main reaction) took place at the catalyst surface while non-catalytic reaction (side reaction) occurred in the gas phase of void space among catalyst particle. The effluents from both parts were the end products. This model was shown in figure 4.4.

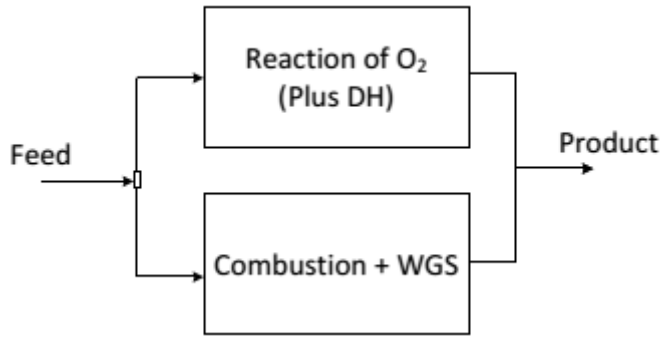

Fig 4.4 Duo-equilibrium reaction model

In the catalytic reactor, the simulation was run with the catalytic reactions in table 4.1, i.e. OCM, oxidative dehydrogenation, partial oxidation, steam reforming, dehydrogenation (DH) and hydrocracking. While, the non-catalytic reactions i.e. combustion and water-gas shift (WGS) was calculated in the gas phase reactor. Both

reactors were assumed to run at the same temperature and pressure until getting the equilibrium. Ratio of catalytic and gas phase was dependent on type of catalyst.

4.3.3 Trio-equilibrium reaction model

The trio-equilibrium reaction model was modified from previous model under the assumption that products from both catalytic and gas phase reaction would react further in the consequent reaction by some others non-oxidized reactions. Then, model consisted of three sub-reactors, shown in figure 4.5, first two sub-reactors were similar to that of the previous model. Another reactor was connected allowing the combined effluents other reactions before the products were final yielded.

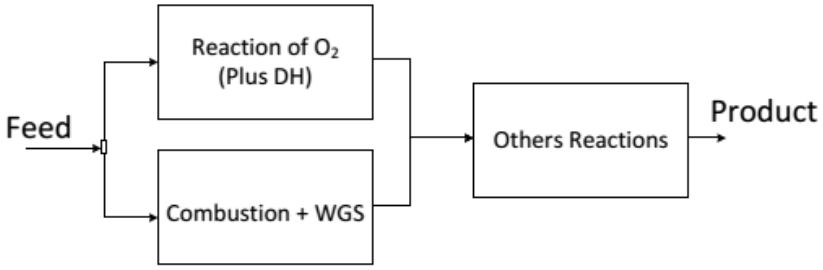

Fig 4.5 Trio-equilibrium reaction model

4.4 Verification of models using statistics

After simulating with the same influents, product components and concentrations from each model were compared to the previous OCM literatures. However, the effluent data reported from literatures were different in two styles. Some reported all components efflux in system and the other described only the reactor performance, such as percent conversion. In this work, both information were utilized to validate the proposed model.

4.4.1 Verification using components in effluence.

For literature reporting all effluent component data, model validation utilizing Residue Sum Square (RSS) shown in equation 4.1 was chosen. RSS value was the value of deviations calculated from summation of square difference between effluent mole flow of chemical equilibrium model (M_{model}) and the experiment (M_{exp})

divided by the experiment mole flow. The small RSS value indicated accuracy of model of all components.

$$RSS = \sum_{i=1}^{N} \left[\frac{(M_{\exp} - M_{model})}{M_{\exp}} \right]^2 \quad (4.1)$$

4.4.2 Verification using reactor performance

For literatures reporting the reactor performance in OCM system, the accuracy of model was tested with respected to variety information such as methane conversion (X_{CH4}), ethane yield (C_2H_6), ethylene yield (C_2H_4) and selectivity (S_i). The description of those varieties was defined in equation 4.2-4.5. Yields of C_2 components were used equivalent in carbon components. Otherwise, maximum yield of C_2 would be limited at only 50% and led to misunderstanding in process.

$$X_{CH_4} = \left(\frac{M_{CH_4,in} - M_{CH_4,out}}{M_{CH_4,in}} \right) x\,100 \quad (4.2)$$

$$Y_{C_2H_6} = \left(\frac{2xM_{C_2H_6,out}}{M_{CH_4,in}} \right) x100 \quad (4.3)$$

$$Y_{C_2H_4} = \left(\frac{2xM_{C_2H_4,out}}{M_{CH_4,in}} \right) x100 \quad (4.4)$$

$$S_i = \frac{Y_i}{X_{CH_4}} \quad (4.5)$$

Average absolute relative deviation (AARD) were statistics calculated from summation of differentiate between the variable (P) from model and experiment divided by number of iterations as shown in equation 4.6.

$$AARD = \frac{1}{N} \sum_{i=1}^{N} \left| \frac{(P_{\exp} - P_{\text{model}})}{P_{\exp}} \right| \quad (4.6)$$

Variables used in the equation 4.6 for this work were methane conversion, ethylene selectivity, ethane selectivity and carbon oxide selectivity. It should be

notice that deviations of all variables could be totally shown in value of AARD. Small value of AARD suggested the validity of model.

After statistic variable showed precision of each model, the best model could be selected. The selected model would be validated further at others operating condition to ensure that the model could be predict the outcome at various conditions.

4.5 Advantage of developed models

After developing the appropriate model for OCM reaction, the model would be utilized in process simulation. The used of equilibrium model would be an optional for the simulation of OCM reaction.

CHAPTER 5

RESULT AND DISCUSSION

This chapter consisted of 5 categories: Equilibrium of oxidative coupling of methane, chemical Equilibrium modeling, model manipulation, model validation and advantage of developed model. The first category explained the OCM system at the equilibrium. Chemical Equilibrium modeling reported the construction and development of each model. Model manipulation was to modify the model to get more accuracy. Model Validation discussed and analyzed the accuracy of models via statistics. Finally, model advantages were implied.

5.1 Equilibrium of Oxidative Coupling of methane

In this research, with the help of Aspen Plus, methane and oxygen were fed into reactor at the variety conditions based on the condition published in the literatures. In the reactor, oxygen was consumed by various reactions (e.g. OCM combustion etc.). The consumed oxygen was reacted with methane to form ethane, ethylene and carbon oxide. After oxygen concentration was very low, concentration of others components were also stable. Thus, it could be compiled that the very small amount of oxygen (mole fraction $\approx 10^{-24}$) left in effluence was in equilibrium with concentration of others products i.e. CH_4, C_2H_6, C_2H_4, CO, CO_2, H_2 and H_2O.

Most kinetic works were generally studied OCM by varying the principle factors such as flow rate, reactor temperature and fraction of catalysts followed by determining the effects of the factors on the effluent components. However, the observing conditions were at the point that O_2 was still too much and not the point reaching the equilibrium.

However, aim of this research is to study OCM using chemical equilibrium principle, then, operating space time must reach equilibrium. Thus, the kinetic studied were simulated further extending the residence time till the system got the equilibrium and the results were used as a reference data (the expected data). The comparison between the reference data and the results calculated from the proposed equilibrium model would suggest the precision of model.

To demonstrate, simulation was set with the condition employed in the previous work of Daneshpayeh et al [9] using $Mn/Na_2WO_4/SiO_2$ as a catalyst. Methane to oxygen feed was at 5 and reactor temperature was 850°C. Both of the results from kinetic model and the experimental data were plotted and shown in part I of figure 5.1. The simulation was allowed to run further till the concentration of each components got equilibrium. The percent conversion of oxygen and methane as well as yield of C_2 products were shown in figure 5.1 part II.

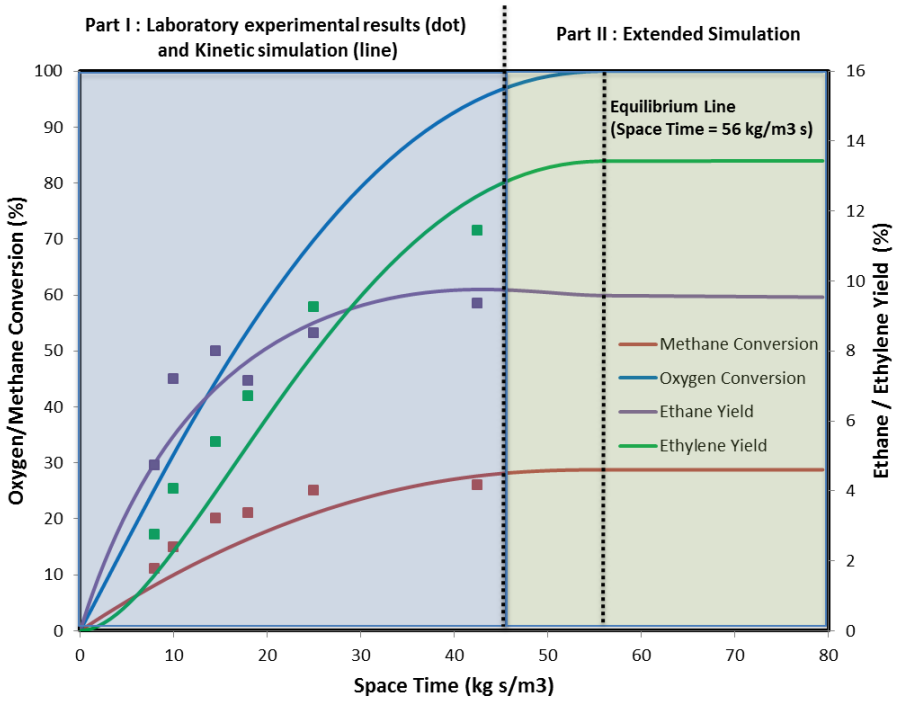

Fig 5.1 Percent conversions of effluents simulated by kinetic model with respect to the space time
(Catalyst =$Mn/Na_2WO_4/SiO_2$, CH_4/O_2 = 5, temperature = 850°C)

In figure 5.1 part I, results from laboratory experiments (dots) and kinetic model (lines) were plotted versus the space time up to 46 kg s/m^3 (41.8 milliseconds). After extending the residence time further with kinetic simulation, it showed the system was reach the equilibrium at the space time of 56 kg s/m^3 (50.9 milliseconds). It should be noticed that the system got equilibrium at the point of almost 100% conversion of O_2. It was shown the very short times of 9.1 milliseconds where the products yield between experiment and kinetic simulation at equilibrium was not significantly different. Thus, data from experiment was reasonable assumed as the reference data. Moreover, this research used kinetic simulation with the

extend time at equilibrium to calculate the reference data which was not only the precious effluents, such as CH_4 C_2H_6 C_2H_4 and CO_x, but also other available components which were not reported in the laboratory such as H_2 and H_2O.

5.2 Chemical equilibrium modeling

Chemical equilibrium modeling procedure was constructed as described in chapter 4. In this research, there were three catalysts to be studied: $Mn/Na_2WO_4/SiO_2$, La_2O_3/CaO and PbO/Al_2O_3. Some properties of catalysts used in this research were listed in table 4.1

Three models mentioned in chapter 4 were consecutively studied for each catalyst, starting from uni-reactor to trio-equilibrium reaction model. The precision of models (difference between data from the proposed model and the data from the reference data) were determined to verify the best model. The chosen model was then validated to find the validation regions.

5.2.1 Uni-equilibrium reaction model

The uni-equilibrium reaction model detailed in chapter 4.2.1 was tested with three types of catalysts, $Mn/Na_2WO_4/SiO_2$, La_2O_3/CaO and PbO/Al_2O_3. Operating conditions were the picked up from the corresponding literatures which was listed in table 4.1. The results were compared to the reference data which was called “the equilibrium composition” to verify the capability of models.

5.2.1.1 The test of OCM reaction over $Mn/Na_2WO_4/SiO_2$ catalyst

Simulations were run with the feed conditions taken from Daneshpayeh et al [11] who study OCM reaction over $Mn/Na_2WO_4/SiO_2$ catalyst. All reactions presented in table 4.2 were input for the competition in the reactor. Simulations were tested with the temperatures, 700, 750, 800, 825 and 850°C. Feed ratios of CH_4/O_2 at a given temperature were varied from 3 to 10. Reaction pressure was fixed at ambient pressure. After the simulation was complete at equilibrium, the effluent yield in mole fractions were plotted against the feed ratio of CH_4/O_2 compared shown in figure 5.2. Dots were the equilibrium composition (the reference data) and line represented the data from the proposed uni-equilibrium reaction model.

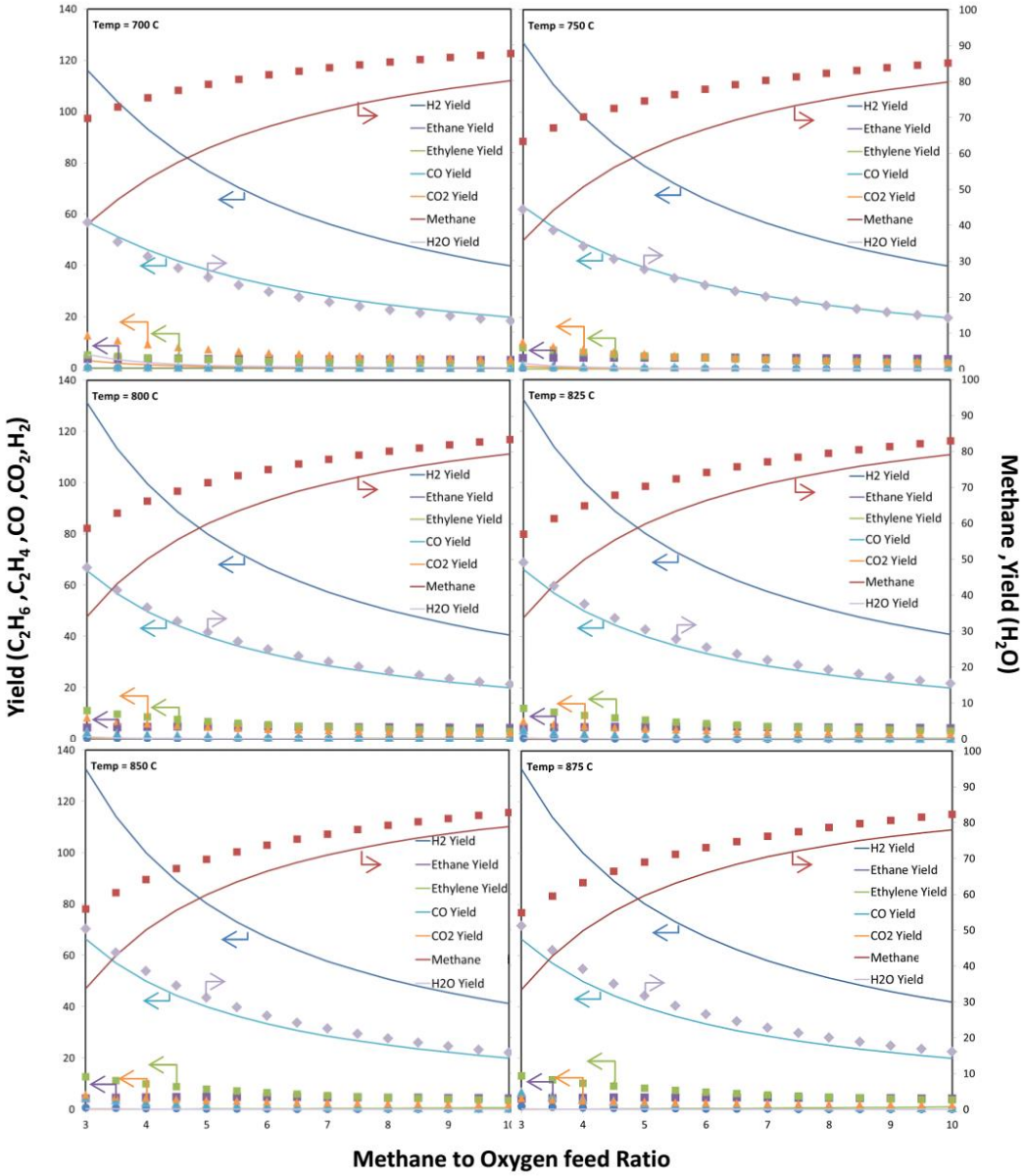

Fig. 5.2 Simulation results from the uni-equilibrium reaction model and equilibrium composition versus the feed ratio of CH_4/O_2 for $Mn/Na_2WO_4/SiO_2$ catalyst at a variety given temperatures

--- Data from uni-equilibrium reaction model ● Equilibrium composition

From figure 5.2, red plot of dots and line represented the methane in equilibrium. It could be described that the higher the feed ratio of CH_4/O_2, the more methane left in the effluent while the other effluents (other colors data) showed conversely. For temperature effect, it was clearly shown that the higher temperature, the closer between two calculated data of methane (red dots versus red line) which suggested the better precision of the proposed model at high temperature. The plots

at 850 or 875 °C were both determine as the best fit for this case. To magnify and show the comparison clearly, data at 850 °C and CH_4/O_2 = 5 was drawn in bar chart and shown in figure 5.3.

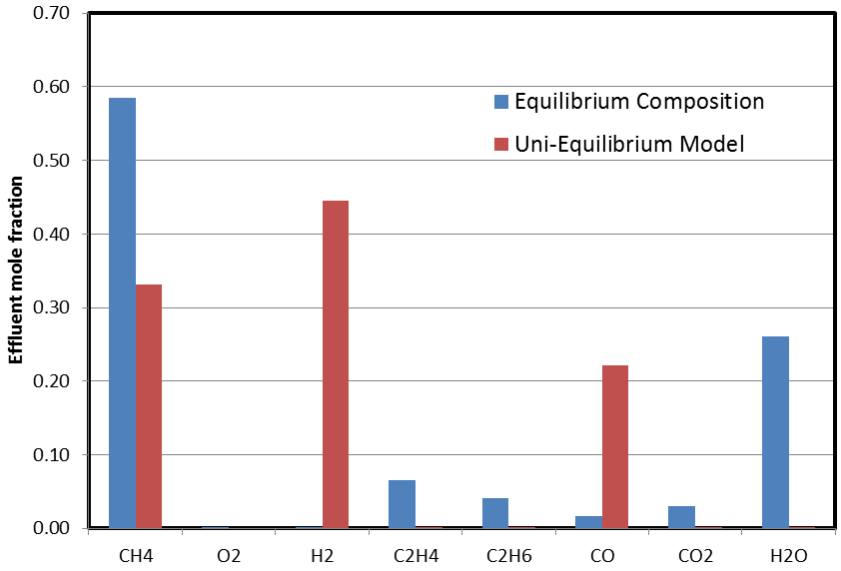

Fig 5.3 Simulation results from uni-equilibrium reaction model and equilibrium composition at equilibrium for $Mn/Na_2WO_4/SiO_2$ catalyst.
(Conditions:, T = 850°C and CH_4/O_2 = 5)

From figure 5.3, the blue and red bars represented the equilibrium composition and the uni-equilibrium reaction model, respectively. The results showed the far difference between those two calculation methods. It suggested the low precision of this proposed model. One important point was that effluents of equilibrium composition consisted of ethylene (C_2H_4), ethane (C_2H_6), carbon monoxide (CO), carbon dioxide (CO_2), water (H_2O) and unreacted methane (CH_4). Dissimilarly, data from proposed model consisted only CO and H_2 including unreacted CH_4 which suggested that only the partial oxidation of CH_4 (Eq.5.1) reacted in the model.

$$CH_4 + 0.5O_2 \longrightarrow CO + 2H_2 \qquad (5.1)$$

The absent of C_2 products including the low precision of these results allowed to conclude that the uni-equilibrium reaction model could not explain the

behavior of the OCM reaction. It should be notified here that the bar plots at other temperatures were ignored according to their similar results to figure 5.3.

5.2.1.2 The test of OCM reaction over La_2O_3/CaO catalyst

This section, simulations using uni-equilibrium reaction model were tested in the same way to section 5.2.1.1. The operating conditions were substituted with the Stransch et.al. [10] model studied over the catalytic of La_2O_3/CaO. After the simulation was completed at equilibrium, the effluent yield in mole fractions were plotted against the feed ratio of CH_4/O_2 compared shown in figure 5.4.

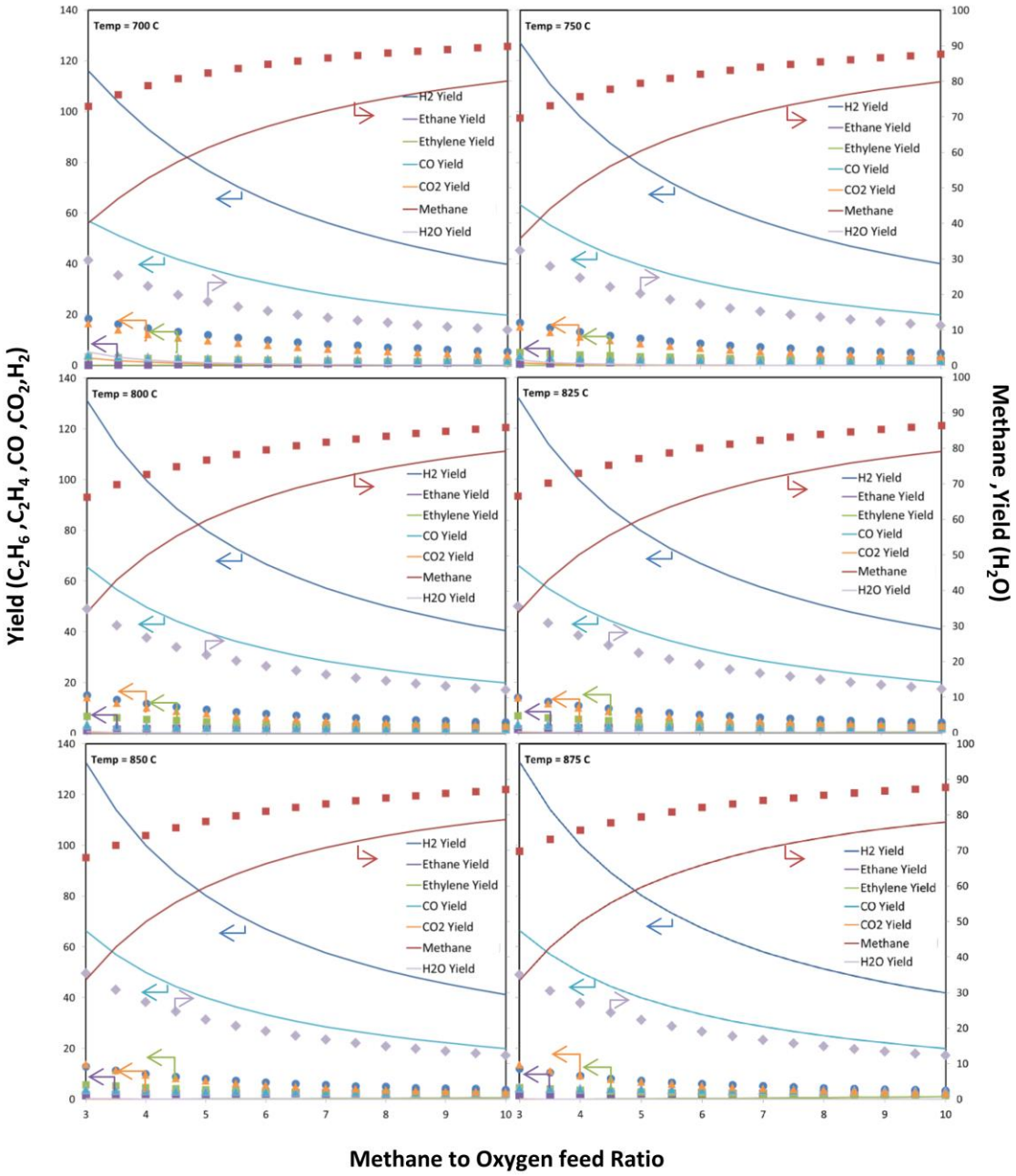

Fig. 5.4 Simulation results from the uni-equilibrium reaction model and equilibrium composition versus the feed ratio of CH_4/O_2 for La_2O_3/CaO catalyst at a variety given temperatures

--- Data from uni-equilibrium reaction model ● Equilibrium composition

From figure 5.4, deviations between two calculation methods were still as high as that of the previous catalyst. The result at 850°C was chosen to plot with bars of effluents mole. The result was depicted in figure 5.5.

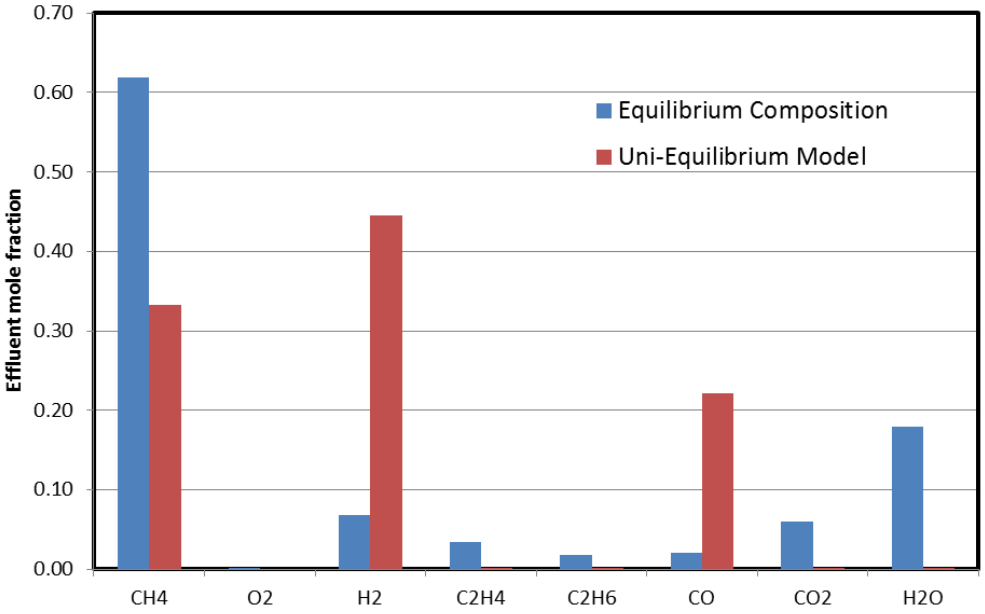

Fig 5.5 Simulation results from uni-equilibrium reaction model and equilibrium composition for La_2O_3/CaO catalyst.
(Conditions: T = 825°C and CH_4/O_2 = 5)

Form figure 5.5, the calculated effluent components showed large deviation from the expected results as the same as that of the previous test using $Mn/Na_2WO_4/SiO_2$. The products components were H_2 and CO and unreacted CH_4 without C_2 products indicated that main reaction in the system was partial oxidation.

5.2.1.3 The test of OCM reaction over PbO/Al_2O_3 catalyst.

The simulation method was repeated with the information from Hinsen et al's work [12] tested over PbO/Al_2O_3 catalyst. Reaction temperature range was 650 – 750 °C. Four plots of effluent yields as the functions of feed ratio of CH_4/O_2 at 650, 700, 725 and 750 °C were illustrated in figure 5.6.

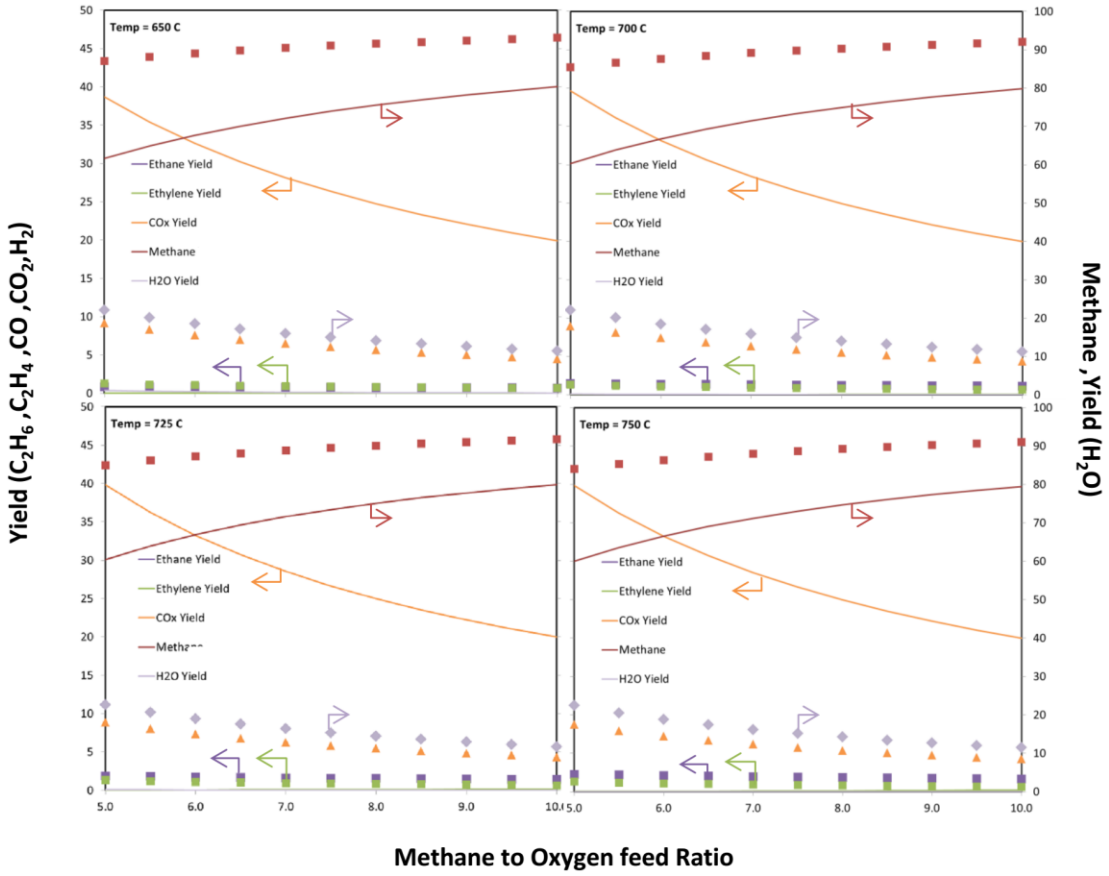

Fig. 5.6 Simulation results from the uni-equilibrium reaction model and equilibrium composition versus the feed ratio of CH_4/O_2 for PbO/Al_2O_3 catalyst at a variety given temperatures

--- Data from uni-equilibrium reaction model ● Equilibrium composition

There were large deviations found in this simulation too. The result at 725°C was chosen to represent the comparison with bar plot and shown in figure 5.7.

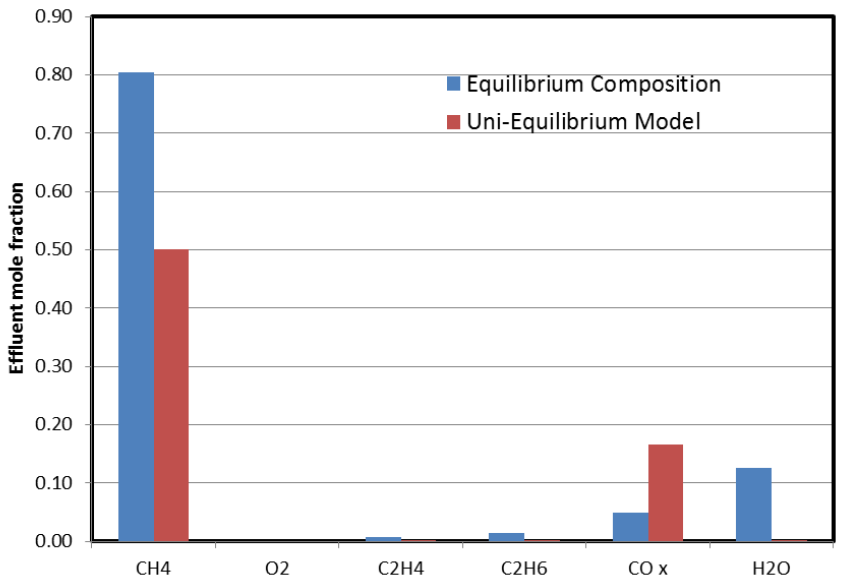

Fig 5.7 Simulation results from uni-equilibrium reaction model and equilibrium composition for PbO/Al_2O_3 catalyst.
(Conditions: T = 725°C and CH_4/O_2 = 8)

Again, with the PbO/Al_2O_3 catalyst, the effluences were the partial combustion products. It should be mentioned here that bar of mole fraction of H_2 was not shown because there was no information of H_2 concentration in the literature. Bar of H_2 mole found from the simulation could make the misunderstanding without the comparative quantity from equilibrium composition. Moreover, CO and CO_2 components were summarized reported in carbon oxide (CO_x) form in literature. Therefore, the model results were also reported in the same pattern.

According to the large deviations from uni-equilibrium reaction model over the three catalysts, $Mn/Na_2WO_4/SiO_2$, La_2O_3/CaO, PbO/Al_2O_3, It can be concluded that this simulation model could not explain the behaviors of the OCM reaction. It was attributed to the limitation of feed oxygen concentration that led partial oxidation to dominate the other reactions such as oxidative coupling of methane, combustion etc.

$$CH_4 + 0.5O_2 \longrightarrow CO + 2H_2 \qquad K_{eq,800\,C} = 2.49 \times 10^{11} \qquad (5.1)$$

$$CH_4 + 1.5O_2 \longrightarrow CO + H_2O \qquad K_{eq,800\,C} = 5.68 \times 10^{29} \qquad (5.2)$$

$$CH_4+2O_2 \longrightarrow CO_2 + H_2O \qquad K_{eq,800\ C} = 9.35 \times 10^{38} \qquad (5.3)$$

By stoichiometric determination, partial oxidation reaction (Eq. 5.1) consumed oxygen per methane at ratio of 0.5 while incomplete combustion (Eq. 5.2) and complete combustion (Eq. 5.3) were 1.5 and 2.0, respectively. To accomplish the lowest Gibbs free energy at limited oxygen, the reaction with the smallest fraction of O_2 paid majority role and directed to the partial oxidation reaction. This was the same reason of combustion at low oxygen concentration would lead to form CO rather than CO_2 even the completed combustion had higher equilibrium constant.

To prove that only the partial oxidation reaction reacted in the system while other reactions were inactive, new simulation was set with the same feed condition but selecting only the partial reaction to be the available reaction computing in the system. This test was run under the hypothesis that the system was run with the solely partial oxidation reaction if the amount of products were identical to that done with all available reaction. The results were shown in figure 5.8.

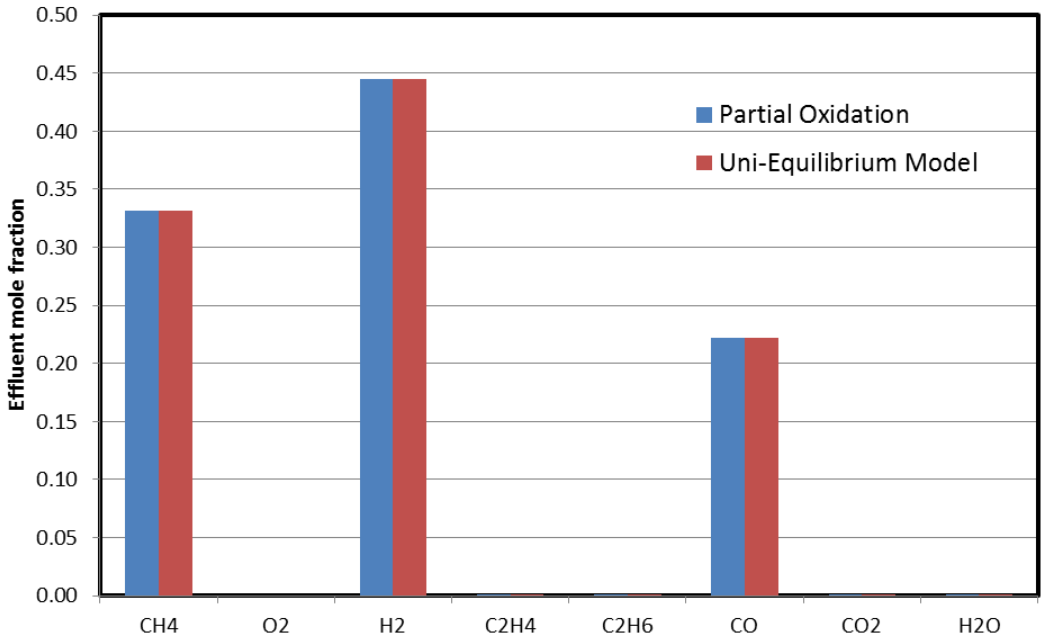

Fig 5.8 Simulation results from uni-equilibrium reaction model with all 22 reactions and solely partial reaction.
(Conditions: catalyst=$Mn/Na_2WO_4/SiO_2$, T =850°C and CH_4/O_2 = 5)

From figure 5.8, it was clearly shown the identity of all effluents produced from both simulations. It proved that uni-equilibrium reaction model support only for the partial combustion reaction which produced the mixture of H_2 and CO.

More attempts were tested on the uni-equilibrium reaction model. One was based on the postulate that catalyst selected the occurring reactions. The selectivity of catalysts led to the limitation of available reactions in the process. The summarizations of the catalyst selectivity were based on literatures published and the conclusions were listed in table 5.1.

Table 5.1 The summarization of the catalyst selectivity.

No.	Reaction	$Mn/Na_2WO_4/SiO_2$ [11]	La_2O_3/CaO [10]	PbO/Al_2O_3 [12]
1	$CH_4+2O_2 \rightarrow CO_2 + H_2O$	✓	✓	✓
2	$2CH_4 + 0.5O_2 \rightarrow C_2H_6 + H_2O$	✓	✓	✓
3	$CH_4 + O_2 \rightarrow CO + H_2O + H_2$	✓	✓	
4	$CO + 0.5O_2 \rightarrow CO_2$	✓	✓	
5	$C_2H_6 + 0.5O_2 \rightarrow C_2H_4 + H_2O$	✓	✓	✓
6	$C_2H_4 + 2O_2 \rightarrow 2CO + 2H_2O$	✓	✓	
7	$C_2H_6 \rightarrow C_2H_4 + H_2$	✓	✓	
8	$C_2H_4 + 2H_2O \rightarrow 2CO + 4H_4$	✓	✓	
9	$CO + H_2O \rightarrow CO_2 + H_2$	✓	✓	
10	$C_2H_4 + 3O_2 \rightarrow 2CO_2 + 2H_2O$			✓

This conceptual system led to ignore the partial oxidation reaction which was solely reaction in the system above. New simulations were tested with the limited reactions in table 5.1. It was noted that the selective reactions using $Mn/Na_2WO_4/SiO_2$ and La_2O_3/CaO catalysts were identical, the reaction number 1-9 (table 5.1). Other conditions such as feed ratio, temperature and pressure were controlled to compare with the result shown in figure 5.3 and 5.5 respectively. The comparison of bar plots resulted from the uni-equilibrium reactions between the different available reactions (all 22 reaction and 9 limit reactions) were depicted in figure 5.9 and 5.10.

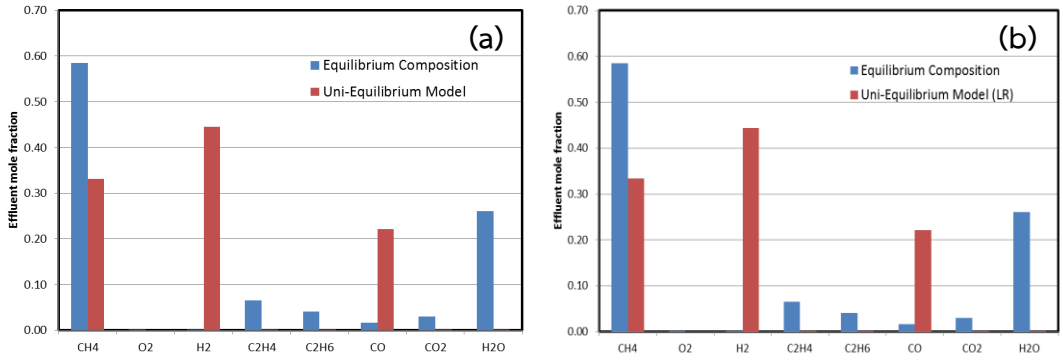

Fig 5.9 Comparison of the simulation results from the uni-equilibrium reaction model for $Mn/Na_2WO_4/SiO_2$ catalyst. (a) all 22 reactions available (b) 9 limited reactions (Conditions: T =850°C and CH_4/O_2 = 5)

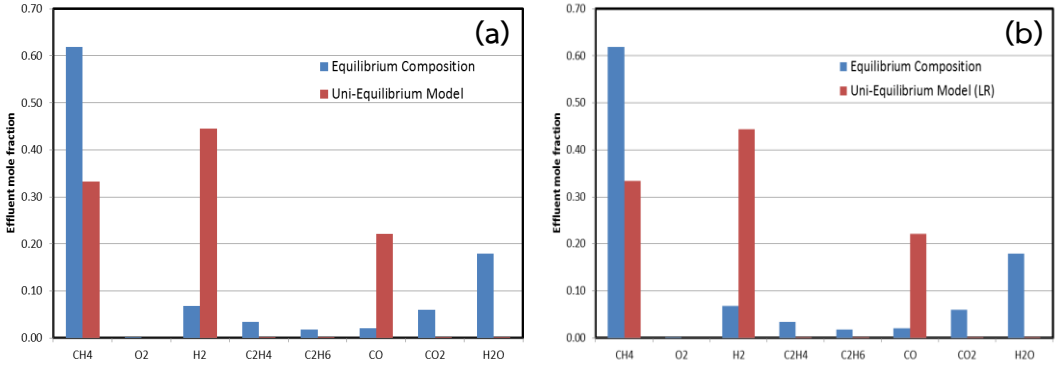

Fig 5.10 Comparison of the simulation results from the uni-equilibrium reaction model for La_2O_3/CaO catalyst. (a) all 22 reactions available (b) 9 limited reactions (Conditions: T =825°C and CH_4/O_2 = 5)

Figure 5.9 and 5.10 showed the comparison of the simulation results from the uni-equilibrium reaction model for $Mn/Na_2WO_4/SiO_2$ and La_2O_3/CaO catalyst, respectively.

Surprisingly, two different simulations with limited reaction using $Mn/Na_2WO_4/SiO_2$ and La_2O_3/CaO catalyst showed the identical bars comparing to those with the partial oxidation reaction solely. The persistence of H_2, CO without partial oxidation reaction in the running process was must be described.

For describing this mechanism, the proposed scheme of elementary reactions for mechanism was written in figure 5.11.

Route 1	$2CH_4 + 0.5O_2 \longrightarrow C_2H_6 + H_2O$	$K_{eq} = 5.00 \times 10^5$
	$\downarrow$	
	$C_2H_6 \leftrightarrow C_2H_4 + H_2$	$K_{eq} = 1.19$
	$\downarrow$	
	$C_2H_4 + 2H_2O \longrightarrow 2CO + 4H_4$	$K_{eq} = 6.89 \times 10^7$
Route 2	$CH_4 + O_2 \longrightarrow CO + H_2O + H_2$	$K_{eq} = 3.76 \times 10^{20}$
Total Reaction	$CH_4 + 0.5O_2 \longrightarrow CO + 2H_2$	$K_{eq} = 2.49 \times 10^{11}$

Fig 5.11 the proposed scheme of reaction mechanism in the uni-equilibrium reaction model

However, products from the simulation did not match to equilibrium compositions. Those suggested that the uni-equilibrium reaction model was the unsatisfactory model for describing the results.

Another attempt was run for PbO/Al_2O_3 catalyst. The selective reactions were reaction number 1, 2, 5 and 10 (table 5.2). The comparison of the simulation results between the unequal reactions used in the calculation were shown in figure 5.12.

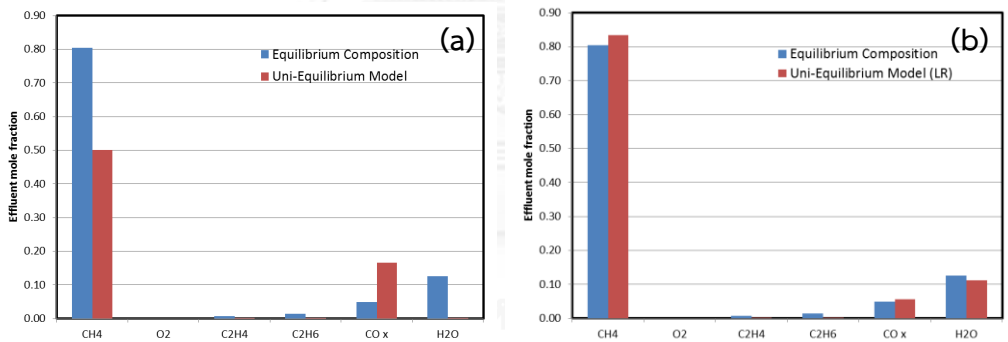

Fig 5.12 Comparison of the simulation results from the uni-equilibrium reaction model for PbO/Al_2O_3 catalyst. (a) all 22 reactions available (b) 4 limited reactions (Conditions: T =725^{o}C and CH_4/O_2 = 8)

From figure 5.12, the limitation of available reactions input in the simulation impacted the products composition. However, main products i.e. C_2H_4 and C_2H_6 were not found. Those confirmed that the uni-equilibrium reaction model with limited selective reactions was not an appropriate model for describing the OCM reaction.

However, this result suggested the good point that the limitation of reactions helped to get better fit.

Deviation of simulation results from uni-equilibrium reaction model was discussed. It was responsible to some inactive reactions which reacted slowly and would not reached equilibrium (i.e. ethylene steam reforming). In fact, ethylene steam reforming was a selective catalytic reaction which suitable with specific catalyst as listed in table 5.2. The steam reforming reaction was selective to the noble metal catalyst like Ni, Pd, Rh, Ru, Pt, or Co while OCM was for Ba, Ca, W, Sn, Sr, Mn, Pb or La. Therefore, steam reforming reaction could be claimed as the inactive reaction which would not function in the OCM catalyst. Thus, the rate of reaction compared to OCM would be very slow and could be neglected from calculation. Moreover, there were others catalytic reactions which were selective to another catalysts as well i.e. partial oxidation, carbon dioxide reforming, dehydrogenation and water gas shift reaction. Thus, these reactions could be neglected from simulation in catalytic part. Moreover, it should be noticed that catalysts for hydrocracking were overlapped with that of the OCM and ODH reactions, Tungsten (W) and lead (Pb). Thus, this research proposed this reaction to be possibly reacted in simulation system.

Table 5.2 Common catalysts for each reaction type

Reaction	Catalyst	Reference
Oxidative Coupling of Methane	Ba, Ca, W, Sn, Sr, Mn, Pb, La	[5]
Oxidative Dehydrogenation of Ethane	Ba, Ca, W, Sn, Sr, Mn, Pb, La	[67]
Partial Oxidation	V, Mo, Pr	[5]
Steam Reforming	Ni, Pd, Rh, Ru, Pt, Co	[68]
Carbon Dioxide Reforming	Ni, Pd, Rh, Ru, Pt, Co	[68]
Hydrocracking	Co, Ni, Mo, W and Pb	[63, 64]
Dehydrogenation	Pt, Sn	[5]
Water-Gas-Shift Reaction	Fe, Cu, Cr, Zn, Ni, Pt, Rh	[69]

After confining the reactions for OCM, the remaining reactions on catalytic part were OCM, ODH and hydrocracking. Ethane dehydrogenation and water-gas shift which could react only in gas phase because the OCM catalysts contained different element. Moreover, gas phase combustion was included all possible hydrocarbon

combustion reactions. The remaining reactions were listed in table 5.3. The numbers of reactions were referred in the next sections.

Table 5.3 Proposed reactions in OCM simulation

No.	Reaction	K equilibrium 600 C	K equilibrium 700 C	K equilibrium 800 C
Catalytic Reaction				
	Oxidative Coupling			
C1	$2CH_4+0.5O_2 \longrightarrow C_2H_6+H_2O$	$4.41x10^{7}$	$3.73 x10^{6}$	$5.00 x10^{5}$
	Oxidative Dehydrogenation			
C2	$C_2H_6 + 0.5O_2 \longrightarrow C_2H_4 + H_2O$	$2.60 x10^{10}$	$5.97 x10^{9}$	$1.79 x10^{9}$
	Hydrocracking [a]			
C3	$C_2H_6 + H_2 \longrightarrow 2CH_4$	$1.98 x10^{4}$	$7.05 x10^{3}$	$3.02 x10^{3}$
C4	$C_2H_4 + 2H_2 \longrightarrow 2CH_4$ [b]	$6.61 x10^{5}$	$3.11 x10^{4}$	$2.55 x10^{3}$
Non-Catalytic Reaction				
	Thermal Dehydrogenation			
G1	$C_2H_6 \leftrightarrow C_2H_4 + H_2$	$2.99 x10^{-2}$	$2.27 x10^{-1}$	1.19
	Thermal Water-Gas Shift			
G2	$CO + H_2O \leftrightarrow CO_2 + H_2$	2.68	1.62	1.09
	Combustion [c]			
G3	$CH_4+1.5O_2 \longrightarrow CO + 2H_2O$	$3.41 x10^{35}$	$2.23 x10^{32}$	$5.69 x10^{29}$
G4	$CH_4+2O_2 \longrightarrow CO_2 + H_2O$	$7.95 x10^{47}$	$9.51 x10^{42}$	$9.35 x10^{38}$
G5	$CO + 0.5O_2 \longrightarrow CO_2$	$2.34 x10^{12}$	$4.26 x10^{10}$	$1.64 x10^{9}$
G6	$C_2H_6+2.5O_2 \longrightarrow 2CO+3H_2O$	$2.63 x10^{63}$	$1.34 x10^{58}$	$6.47 x10^{53}$
G7	$C_2H_6+3.5O_2 \longrightarrow 2CO_2+H_2O$	$1.43 x10^{88}$	$2.43 x10^{79}$	$1.75 x10^{72}$
G8	$C_2H_4 + 2O_2 \longrightarrow 2CO + 2H_2O$	$1.01 x10^{53}$	$2.24 x10^{48}$	$3.60 x10^{44}$
G9	$C_2H_4+3O_2 \longrightarrow 2CO_2+2H_2O$	$5.51 x10^{77}$	$4.06 x10^{69}$	$9.73 x10^{62}$

[a] Additional reactions proposed in this research

[b] Reversible reactions of combination of reaction C3 and G1

[c] Combustion reactions were cover all incomplete and complete of all components

After scoping the feasible reactions in OCM, new simulations with three catalysts were shown separately in figure 5.13 to 5.15.

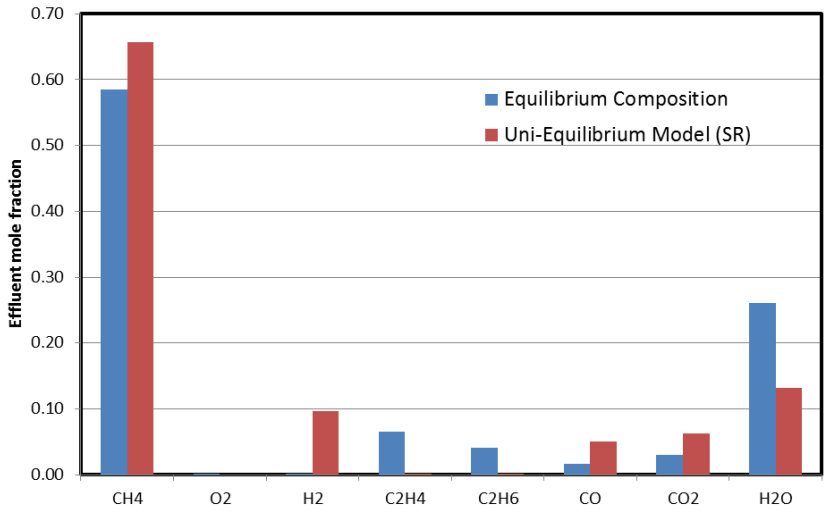

Fig 5.13 Effluents simulated by the uni-equilibrium reaction model with the 13 selected reactions for $Mn/Na_2WO_4/SiO_2$ (Conditions: T =850°C and CH_4/O_2 = 5)

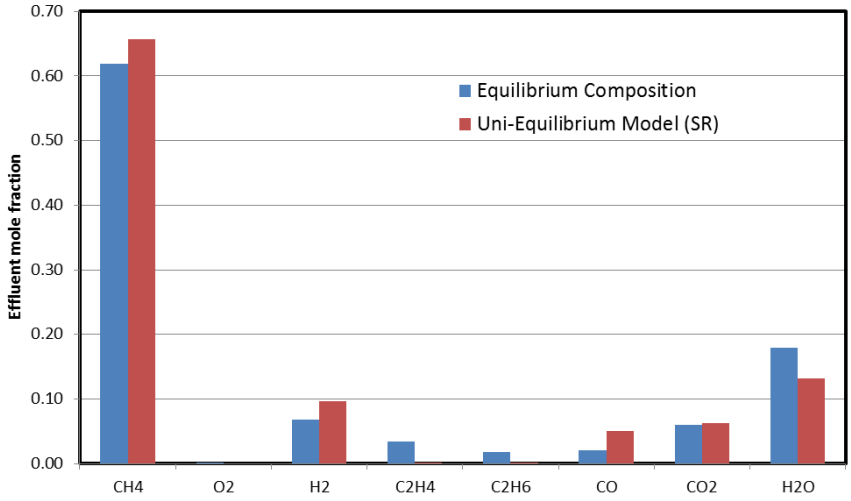

Fig 5.14 Effluents simulated by the uni-equilibrium reaction model with the 13 selected reactions for La_2O_3/CaO (Conditions: T =825°C and CH_4/O_2 = 5)

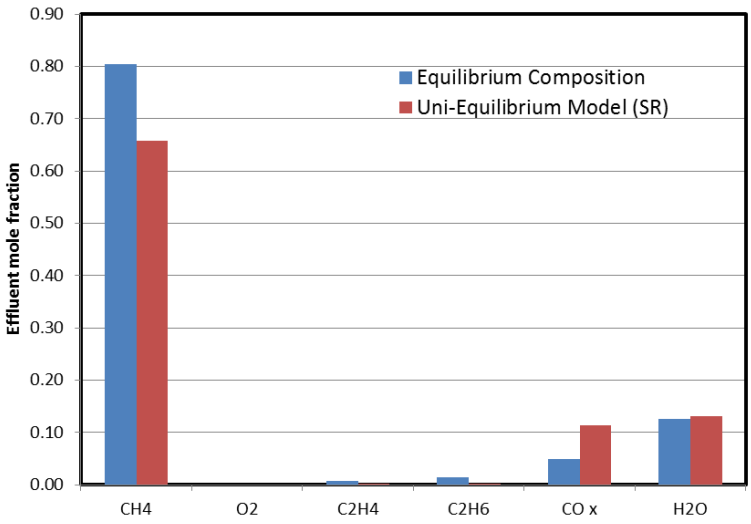

Fig 5.15 Effluents simulated by the uni-equilibrium reaction model with the 13 selected reactions for PbO/Al_2O_3 (Conditions: T =725°C and CH_4/O_2 = 8)

New simulation results were slightly better than previous prediction. As seen in figure 5.13 to 5.15, not only CO_2 and H_2O were formed but also more reasonable effluent composition. Nevertheless, there was still major deviation of no C_2H_4 and C_2H_6.

This deviation was attributed to the competition between reactions. In this case, OCM reaction (C1) and combustion reactions (G3-G10) were competed in reactor. Because combustion reaction have the higher equilibrium constant (K) than that of OCM reaction, the combustion reaction will react mostly in completion. Thus, in figures, there were only CO and CO_2 formed. So the uni-equilibrium calculation could not predict the reactions to competition for non-equilibrium reactions.

5.2.2 Duo-equilibrium reaction model

From previous section, the single equilibrium calculation could not predict competitive reactions between non-equilibrium reactions. Then, model was developed to allow the competition between the reactions. From one single reactor that all reactions were calculated in the same stage, it was split the calculation to two different parts, catalytic and gas phase, total products of those two parts were the output of the simulation. Each spitted part was specified the reaction to

competition. The fraction volume input in catalytic and non-catalytic reactor was assumed to be equal to the void and solid fraction of catalyst which was a specific property of catalyst as shown in table 4.1.

The duo-equilibrium reaction model was studied with two different specified reactions as described below.

5.2.2.1 The duo-equilibrium reaction model A

In this model, the first simulation part, the reactions reacted at catalytic surface were oxidative coupling of methane (OCM) and oxidative dehydrogenation (ODH) of ethane to ethylene. The other simulation part allowed the spontaneous possible gas phase reactions (the non-catalytic reaction) such as combustion and water-gas shift reactions (WGS). The duo-equilibrium reaction model was drawn and shown in figure 5.16. Table 5.6 summarized the equations used in both two parts. It should be noticed that the combustion reactions in gas phase were consisted of both complete and incomplete combustion of CH_4, C_2H_6 and C_2H_4. Although the combustion of C_2H_6 and C_2H_4 were included in calculation, these two reactions did not affect the effluent composition in this research. It was responsible for the pure feed of methane with no C_2H_6 and C_2H_4 impurity. Thus, there was no C_2 reactant to react with the combustion reactions.

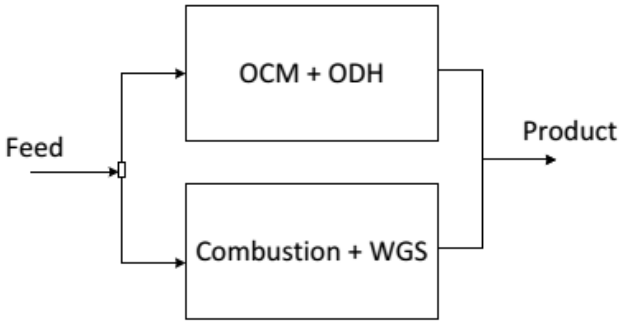

Fig 5.16 The duo-equilibrium reaction model A

It should be noted that fraction volume between reactors of catalytic and non-catalytic reactor was assumed to be equal to void and solid fraction of catalyst which was specified to a type of catalyst.

Table 5.4 Suggested reactions in each calculation phase.

Catalytic Phase	Gas Phase
$CH_4 + 0.5\ O_2 \longrightarrow C_2H_6 + H_2O$	$CH_4 + 1.5O_2 \longrightarrow CO + 2H_2O$
$C_2H_6 + 0.5\ O_2 \longrightarrow C_2H_4 + H_2O$	$CH_4 + 2O_2 \longrightarrow CO_2 + H_2O$
	$CO + H_2O \longrightarrow CO_2 + H_2$
	$CO + 0.5O_2 \longrightarrow CO_2$
	$*C_2H_6 + 2.5O_2 \longrightarrow 2CO + 3H_2O$
	$*C_2H_6 + 3.5O_2 \longrightarrow 2CO_2 + H_2O$
	$*C_2H_4 + 2O_2 \longrightarrow 2CO + 2H_2O$
	$*C_2H_4 + 3O_2 \longrightarrow 2CO_2 + 2H_2O$

* Required when impurity in feed were consisted of C_2 hydrocarbon and if there was another hydrocarbon in feed combustion of the hydrocarbon should be included.

Table 5.4 listed the reaction calculated in catalytic and gas phase for the duo-equilibrium reaction model A. Simulation was succeeded by feeding the CH_4/O_2 ratio in gas phase per catalytic phase with the void to solid fraction of catalyst. This provided the different amount of reactants in both calculation parts and led to the different products formed in the different catalyst.

The simulation results from duo-equilibrium reaction model for $Mn/Na_2WO_4/SiO_2$ catalyst at six different reaction temperatures were shown in figure 5.17. Data from the duo-equilibrium reaction model were shown in line pattern (---) and Data from equilibrium composition were dots (●).

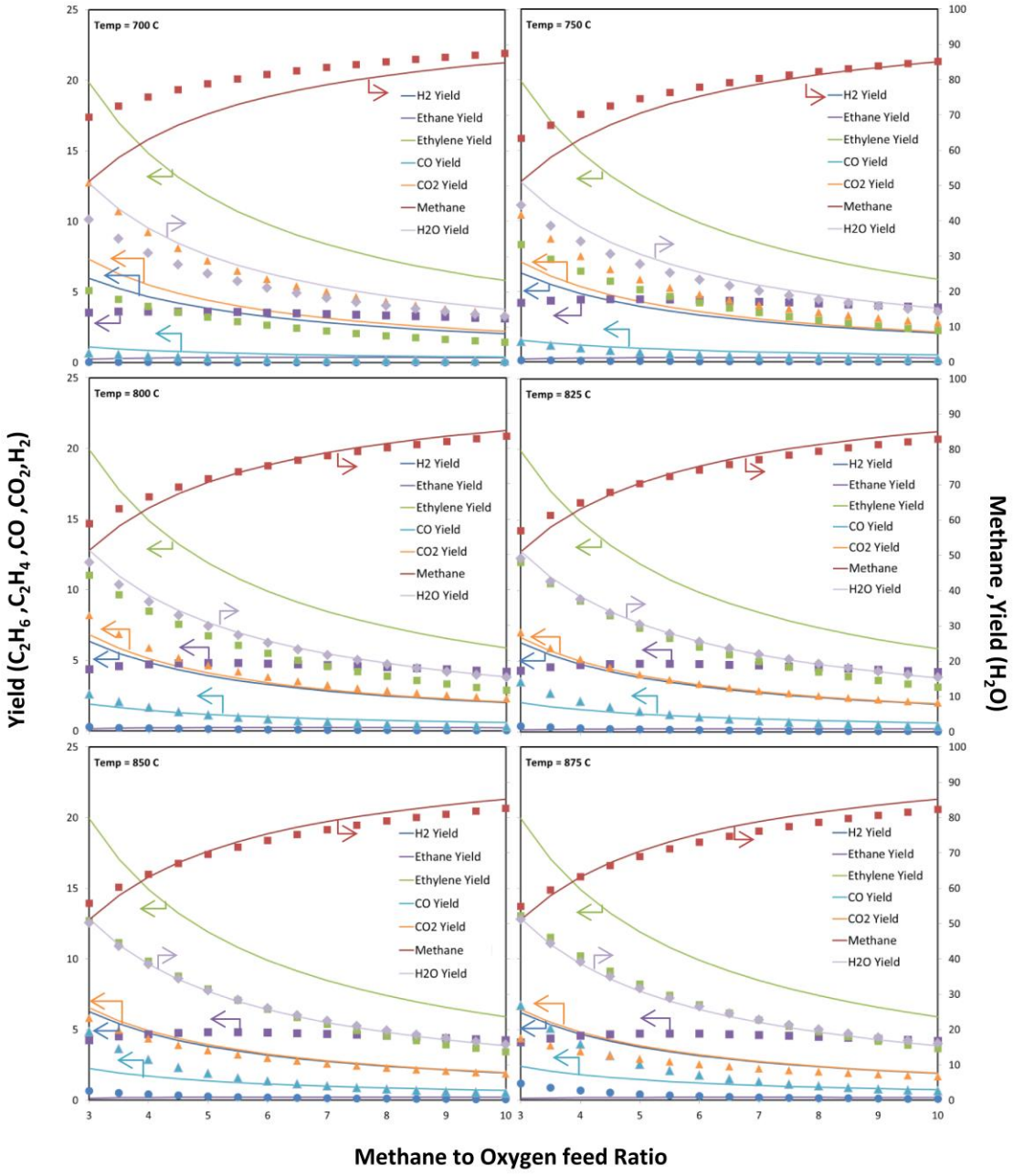

Fig 5.17 Simulation results from duo-equilibrium reaction model versus feed ratio for $Mn/Na_2WO_4/SiO_2$ catalyst at variety of reaction temperature

--- Data from the duo-equilibrium reaction model ● Equilibrium composition

From figure 5.17, the amount of most effluents was got closer to the expected results. Carbon monoxide and carbon dioxide components were reasonably closed at high temperature. As well as methane and water vapor that gave less deviate from previous model. Moreover, there were C_2 components formed

in this model. As seen in the figure that ethylene (green line) was formed in the system.

Simulation results from duo-equilibrium reaction model versus for La_2O_3/CaO catalyst at variety of reaction temperatures were shown in figure 5.18.

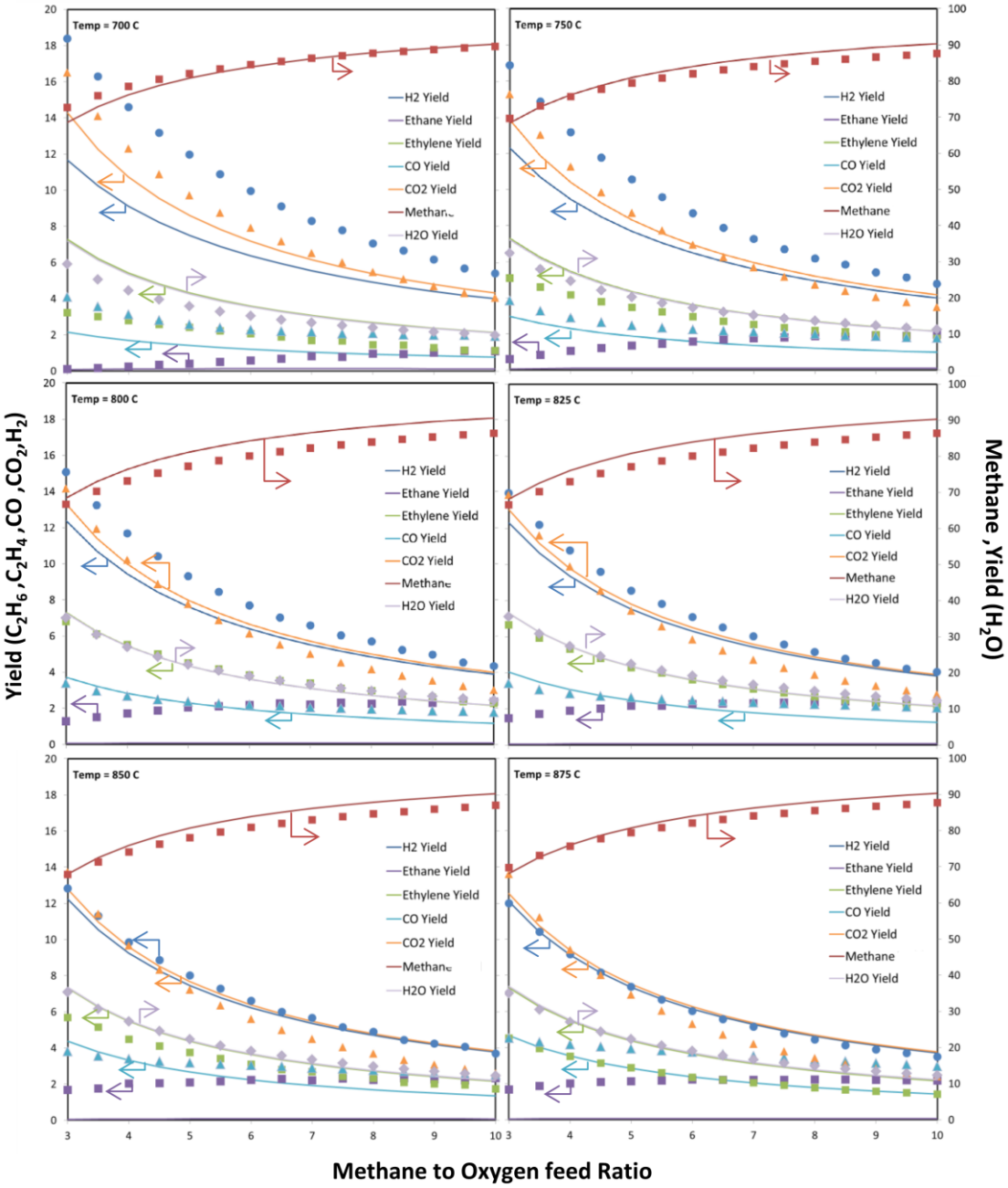

Fig 5.18 Simulation results from duo-equilibrium reaction model versus feed ratio for La_2O_3/CaO catalyst at variety of reaction temperature

--- Data from the duo-equilibrium reaction model ● Equilibrium composition

The results found that the simulation over the catalyst of La_2O_3/CaO showed the better fit as the same as $Mn/Na_2WO_4/SiO_2$ catalyst. Temperature effect was in agreement with the previous catalyst which could be concluded that the higher the temperature, the better the prediction results obtained. The deviation of each component would be shown with bar curve in figure 5.21.

Simulation results from duo-equilibrium reaction model versus feed ratio for PbO/Al_2O_3 catalyst at variety of reaction temperature were shown in figure 5.19.

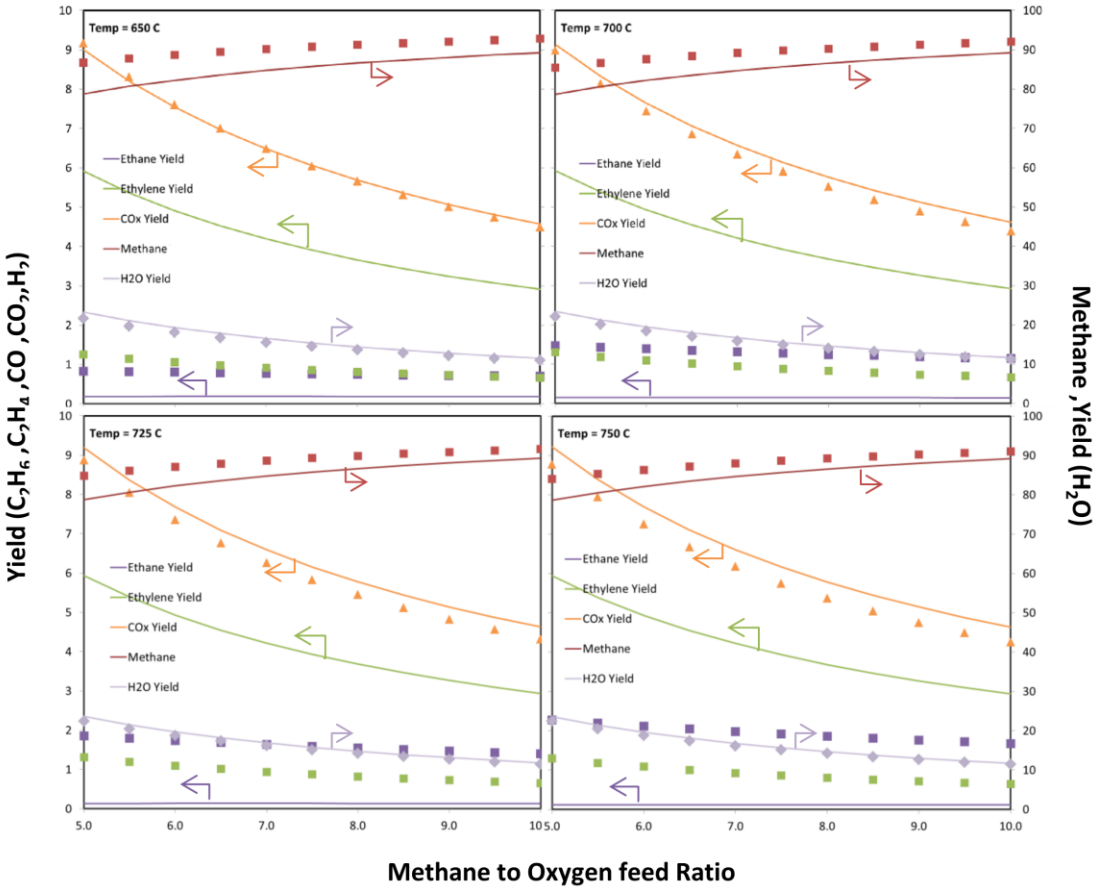

Fig 5.19 Simulation results from duo-equilibrium reaction model versus feed ratio for PbO/Al_2O_3 catalyst at variety of reaction temperature

--- Data from the duo-equilibrium reaction model ● Equilibrium composition

The results showed the better fit compared to those run with the uni-equilibrium reaction model as well as two previous catalysts. It should be noted that

this simulation was varied with the narrow range of temperature because it was within the scope studying for this catalyst.

The bar charts plotted from a set of data simulated with the duo-equilibrium reaction model condition were shown bar charts as in figure 5.20 to 5.22.

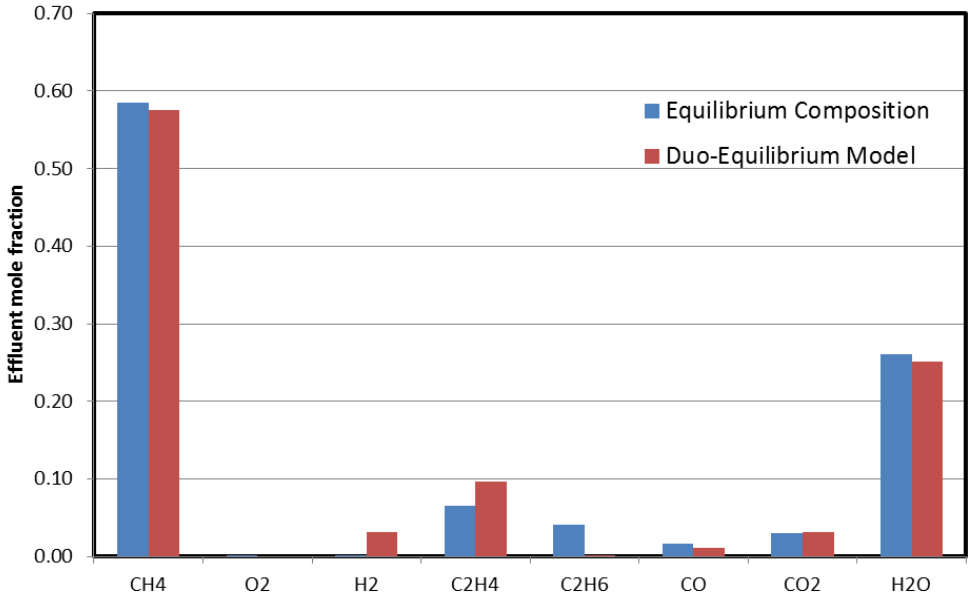

Fig 5.20 Effluent mole fraction simulated by the duo-equilibrium reaction model A for $Mn/Na_2WO_4/SiO_2$
(Conditions: T =875°C and CH_4/O_2 = 5)

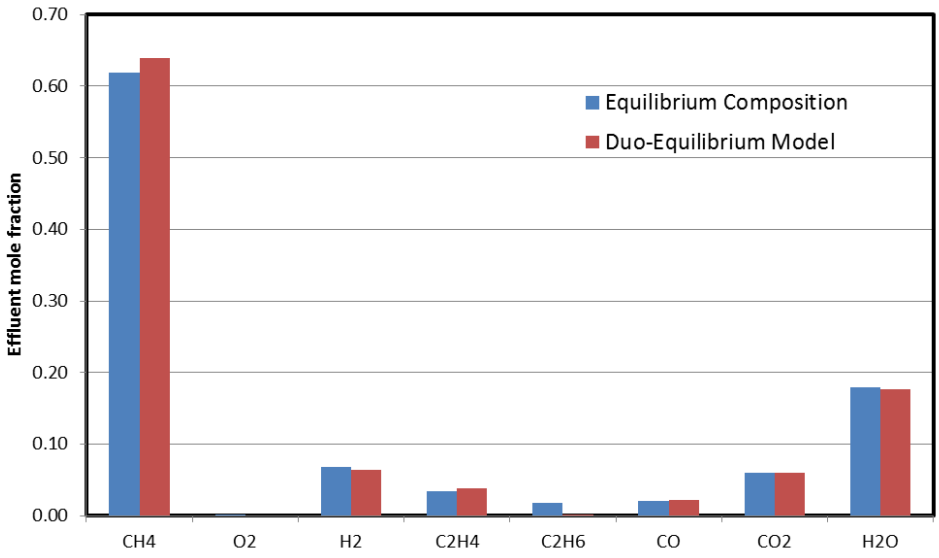

Fig 5.21 Effluent mole fraction simulated by the duo-equilibrium reaction model A for La_2O_3/CaO
(Conditions: T =875°C and CH_4/O_2 = 5)

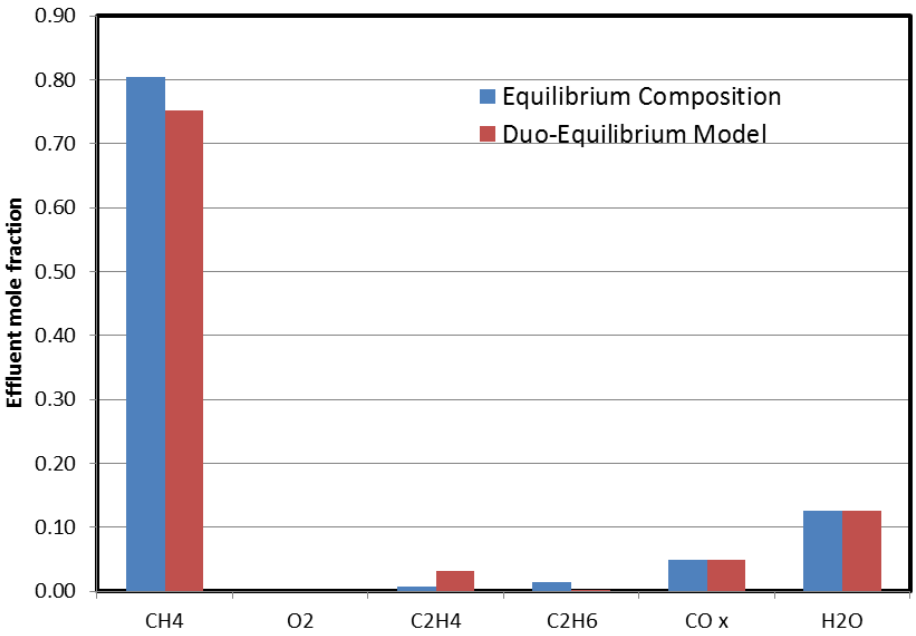

Fig 5.22 Effluent mole fraction simulated by the duo-equilibrium reaction model A for PbO/Al_2O_3 (Conditions: T =750°C and CH_4/O_2 = 5)

From figure 5.20 – 5.22, the simulation results from the duo-equilibrium reaction model A were much better than the uni-equilibrium reactors model. As seen in figure 5.20 to 5.22, there were C_2H_4 components formed in the simulation. Moreover, the others components mole fraction were less deviated from equilibrium composition. This indicated that the splitting calculation supported the methodology for OCM system. However, C_2H_6 components were still missed. It was reported at the nearly zero fraction of C_2H_6 ($x_{C2H6} \approx 0.0017$) which was much far from the expected amount ($x_{C2H6} \approx 0.014 - 0.04$). This error was taken in account and discussed for finding the method to reduce this deviation.

5.2.2.1 The duo-equilibrium reaction model B

The duo-equilibrium reaction model B model was designed to compete with model A. The difference between model A and B was only on the substitution of ODH with dehydrogenation (DH) reaction and the model scheme was shown in figure 5.23

Dehydrogenation : $C_2H_6 \rightleftharpoons C_2H_4 + H_2$ (5.4)

This dehydrogenation reaction in the catalytic phase was expected to adjust the yield of C_2, C_2H_6 and C_2H_4. The simulations were expected to yield more C_2H_6 at the output.

Because the equilibrium constants of the dehydrogenation reaction were 2.99 $x10^{-2}$, 2.27 $x10^{-1}$, and 1.19 at 600, 700 and 800 $^{\circ}C$, respectively, it suggested that at the reactor temperature lower than 800 $^{\circ}C$, the equilibrium shifted to the left while at the temperature higher than 800$^{\circ}C$, the equilibrium shifted to the right. Then, at the low temperature, the reaction trend to go back and yielded C_2H_6. Conversely, the reaction consumed C_2H_6 at the high temperature and produced C_2H_4.

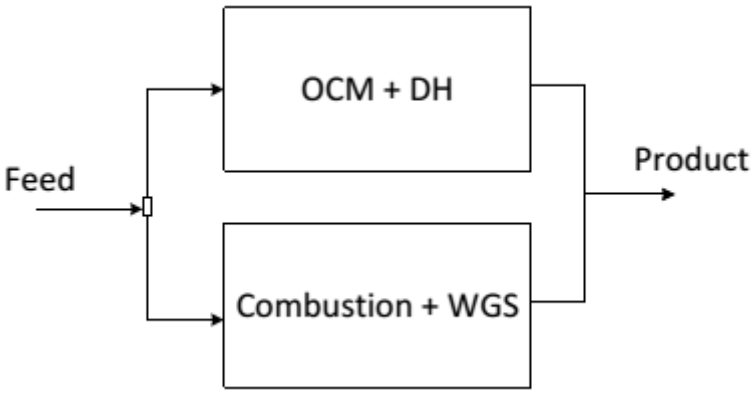

Fig 5.23 The duo-equilibrium reaction model of B

Figure 5.24-5.26 showed the compaison of bar graphs of components calculated from two different duo-equilibrium model A and B over three catalysts.

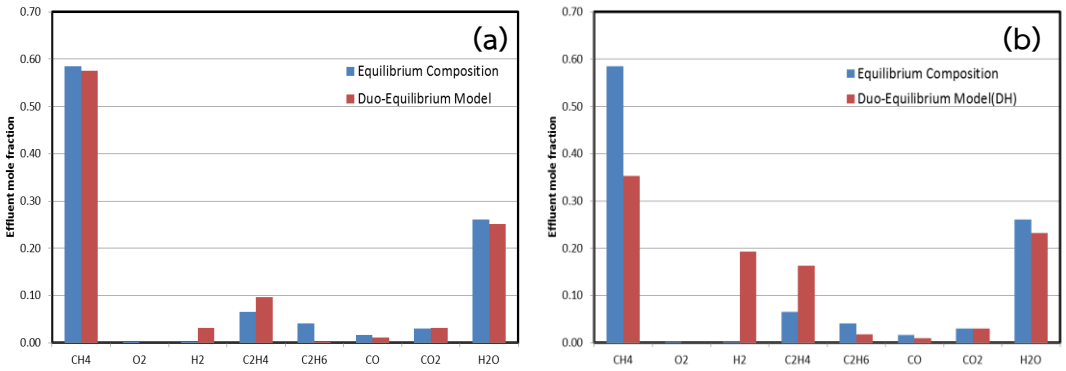

Fig 5.24 Comparison between simulation results from the duo-equilibrium reaction model A and B for $Mn/Na_2WO_4/SiO_2$ (Conditions: T = 850$^{\circ}C$ and CH_4/O_2 = 5)
(a) model A (b) model B

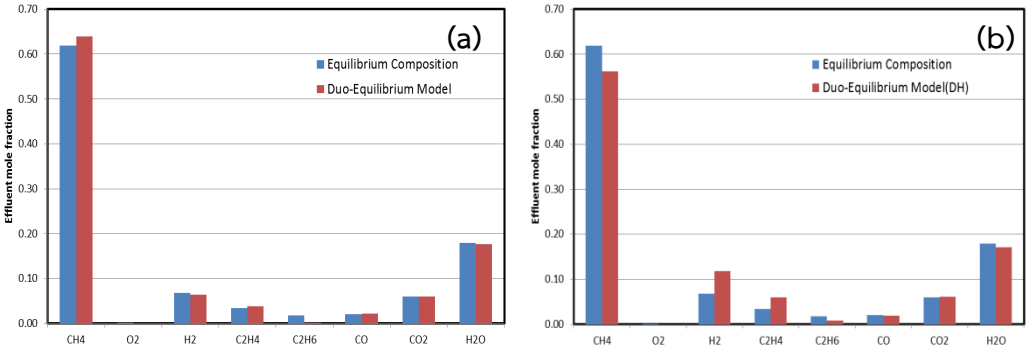

Fig 5.25 Comparison between simulation results from the duo-equilibrium reaction model A and B for La_2O_3/CaO (Conditions: T = 825°C and CH_4/O_2 = 5)
(a) model A (b) model B

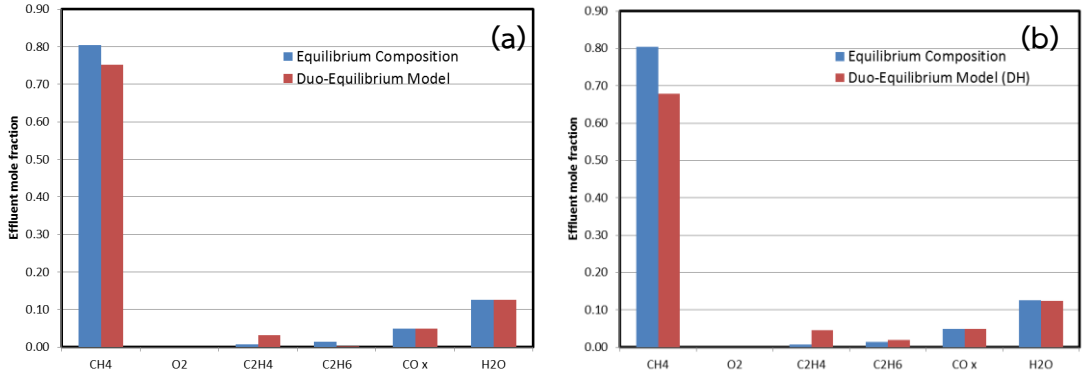

Fig 5.26 Comparison between simulation results from the duo-equilibrium reaction model A and B for PbO/Al_2O_3 (Conditions: T= 725°C and CH_4/O_2 = 8)
(a) model A (b) model B

From figure 5.24 to 5.26, using DH instead of ODH provided worse results for all catalysts. Despite ethane was formed in reactor, ethylene and hydrogen composition was too high as well as methane was over-consumed. This was attributed to the OCM reaction in the catalytic reactor. Instead of sharing O_2 for OCM and ODH, O_2 was consumed solely by OCM at which CH_4 was simultaneously spent out in such a high ratio. Moreover, production of C_2H_4 was exceed than C_2H_6 at 850°C because the DH reaction would slightly forward at the equilibrium constant exceed than 1. From this model, it could be concluded that the formation of ethylene in catalyst phase should be from by ODH reaction rather than DH.

5.2.3 Trio-equilibrium reaction model

This model was developed from the duo-equilibrium reaction model A which the catalytic part composed of OCM and ODH whilst the gas phase reactor composed of the combustion and water gas shift reaction. The simulation results were lack of C_2H_6 and a higher yield of C_2H_4. Therefore, the model was developed by adding a new calculation for adjusting the ethane yield by adding one more calculation just after the duo-equilibrium reaction model. The additional reactor was trial between two reactions, the results were detailed in next section.

5.2.3.1 Trio-equilibrium reaction model A

Since the results from the duo-equilibrium reaction model A showed much deviation from equilibrium composition. Amount of produced H_2 and C_2H_4 were too high (figure 5.24-5.26), which required the reduction by any consuming reaction. Then, the dehydrogenation reaction; $C_2H_6 \rightleftharpoons C_2H_4 + H_2$, was a choice for this objective. It was expected that the amount of H_2 form in gas phase would shifted dehydrogenation backward and ethane would form by reverse dehydrogenation. The scheme of the developed model was looked like the series connection between the duo-equilibrium reactions model connected to the DH reactor as shown in figure 5.27.

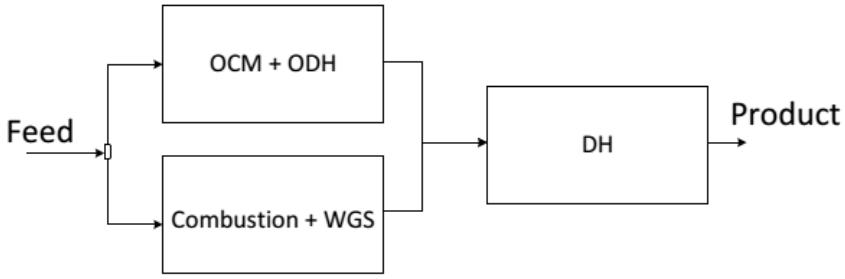

Fig 5.27 Scheme of Trio-equilibrium reaction model A

The comparison of simulation results between duo-equilibrium model and the trio-equilibrium reactors model were shown in figure 5.28 to 5.30 for the three catalysts.

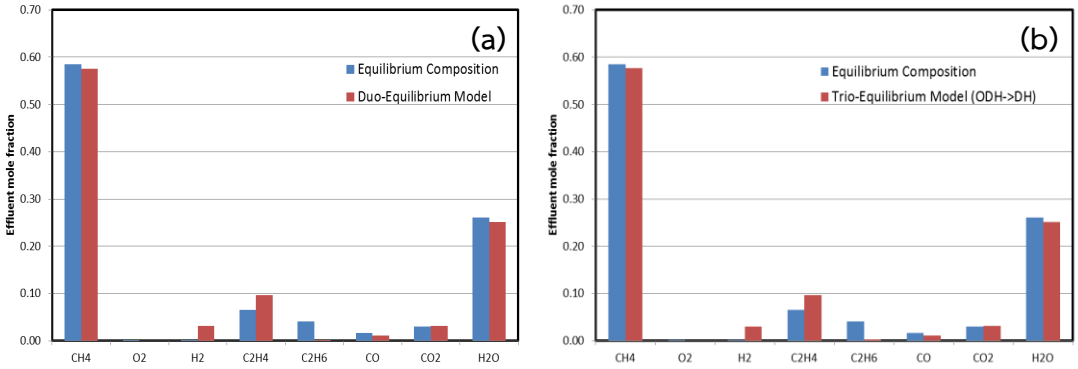

Fig 5.28 Comparison of results from the the duo-equilibrium reaction model A and the Trio-equilibrium reaction model A for $Mn/Na_2WO_4/SiO_2$ (Conditions: T = 850°C and CH_4/O_2 = 5)
(a) The duo-equilibrium reaction model A
(b) The Trio-equilibrium reaction model A

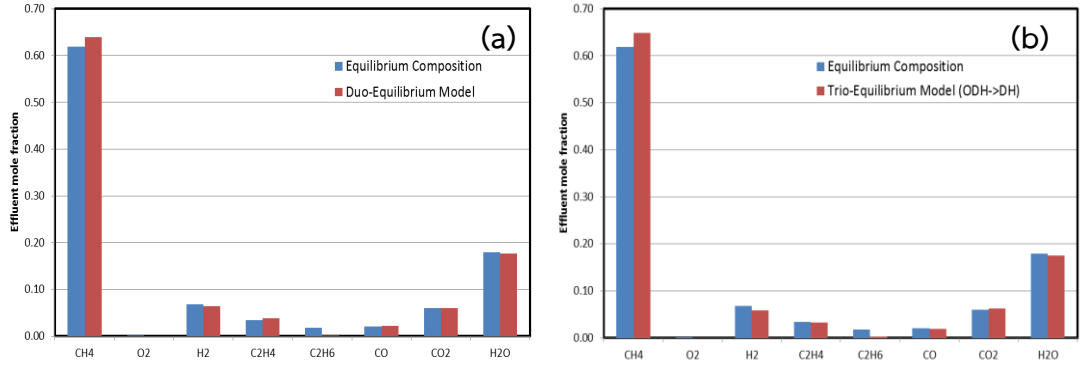

Fig 5.29 Comparison of results from the duo-equilibrium reaction model A and the Trio-equilibrium reaction model A for La_2O_3/CaO (Conditions: T = 825°C and CH_4/O_2 = 5)
(a) The duo-equilibrium reaction model A
(b) The Trio-equilibrium reaction model A

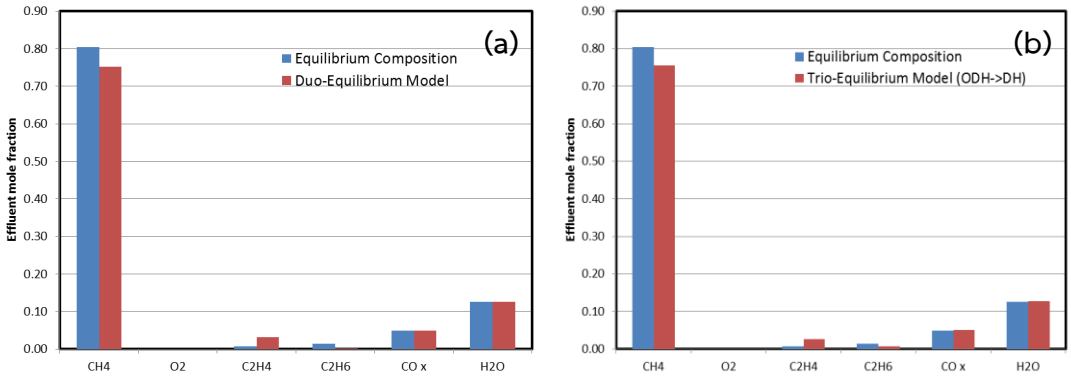

Fig 5.30 Comparison of results from the duo-equilibrium reaction model A and the Trio-equilibrium reaction model A for PbO/Al_2O_3
(Conditions: T = 750°C and CH_4/O_2 = 8)
(a) The duo-equilibrium reaction model A
(b) The Trio-equilibrium reaction model A

The results from figure 5.28 to 5.30 showed that the DH reaction at the end of simulation provided non-significantly changes of effluents. The results from both catalysts, $Mn/Na_2WO_4/SiO_2$ and La_2O_3/CaO (figure 5.28 and 5.29) showed very slightly backward of dehydrogenation reaction. The hydrogen concentration was slightly decreased while ethane was increased. However, with the PbO/Al_2O_3 catalyst the small increase of C_2H_6 was found. It should be reminded again that in PbO/Al_2O_3 literature, there was no report about H_2 components. Thus, only decreasing of ethylene and increasing of ethane were noticed. These changes were attributable to the reactor temperature used in the calculation. As mentioned above, the equilibrium constant of DH was lower than 1 at the temperature lower than 800°C. Therefore, the system of PbO/Al_2O_3 catalyst that the DH was calculated at 750°C could got the equilibrium with some backward reaction of DH which gave C_2H_6. However, overall considered from the results, this model was still be unsatisfied to explain the behavior of OCM.

5.2.3.2 Trio-equilibrium reaction model B

This model was also developed from the duo-equilibrium reaction model A which OCM and ODH were run at the catalytic part and the combustion with water gas shift reactions were competitive at the gas phase reactor. In this model the

output from the duo-equilibrium reaction model was calculated by the ethylene hydrocracking reaction; $C_2H_4 + H_2 \longrightarrow 2\ CH_4$. This reaction was expected to consume the excess of C_2H_4 and H_2 and compensated of CH_4. The ethylene hydrocracking was the combination reactions between ethane cracking (Eq.5.5) and reverse dehydrogenation of ethane (Eq. 5.6). The used of the combination reactions was due to no ethane exit in simulation system.

Reverse dehydrogenation of ethane: $C_2H_4 + H_2 \longrightarrow C_2H_6$ (5.5)

Ethane hydrocracking: $C_2H_6 + H_2 \longrightarrow 2\ CH_4$ (5.6)

Ethylene Hydrocracking reaction: $C_2H_4 + 2H_2 \longrightarrow 2\ CH_4$ (5.7)

The flow scheme of this model was depicted in figure 5.31.

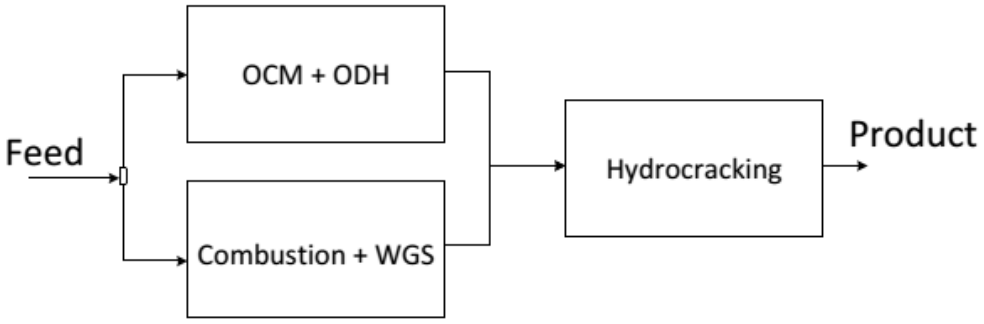

Fig 5.31 Scheme of Trio-equilibrium reaction model B

Afterward, simulations were run with the corresponding operating condition, the results of the trio-equilibrium reactors model were shown for $Mn/Na_2WO_4/SiO_2$, La_2O_3/CaO and PbO/Al_2O_3 catalyst in figure 5.32 to 5.34, respectively (in comparison with the duo-equilibrium reactors model).

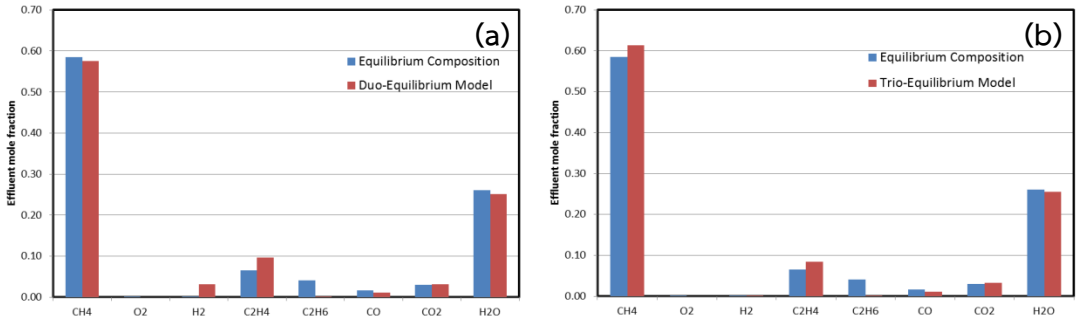

Fig 5.32 Comparison of results from the the duo-equilibrium reaction model A and the Trio-equilibrium reaction model B for $Mn/Na_2WO_4/SiO_2$ (Conditions: T = 850°C and CH_4/O_2 = 5)
(a) The duo-equilibrium reaction model A
(b) The Trio-equilibrium reaction model B

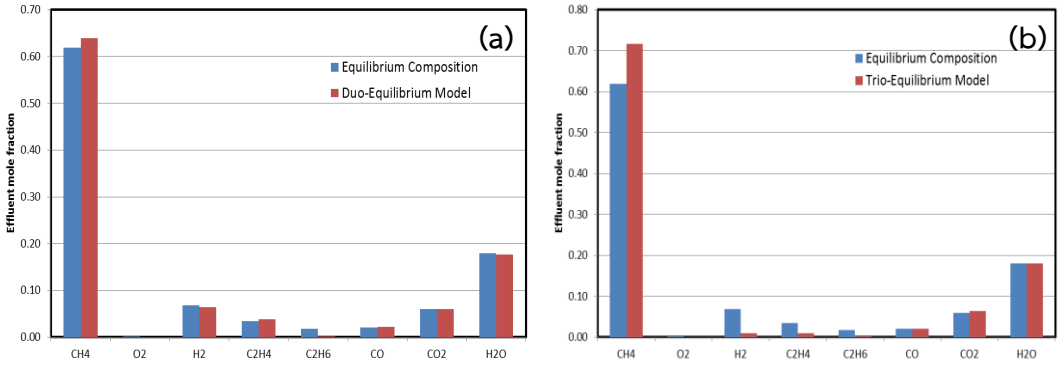

Fig 5.33 Comparison of results from the the duo-equilibrium reaction model A and the Trio-equilibrium reaction model B for La_2O_3/CaO (Conditions: T = 850°C and CH_4/O_2 = 5)
(a) The duo-equilibrium reaction model A
(b) The Trio-equilibrium reaction model B

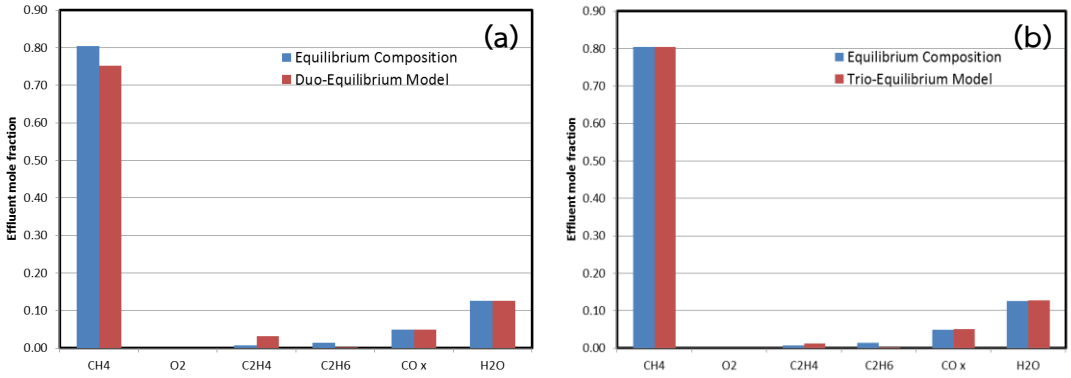

Fig 5.34 Comparison of results from the duo-equilibrium reaction model A and the Trio-equilibrium reaction model B for PbO/Al_2O_3 (Conditions: T = 750°C and CH_4/O_2 = 8) (a) The duo-equilibrium reaction model A (b) The Trio-equilibrium reaction model B

Figure 5.32–5.34, the calculation gave better results for both $Mn/Na_2WO_4/SiO_2$ and PbO/Al_2O_3 catalyst. As seen in figure 5.32, H_2 mole fraction from this model was nearly identical to the equilibrium composition. This indicated that the addition of hydrocracking reaction after the duo-equilibrium reaction model was appropriated for $Mn/Na_2WO_4/SiO_2$ and PbO/Al_2O_3 catalyst. However, C_2H_6 mole fraction in both catalysts were still nearly zero which required the manipulation further in section 5.3.

For La_2O_3/CaO catalyst, the addition of hydrocracking caused more deviation. Figure 5.33 showed the results that C_2H_4 as well as H_2 component were consumed and left at a small amount. Moreover, C_2H_6 mole fraction was still nearly zero. Thus, it could be concluded that the duo-equilibrium reaction model connecting with hydrocracking was the unsatisfactory model for La_2O_3/CaO catalyst.

These results conformed to type of catalyst used in OCM that The lanthanum element did not support with hydrocracking reaction to occur in system. Thus, it could be recapitulated that the appropriate reaction model was OCM and ODH in parallel with combustion and water-gas shift reaction while the hydrocracking reaction was required if there were element in catalyst that supported the reaction to react.

In conclusion, the development of the proposed model got better and better results from the uni-equilibrium reaction model through the Trio-equilibrium reaction

model. The best fit model was selective to the catalyst types, i.e. the trio-equilibrium reaction model B was suit to both $Mn/Na_2WO_4/SiO_2$ and PbO/Al_2O_3 catalysts while the duo-equilibrium reaction model A was the best for La_2O_3/CaO catalyst. However, the persistence problem was the too small amount of C_2H_6 components. Neither the DH reaction nor the hydrocracking reaction could not use to adjust the fraction of C_2H_6 at the equilibrium. Thus, this research proposed the methodology to manipulate equilibrium model by adding the parameter into the model. This parameter was acquired from experiment data.

5.3 Model manipulation

Before the explanation of the manipulation of model, the discussion on C_2H_6 component must be clearified for understanding the role of C_2H_6 in OCM reaction.

5.3.1 Discussion on the role of C_2H_6 in OCM

In simulation process, C_2H_6 was the product of the oxidative coupling reaction (OCM); $2CH_4 + 0.5O_2 \longrightarrow C_2H_6 + H_2O$. Produced C_2H_6 was then consumed by the oxidative dehydrogenation reaction (ODH); $C_2H_6 + 0.5O_2 \longrightarrow C_2H_4 + H_2O$ as shown in figure 5.35.

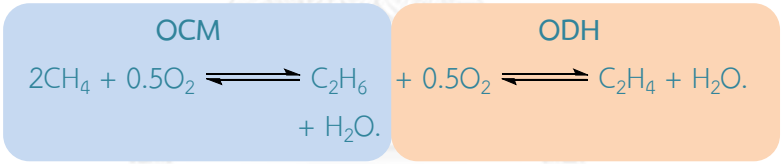

Fig 5.35 Scheme of ethane formation and consumption

At the equilibrium, all components must be in equilibrium and left in the reactor. The absence of C_2H_6 in the calculation under the equilibrium concept might be explained as followed. The pathway of the C_2H_4 production was formed via two elementary reactions OCM and ODH as followed.

OCM: $2CH_4 + 0.5O_2 \rightleftharpoons C_2H_6 + H_2O.$ K_1

ODH: $C_2H_6 + 0.5O_2 \rightleftharpoons C_2H_4 + H_2O.$ K_2

Overall reaction: $2CH_4 + O_2 \rightleftharpoons C_2H_4 + 2H_2O.$ $K_{overall} = K_1.K_2$

Because C_2H_6 functioned as the intermediate in the process, theoretically of chemical equilibrium, intermediate would not exist in the final products because the reactions were already combined to form the overall reaction. The calculation of products at equilibrium could be done with the overall reaction. Simulations in this pathway led to the nearly zero of C_2H_6 at the end.

In fact, C_2H_6 should still remain with a substantial amount to maintain the the production of C_2H_4 via oxidative dehydrogenation reaction. This concept was respected to the method calculating the amount of intermediate at steady state which published elsewhere. [70]

There were many reports for ethane yield of OCM which was summarized in table 5.5 for variety of catalysts. Moreover, there was an interested issue that yield of ethane were almost constant with small standard deviation at any range of operating condition (i.e. temperature and CH_4/O_2 feed ratio).

Table 5.5 Yield of ethane for each catalyst [10, 11, 71-74]

Catalyst	Temperature (°C)	CH_4/O_2	Average ethane yield (%mole)	Standard deviation
$Mn/Na_2WO_4/SiO_2$	775-875	4-10	9.07	0.41
La_2O_3/CaO	750-875	5-10	4.16	0.60
PbO/Al_2O_3	700-750	5-10	3.22	0.62
La/MgO	750-850	4	7.75	0.48
Li/MgO	700-820	4	4.14	0.54
Sn-Ba-TiO_3	725-775	2-4.5	5.32	0.60

As the fraction of C_2H_6 must remain in the system, thus, it was possible to specify yield of ethane to be constant. The value was specified as published in the literatures. They were 9.07, 4.16 and 3.22 % mole for $Mn/Na_2WO_4/SiO_2$, La_2O_3/CaO and PbO/Al_2O_3 catalyst, respectively.

5.3.2 Manipulation of Duo-equilibrium reaction model

As mention in previous section, the existence of intermediate of the chemical reaction was accepted and the chemical equilibrium concept could not describe the

intermediate behavior because the combination reaction did not suggest the existence of intermediate. In this section, the manipulation for running the program was described and verified the results.

Up to this section, the best fit model of the simulation for $Mn/Na_2WO_4/SiO_2$ and PbO/Al_2O_3 was the Trio-equilibrium reaction model type B which was the connection between the parallel set of OCM/ODH and combustion/WGS series with the hydrocracking reaction. The model shown best fit for La_2O_3/CaO was the duo-equilibrium reaction model which was the set of parallel between OCM/ODH and combustion/WGS

With respect to the C_2H_6 yield found in the experimental research [10, 11, 71-74], the first manipulation for upgrading the results was decided to appoint the C_2H_6 constant molar extension at the equilibration. The constant molar of C_2H_6 was taken from the average ethane yield listed in table 5.5.

One more manipulation was a change of input in catalytic reactor.

OCM : $2CH_4 + 0.5O_2 \longrightarrow C_2H_6 + H_2O$ (5.6)

ODH : $C_2H_6 + 0.5O_2 \longrightarrow C_2H_4 + H_2O$ (5.7)

Overall reaction : $2CH_4 + O_2 \longrightarrow C_2H_4 + H_2O$ (5.8)

Instead of inputting the OCM and ODH in the catalytic reactor, the ODH was substituted with the overall reaction (equation 5.8).

Then, two important points for manipulating the model was (1) fix the extension molar of C_2H_6 equal to specific yield (2) substitute the ODH reaction in the catalytic reactor with the overall reaction of OCM. The comparison results between the duo-equilibrium reaction model with/ without the specific ethane yield for La_2O_3/CaO was shown in figure 5.36.

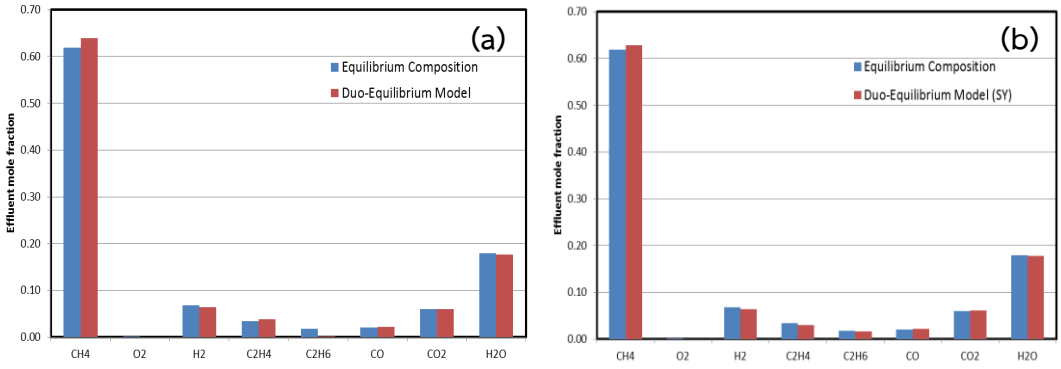

Fig 5.36 Comparison of results from the duo-equilibrium reaction model with/without specific ethane yield for La_2O_3/CaO catalyst

(Conditions: T = 825°C and CH_4/O_2 = 5)

(a) The duo-equilibrium reaction model A

(b) The duo-equilibrium reaction model A with specified ethane yield at 4.16

From figure 5.36, it is clearly shown that after the manipulation, the prediction results from the duo-equilibrium reaction model showed almost identical to the expected results. Thus, this model was appropriate for the OCM for La_2O_3/CaO catalyst.

The comparison of results from the duo-equilibrium reaction model with/without specific ethane yield for $Mn/Na_2WO_4/SiO_2$ and PbO/Al_2O_3 catalyst were shown in figure 5.37 and 5.38, respectively.

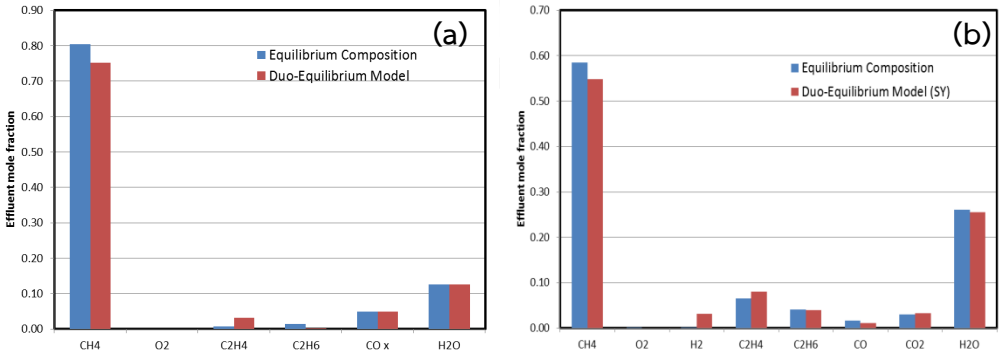

Fig 5.37 Comparison of results from the duo-equilibrium reaction model with/without specific ethane yield for $Mn/Na_2WO_4/SiO_2$ catalyst

(Conditions: T = 850°C and CH_4/O_2 = 5)

(a) The duo-equilibrium reaction model A

(b) The duo-equilibrium reaction model A with specified ethane yield at 9.07

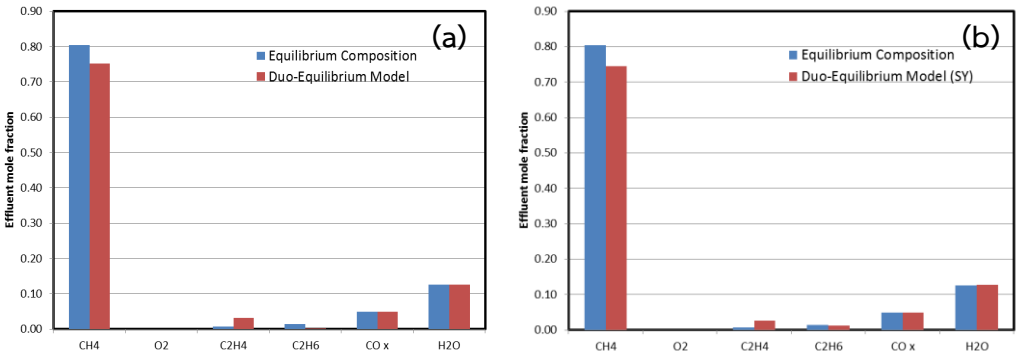

Fig 5.38 Comparison of results from the duo-equilibrium reaction model with/without specific ethane yield for PbO/Al_2O_3 catalyst
(Conditions: T = 750°C and CH_4/O_2 = 8)
(a) The duo-equilibrium reaction model A
(b) The duo-equilibrium reaction model A with specified ethane yield at 3.22

From figure 5.37 and 5.38, the manipulated duo-equilibrium reaction model could provide better outcome of effluents for $Mn/Na_2WO_4/SiO_2$ and PbO/Al_2O_3. The C_2H_6 components were closed to equilibrium composition. However, there were still deviation of H_2 and C_2H_4. Hence, the manipulation technique used in duo-equilibrium reactors model did not suit for $Mn/Na_2WO_4/SiO_2$ and PbO/Al_2O_3. More tests were tried with the trio-equilibrium reactions model.

5.3.3 Manipulation of Trio-equilibrium reaction model

This model was developed from the trio-equilibrium reaction model B mentioned in section 5.2.3.2. This model gave good result for $Mn/Na_2WO_4/SiO_2$ and PbO/Al_2O_3. After the model was manipulated as mentioned above, the simulations were tested and the results were shown in figure 5.39 for $Mn/Na_2WO_4/SiO_2$ catalyst and figure 5.40 for PbO/Al_2O_3.

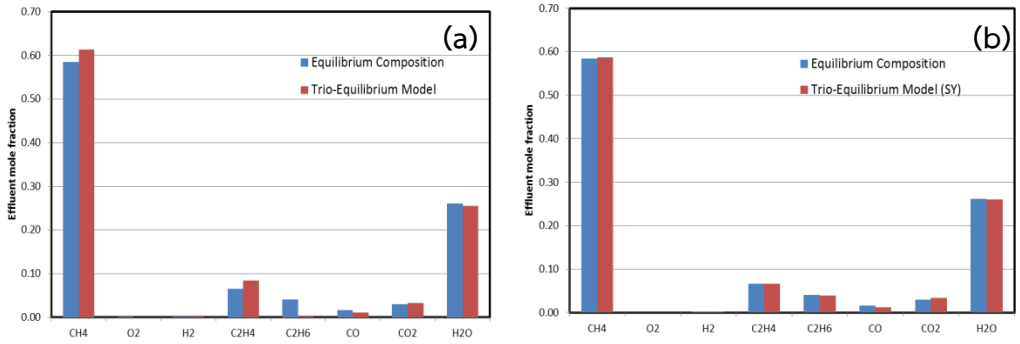

Fig 5.39 Comparison of results from the Trio-equilibrium reaction model with/without specific ethane yield for $Mn/Na_2WO_4/SiO_2$ catalyst (Conditions: T = 850°C and CH_4/O_2 = 5)

(a) The Trio-equilibrium reaction model B

(b) The Trio-equilibrium reaction model B with specified ethane yield at 9.07

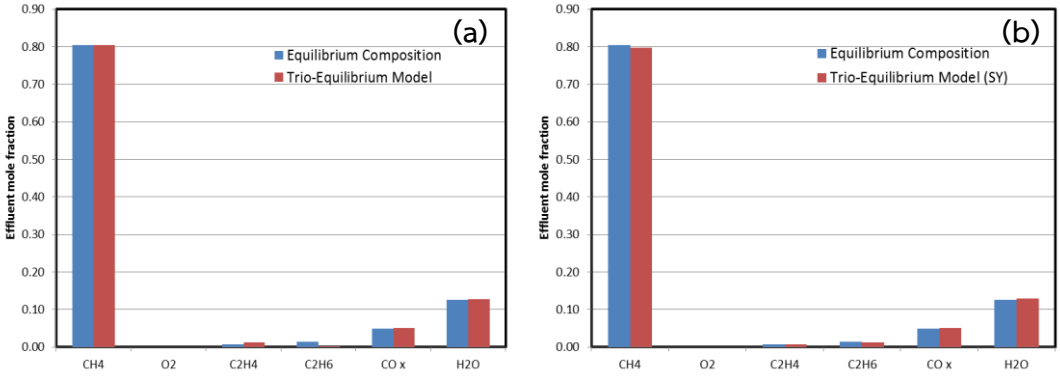

Fig 5.40 Comparison of results from the Trio-equilibrium reaction model with/without specific ethane yield for PbO/Al_2O_3 catalyst (Conditions: T = 725°C and CH_4/O_2 = 8)

(a) The Trio-equilibrium reaction model B

(b) The Trio-equilibrium reaction model B with specified ethane yield at 3.22

Figure 5.39 showed the comparison results of the trio-equilibrium reaction model with/without specific ethane yield for $Mn/Na_2WO_4/SiO_2$ catalyst and figure 5.40 was for PbO/Al_2O_3. The results from the manipulating techniques were shown that both simulations for $Mn/Na_2WO_4/SiO_2$ and PbO/Al_2O_3 were best fit. Concentrations of all components were matched to the expected results. The deviations of H_2, C_2H_6 as well as CH_4 from the previous trio-equilibrium model were diminished with the manipulation technique. It could be concluded that the suitable model for both

$Mn/Na_2WO_4/SiO_2$ and PbO/Al_2O_3 catalyst was the trio-equilibrium reaction model with specific ethane yield.

For La_2O_3/CaO catalyst, simulation in the trio equilibrium model manipulated with specific yield of ethane was tested. The results showed in figure 5.41 were different from that of the previous two catalysts.

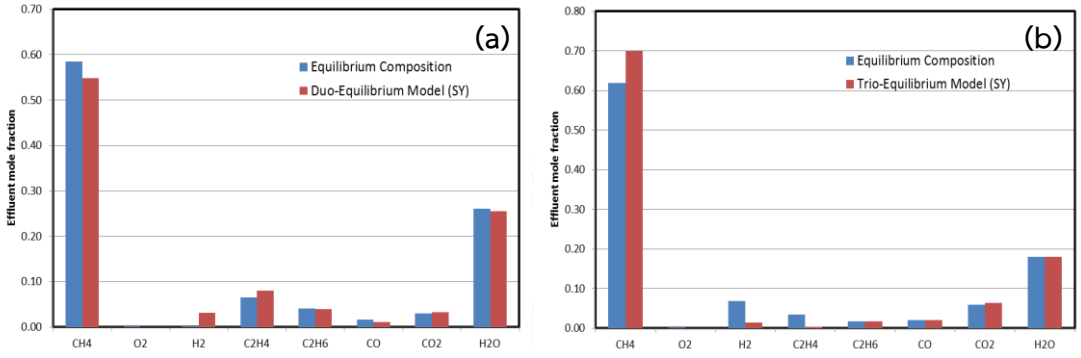

Fig 5.41 Comparison of results from the duo-equilibrium and Trio-equilibrium reaction model with specific ethane yield for La_2O_3/CaO catalyst
(Conditions: T = 825°C and CH_4/O_2 = 5)
(a) The duo-equilibrium reaction model with specific yield at 4.16
(b) The trio-equilibrium reaction model with specified ethane yield at 4.16

From the figure 5.41, hydrogen, ethylene and some other components fractions were deviated more than the previous model which was suggesting the unsatisfactory model for the La_2O_3/CaO catalyst. However from section 5.3.2, the simulation from the duo-equilibrium reaction model with specific ethane yield gave the best fit. Therefore, the model of the most appropriate for La_2O_3/CaO catalyst was the duo-equilibrium reaction model with specific ethane yield model.

In summary, the best fit equilibrium model gave better results by specification of ethane yield. By manipulating the duo-equilibrium model A, methane component as well as ethylene and ethane were reasonably matched with equilibrium composition. Then, for the La_2O_3/CaO catalyst, the best model was the duo-equilibrium model where the catalytic reaction were composed with OCM and ODH while the das phase reactor were composed of the combustion and the water gas shift reactions. For the catalysts of $Mn/Na_2WO_4/SiO_2$ and PbO/Al_2O_3, the best fit was the trio-equilibrium reactors model with hydrocracking reaction.

Moreover, these manipulation models could fit the equilibrium composition at various temperature and methane to oxygen feed ratio. The validation was then described in next section.

5.3.4 Verification and Validation of Manipulation Model

In this section, the verification and validations of the best fit models were accessed. The best fit developed models were simulated with the operating condition similar to equilibrium composition of the same catalyst. For $Mn/Na_2WO_4/SiO_2$ and PbO/Al_2O_3, the temperature range of 700 – 875 $^{\circ}C$ and feed CH_4/O_2 of 3 – 10. The temperature of 650 – 750 $^{\circ}C$ and feed CH_4/O_2 of 5 – 10 were for the PbO/Al_2O_3 catalyst.

Plots for effluent fractions at the six temperatures with respect to the feed ratio of CH_4/O_2 were shown in figure 5.42 – 5.44. It should be mentioned here that results from other temperatures were not plotted.

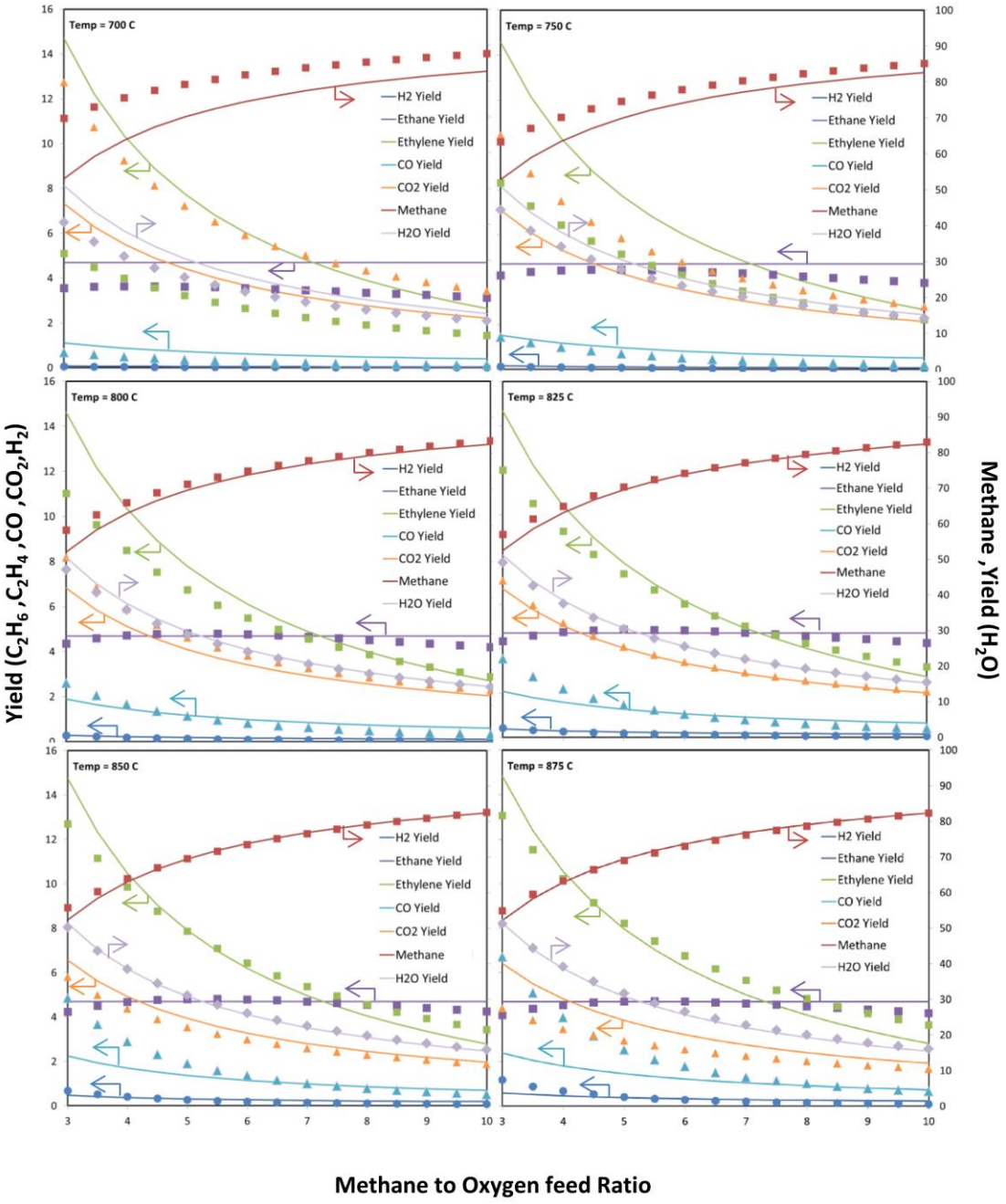

Fig 5.42 Simulation results from the best fit developed model (line) and the equilibrium composition (dots) for $Mn/Na_2WO_4/SiO_2$ catalyst

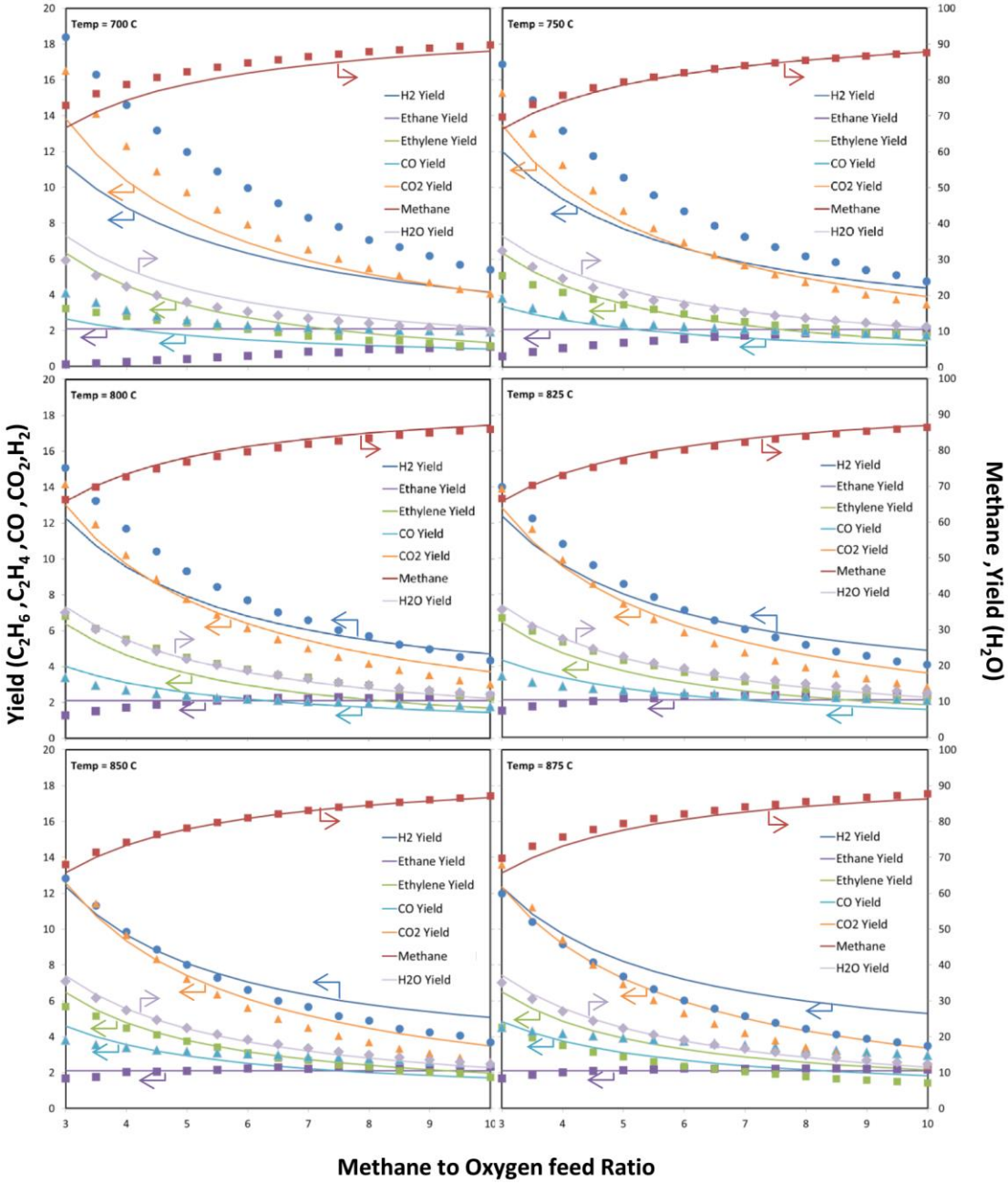

Fig 5.43 Simulation results from the best fit developed model (line) and the equilibrium composition (dots) for La_2O_3/CaO catalyst

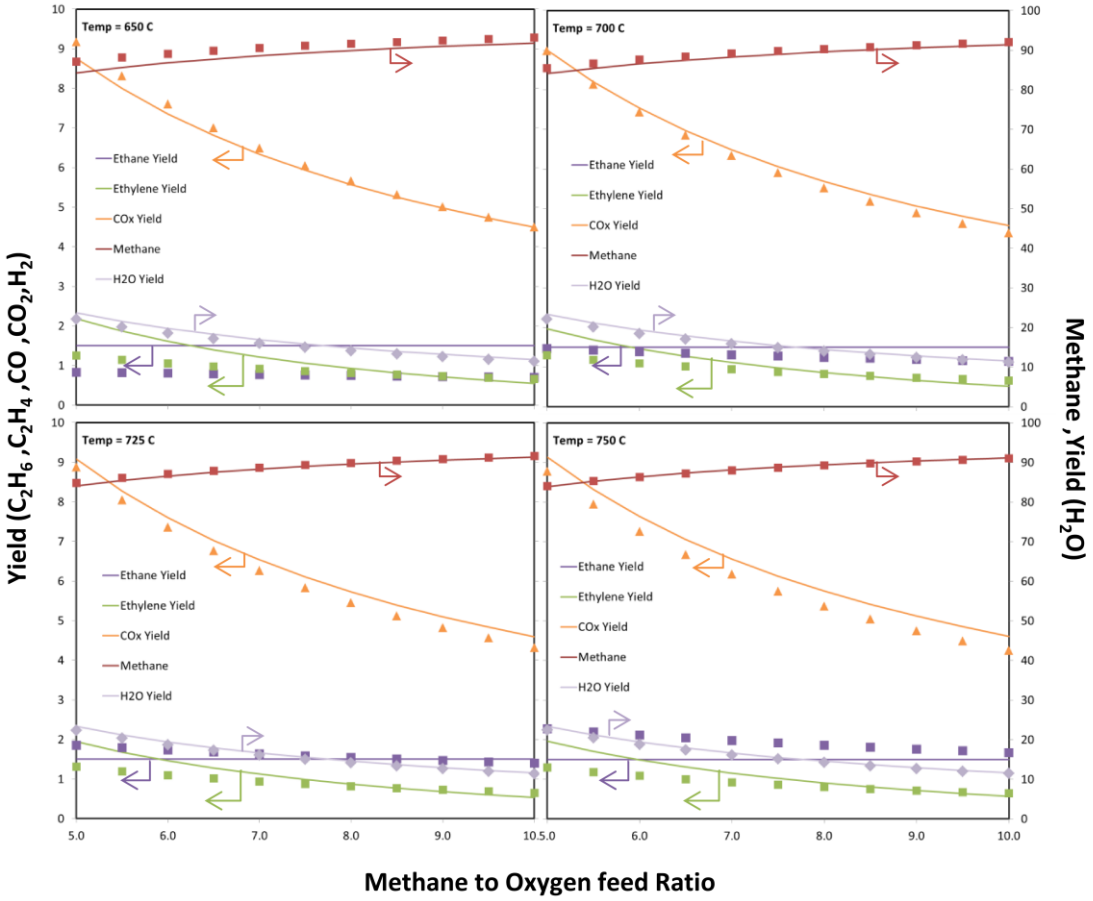

Fig 5.44 Simulation results from the best fit developed model (line) and the equilibrium composition (dots) for PbO/Al_2O_3 catalyst

From figure 5.42–5.44 showed the simulation results from the best fit developed model (line) and the equilibrium composition (dots) for three catalysts. All components showed the good agreement of simulation data between dot and line of the same color. The model showed the accurately predict the variation of methane to oxygen feed ratio with small deviation. However, It should be noticed that the accuracy of the model were depended on temperature. The higher the temperature, the closer the prediction of results.

In conclusion, the manipulated models could predict the OCM reaction at various operating conditions. The validity range of the models would be discussed further in section 5.4.2.2.

5.4 Verification of models

5.4.1 Verification of models using statistics RSS

In this chapter, the statistic of RSS was used to verify the precision of simulation. The verification was done by running the OCM reaction in the suitable developed models with the condition similar to that of literatures. The RSS of the differences between data from developed model and the reference data were calculated. Table 5.6 summarized the RSS value of studied model for all three catalysts. Because the tight fit of the model to the data was suggested with the small value of RSS, then models with best fit for a catalyst were labeled with superscript of alphabet "A" for normal equilibrium models and "B" for manipulated models.

Table 5.6 RSS of the developed models for three catalysts

Model	RSS		
	$Mn/Na_2WO_4/SiO_2$	La_2O_3/CaO	PbO/Al_2O_3
Equilibrium Models			
Uni-equilibrium reaction model	171.10	124.75	8.84
Uni-equilibrium reaction model with 10 literature reactions	171.69	125.47	5.01
Uni-equilibrium reaction model with selected reactions	8.34	4.23	3.80
Duo-equilibrium reaction model with oxidative dehydrogenation	1.24	0.95^{A}	12.04
Duo-equilibrium reaction model with dehydrogenation	4.79	3.31	32.90
Trio-equilibrium reaction model with oxidative dehydrogenation and dehydrogenation	4.17	3.71	14.67
Trio-equilibrium reaction model with hydrocracking	1.09^{A}	2.23	1.50^{A}
Manipulated Equilibrium Models			
Manipulated Duo-equilibrium reaction model with ethane yield specifying	0.14	0.03^{B}	6.67
Manipulated Trio-equilibrium reaction model with ethane yield specifying	0.09^{B}	1.46	0.01^{B}

[a] Best fit model for equilibrium model

[B] Best fit model for manipulated model

As seen in the table 5.6, the best models over PbO/Al_2O_3 and $Mn/Na_2WO_4/SiO_2$ were the trio-equilibrium reaction model. While the OCM reaction over the catalyst of La_2O_3/CaO was used to predict well with the duo-equilibrium reaction model. Thus, it could be concluded that the base reactions in OCM system were the same pattern in any types of catalysts. The catalytic reactions were OCM and ODH while gas phase reactions were combustion and water-gas shift (WGS). However, the difference between types of catalysts depended on the composition of the catalyst. The catalysts which contained element that supported hydrocracking reaction, such as Pb and W, were selective to hydrocracking reaction in OCM as well.

However, the equilibrium model could not predict the ethane composition correctly. Thus, this research proposed the manipulation for equilibrium model by specifying ethane yield at constant. The specified ethane yield was counted as one parameter of manipulated model which required experiment. The results for manipulated models gave the better results comparing to normal equilibrium models. Table 5.7 showed the conclusion of catalysts properties and the best model for predicting the behavior of OCM reaction including its parameters.

Table 5.7 Catalyst properties and its appropriate proposed models

Category	**Catalyst**		
	$Mn/Na_2WO_4/SiO_2$	La_2O_3/CaO	PbO/Al_2O_3
Type of catalyst	Transition	Rare Earth Metal	Post-Transition
Void fraction	0.4	0.78	0.7
Catalyst Density (kg/m^3)	1100	3600	2000
Best fit Model	Trio-equilibrium reaction model	Duo-equilibrium reaction model	Trio-equilibrium reaction model
Number of Reactions	5	4	5
Catalytic Reactions	OCM,ODH	OCM,ODH	OCM,ODH
Gas Phase Reactions	Combustion, WGS	Combustion, WGS	Combustion, WGS
Post Gas Phase Reactions	Hydrocracking	-	Hydrocracking
Manipulating Parameters			
Specific ethane yield	9.07	4.16	3.22

5.4.2 Validation of the developed models by reactor performance

In this section, the precision of the models were determined by comparing results with reactor performances reported from literatures. Reactor performances to be compared in this section were methane conversion (X_{CH4}), ethane selectivity (S_{C2H6}), ethylene selectivity (S_{C2H4}), ethane yield (Y_{C2H6}) and ethylene yield (Y_{C2H4}). The definitions of these variables were expressed in section 4.4.

5.4.2.1 Validation by comparing with laboratory experiment

The trio-equilibrium reaction model was run with/without the specific ethane yield over $Mn/Na_2WO_4/SiO_2$ catalyst with the conditions used in Daneshpayeh et al [9]. Methane conversion and C_2 selectivity from both trials were calculated and compared to the reactor performances reported from laboratory experimental results. The simulations were tested at both 800°C and 850°C for confirmation of results. The results were shown in figure 5.45 (a) and (b), respectively.

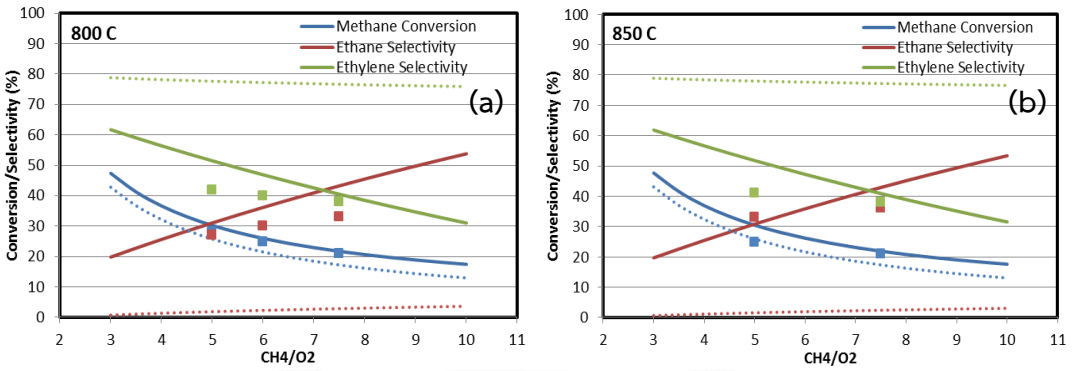

Fig 5.45 The performance plots with respect to feed ratio (CH_4/O_2) for $Mn/Na_2WO_4/SiO_2$ catalyst (a) 800°C (b) 850°C

(Dot) experimental results

(Dash) the trio-equilibrium reaction model

(Solid) the manipulated trio-equilibrium model

From figure 5.45, the reactor performances to be compared were methane conversion (Blue), ethane selectivity (Red) and ethylene selectivity (Green). In figure 5.45 (a), it was clearly shown all performance calculated from the trio-equilibrium reaction model with specific ethane yield (solid line) were close to that of the experimental results (dots). While the calculations from the trio-equilibrium reaction

model without specific ethane yield (dash line) showed quite far from the expected results (dots). The same results for all performances were shown at 850°C of simulation test (figure 5.45 (b)). Thus, the equilibrium reaction model without manipulation could not accurately predict the outcome of OCM reaction.

Take a closer look to the trio-equilibrium reaction model which was manipulated by specifying the ethane yield, it could be a promising tool for predicting reactor performances at a variety of temperature and methane feed ratio. However, it should be noticed that methane conversion of the models were fit to the experiment but C_2 selectivity were lower than the expected results. This indicated that there was another reaction that converted methane into others component which didn't reported in any literatures. The reaction was supposed to be the decomposition of methane which converted methane into carbon and hydrogen (Eq. 5.9). This reaction was the side reaction occurred at high temperature and caused the formation of coke [75].

$$CH_4 \longrightarrow C + 2H_2 \qquad (5.9)$$

It was believed that this side reaction brought about the deviation occurring for both kinetic model and the equilibrium model. Since, the product of this reaction was solid of coke, it could not be put as the available reaction in the simulation program. However, the percentage error caused by this side reaction was in the acceptable range which could be ignored.

For La_2O_3/CaO catalyst, the duo-equilibrium reaction model was used for simulation. Conditions were imitated from Stransch et al [8]. The results compared with that from the experiments were expressed in figure 5.46

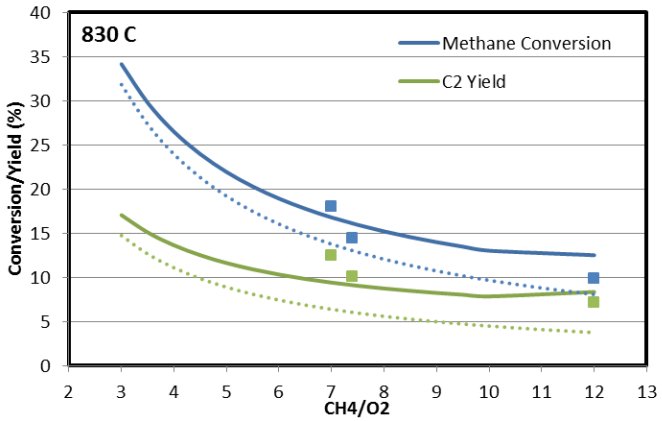

Fig 5.46 The performance plots with respect to feed ratio (CH_4/O_2) for La_2O_3/CaO catalyst at 830° C

(Dot) experimental results

(Dash) the trio-equilibrium reaction model

(Solid) the manipulated trio-equilibrium model

The reported reactor performances over La_2O_3/CaO catalyst of Stransch et al [8] were methane conversion and yield of C_2 hydrocarbon. The blue line showed methane conversion of model which was considerable close to experiment. The green line showed yield of C_2 which acceptable deviate from experiment. Thus, the manipulated duo-equilibrium reaction model could predict the results that fit with the experiment. It should be notice that the dash line of equilibrium model without manipulation showed the same trend as the experimental results but with large deviation. Thus, without manipulation, the duo-equilibrium reaction model could roughly predict the outcome of OCM for ethane and ethylene components.

In summary, the equilibrium model without manipulation could roughly predict reactor performance while the manipulation of the model could predict with better accuracy. However, the model had some limitation in prediction of decomposition reaction which did not including in calculation system.

5.4.2.2 Validity region of developed model at variety of operating conditions

The comparisons of reactor performance calculated from best manipulated model and equilibrium composition at various operating conditions were shown in this section. It was aimed to find the validity region based on the performance of OCM process within 20% deviation. The interest performances were methane

conversion, selectivity of ethane and selectivity of ethylene. The studied operating conditions for $Mn/Na_2WO_4/SiO_2$ and La_2O_3/CaO were at temperature 700-925°C and methane to oxygen feed ratio 3-12 while PbO/Al_2O_3 was at 650-850°C and feed ratio 5-16.

The validity region was determined using the AARD. The validity of the developed model was strong accepted at the 15% lower of AARD and accepted under the considerable at 20% lower of AARD.

The best fit developed models were written again below; the trio equilibrium model with specific ethane yield for $Mn/Na_2WO_4/SiO_2$ and PbO/Al_2O_3, the duo-equilibrium reaction model with specific ethane yield for La_2O_3/CaO catalyst

Table 5.8 indicated operating conditions of $Mn/Na_2WO_4/SiO_2$ catalyst which provided the AARD lower than 10% (+), AARD between 10-15% (•), AARD between 15 – 20% (o) and AARD more than 20% (x).

Table 5.8 AARD with respect to CH_4/O_2 feed ratios at variety of reaction temperatures for $Mn/Na_2WO_4/SiO_2$.

CH_4/O_2 Feed Ratio	Temperature ($^{\circ}$C)									
	700	725	750	775	800	825	850	875	900	925
3	X	X	X	X	O	•	+	+	X	X
3.5	X	X	X	O	•	+	+	+	X	X
4	X	X	X	O	•	+	+	+	X	X
4.5	X	X	X	O	+	+	+	+	X	X
5	X	X	X	•	+	+	+	+	X	X
5.5	X	X	O	•	+	+	+	+	X	X
6	X	X	O	•	+	+	+	+	X	X
6.5	X	X	O	+	+	+	+	+	X	X
7	X	X	O	+	+	+	+	+	X	X
7.5	X	X	•	+	+	+	+	+	X	X
8	X	X	•	+	+	+	+	+	X	X
8.5	X	X	•	+	+	+	+	+	X	X
9	X	X	•	+	+	+	+	+	X	X
9.5	X	X	•	+	+	+	+	+	X	X
10	X	X	•	+	+	+	+	+	X	X
11	X	X	X	X	X	X	X	X	X	X
12	X	X	X	X	X	X	X	X	X	X

+ AARD less than 10% • AARD between 10-15% O AARD between 15-20% X AARD more than 20%

As seen in the table, the operating conditions which the manipulated trio-equilibrium reaction model could predict effluence of $Mn/Na_2WO_4/SiO_2$ catalyst with the AARD less than 15% were at temperature 775-875°C and methane to oxygen feed ratio were 4-10. It should be noticed that at higher temperature than 875°C or methane to oxygen ratio more than 10, all of the AARD values were excess than 20%. The deviations were caused by the reference value that simulated from kinetic were deviated. The kinetic model of Daneshpayeh et al [9] was confirmed their accuracy only at temperature 700-875°C and methane to oxygen feed ratio 3-10.

With respect to AARD calculation, for La_2O_3 catalyst, the accuracy of the developed model at the variety of temperature and feed ratio of CH_4/O_2 were shown in table 5.9.

Table 5.9 AARD with respect to CH_4/O_2 feed ratios at variety of reaction temperatures for La_2O_3/CaO.

CH_4/O_2 Feed Ratio	Temperature (°C)									
	700	725	750	775	800	825	850	875	900	925
3	X	X	X	X	O	•	•	X	X	X
3.5	X	X	X	X	•	+	+	O	X	X
4	X	X	X	O	•	+	+	O	X	X
4.5	X	X	X	•	•	+	+	O	X	X
5	X	X	O	•	•	+	+	O	X	X
5.5	X	X	O	•	•	+	+	O	X	X
6	X	X	•	+	•	+	+	O	X	X
6.5	X	X	+	•	•	+	+	O	X	X
7	X	X	+	+	•	+	+	O	X	X
7.5	X	X	+	•	•	+	+	O	X	X
8	X	X	+	•	•	+	+	O	X	X
8.5	X	X	+	•	•	+	+	O	X	X
9	X	X	+	+	•	+	+	O	X	X
9.5	X	•	+	•	•	+	+	O	X	X
10	X	O	+	•	•	+	+	O	X	X
11	X	X	X	X	X	X	X	X	X	X
12	X	X	X	X	X	X	X	X	X	X

+ AARD less than 10% • AARD between 10-15% O AARD between 15-20% X AARD more than 20%

As seen in the table, the operating conditions which the manipulated duo-equilibrium reaction model could predict effluence of La_2O_3/CaO with the AARD less than 15% was at temperature 750-850°C and methane to oxygen feed ratio were 5-

10. Again, the values of AARD for temperature more than 875°C or methane to oxygen feed ratio more than 10 were deviated more than 20%. It was also caused by deviation of kinetic model which simulated out of literature ranges.

PbO/Al_2O_3 could be predicted by the trio equilibrium model with specifying the ethane yield. Table 5.10 indicated operating condition which had AARD lower than 15%.

Table 5.10 AARD with respect to CH_4/O_2 feed ratios at variety of reaction temperatures for PbO/Al_2O_3.

CH_4/O_2 Feed Ratio	Temperature (°C)								
	650	675	700	725	750	775	800	825	850
5	X	X	O	O	X	X	X	X	X
5.5	X	X	O	O	X	X	X	X	X
6	X	X	•	•	O	X	X	X	X
6.5	X	X	•	•	O	X	X	X	X
7	X	X	+	+	•	X	X	X	X
7.5	X	X	+	+	•	X	X	X	X
8	X	X	+	+	•	X	X	X	X
8.5	X	X	•	+	+	O	X	X	X
9	X	X	•	+	+	O	X	X	X
9.5	X	X	O	+	+	•	X	X	X
10	X	X	O	+	+	•	X	X	X
11	X	X	X	•	+	•	O	X	X
12	X	X	X	•	•	•	•	X	X
14	X	X	X	X	O	O	O	O	X
16	X	X	X	X	X	O	X	O	O

+ AARD less than 10% • AARD between 10-15% O AARD between 15-20% X AARD more than 20%

As seen in the table, the operating conditions which the manipulated trio-equilibrium reaction model could predict outcome of PbO/Al_2O_3 with the AARD less than 15% was at temperature 700-750°C and methane to oxygen feed ratio were 6-10. This type of catalyst also reported AARD value over than 20% at temperature more than 750°C or methane to oxygen feed ratio more than 10. It was corresponding to reference data which simulated by kinetic simulation were out of range suggested by literature.

In summary, each model had its individual accuracy range. Table 5.11 concluded ranges of operations for each model and catalyst. It should be noticed that, for all models, the best conditions were at high temperature.

Table 5.11 The validity for the developed equilibrium model.

Catalyst	$Mn/Na_2WO_4/SiO_2$	La_2O_3/CaO	PbO/Al_2O_3
Pressure (atm)	1	1	1
Temperature (^{o}C)	775-875	750-850	700-750
CH_4/O_2 mole ratio	4-10	5-10	6-10

5.5 The advantage of the proposed model

According to the results explained previously, this research succeeded to construct and develop the competitive model for predicting the OCM reaction. The models were able to predict the components composition and performances correctly. The models were proposed with confidence to be an alternative tool for predicting the outcomes as required. This section described the advantages of the proposed models which were two categories, the ease in prediction and extrapolated prediction.

5.5.1 Ease in prediction

The comparison of some utility responses was summarized in table 5.12.

Table 5.12 Comparison between kinetic model and the proposed model.

Topic	Kinetic Model	Equilibrium Model
Number of Parameters	a lot	small
Accuracy	High	Moderate
Limitation	within regression range of experiments	only at the equilibrium
Iteration time	fast	Very fast
Data required for Construction	a lot of data from experiment	A few data from experiment
Reactor Design Availability	Yes	No

As kinetic model was developed from regression of the experiment data into rate law equations, a lot of experiment data were required to construct the model. The accuracy of the kinetic model within the range of regression was high.

For the equilibrium model, it was developed from theory with some manipulations which required only a few data to determine the parameters. The calculation procedure for equilibrium was simple. Nevertheless, equilibrium model had the limitation to predict only at equilibrium time while kinetic model could predict the effluence as a function of time and able to use for reactor design.

Table 5.13 summarized the comparison of parameters of both models, kinetic model and equilibrium model (EB) for three catalyst. It was obviously seen that equilibrium model have lower parameters than that of kinetic model with average error slightly more than kinetic model but still less than 20%. Thus, the use of equilibrium model was more convenient because it required less parameter than kinetic model with the same level of accuracy.

Table 5.13 Parameters comparison between kinetic and equilibrium model

Catalyst	$Mn/Na_2WO_4/SiO_2$		La_2O_3/CaO		PbO/Al_2O_3	
	Kinetic	EB	Kinetic	EB	Kinetic	EB
Number of Reactions	10	5	10	4	4	5
Number of Parameters	42	2	54	2	16	2
Number of reactors	1	3	1	2	1	3
AARD (%)	9.15	9.74*	14	15.56*	-	15.17*

*Range of operating conditions in table 5.11

In conclusion, the ease of use was the advantage of the proposed equilibrium model. To predict the OCM reaction, only two parameters were required to input for simulation. The results would be obtained in a few seconds. However, this model could not be used in reactor design and was limited to predict only at the equilibrium. However, OCM reaction model reached equilibrium in very short time (milliseconds). Therefore, these equilibrium models could be defined an alternative in process simulation.

5.5.2 The extrapolated prediction of OCM reaction

One of the interesting of the equilibrium model was its capable to extrapolate the results for another OCM reaction catalyzed by the other catalysts. Generally, the simulation of the OCM reaction was obtained after the kinetic study which must take many laboratory experiments. Therefore, a new prediction method with much more convenient would be valued for OCM reaction simulation.

The beginning information was only the information from one experiment of that catalyst (feed condition and reactor performance). These information were used to calculate the equilibrium model parameters, split fraction and specific ethane yield. Concept for calculating the void fraction was illustrated in the figure 5.47.

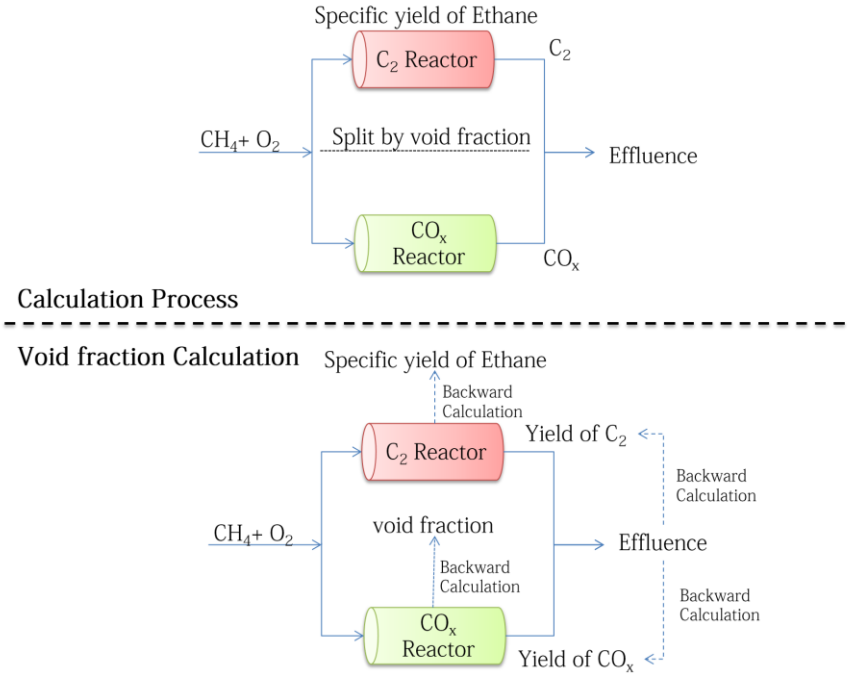

Fig 5.47 Scheme of calculation process and void fraction calculation

Because the calculation pathway of equilibrium model was flowed as the calculation process shown in figure 5.47. Beginning with the given CH_4/O_2 feed, the calculation was split into two parts with the function of the constant void fraction. The first fraction was consumed and produced the stoichiometric yield of C_2. The other fraction of CH_4 was reacted and produced CO_x with permanent stoichiometric ratio.

To calculate the void fraction of catalyst, the backward of flow was explained. Known effluent fractions from the experiment provided ratio of C_2 and COx of product which could be converted stoichiometric to fraction of CH_4 spent in each reactor. The ratio of CH_4 from both calculation parts would similar to the void fraction of catalyst. Therefore, split fraction was developed mathematically from oxygen and carbon balance and expressed in term of CO_x yield (Y_{COx}) in equation 5.10.

$$Split\ fraction = \left(\frac{1.5Y_{COx}}{100}\right)\left(\frac{CH_{4,Feed}}{O_{2,Feed}}\right) \tag{5.10}$$

Another parameter for equilibrium model was ethane yield which generally reported in literatures. The calculation of ethane yield was expressed again in equation 5.11.

$$Specific\,Ethane\,Yield = \frac{Ethane\ mole\,Efflux}{2\,x\,Methane\ mole\,Feed} \tag{5.11}$$

After the split fraction and ethane yield was obtained, the selection of appropriate model for calculation was required. In this research, there were two best fit models available, the duo-equilibrium reaction model with specific ethane yield and the trio-equilibrium reaction model with specific ethane yield. It was suggested that the catalyst composed of element that support hydrocracking, for example Co, Ni, Mo, W and Pb, would accelerate the hydrocracking reaction at the surface. Thus, the model of trio-equilibrium reaction model with specific ethane yield should be selected. In contrast, catalysts that did not contain element supporting hydrocracking reaction were suggested to use the model of duo-equilibrium reaction model with specific ethane yield.

Example of extrapolated prediction with La/MgO[74], SrO/Nd_2O_3[74] and $SnBaTiO_3$ catalyst [73] were studied. The beginning information were CH_4/O_2 = 4 over La/MgO at 800°C, CH_4/O_2 = 4 over SrO/Nd_2O_3 at 850°C and CH_4/O_2 = 3 over $SnBaTiO_2$ at 750°C. The split fraction and specific ethane yield over La/MgO, SrO/Nd_2O_3 and $SnBaTiO_3$ were calculated with equation 5.10 and 5.11. The values of split fraction and ethane yield were 0.734, 0.752, 0.683 and 7.8, 6.4, 4.8 for La/MgO, SrO/Nd_2O_3 and $SnBaTiO_3$ catalyst respectively. Moreover, these three types of catalysts did not

compose of hydrocracking catalyst element. Thus, the duo-equilibrium reaction model with specific ethane yield was selected. Table 5.14 showed the reported data from literature and calculated parameters for equilibrium models.

Table 5.14 Calculated parameter with extrapolated equations

Catalyst	CH_4/O_2	Temp (°C)	Reported Reactor Performance			Calculated Model Parameters	
			Methane Conversion	Ethane Selectivity	Ethylene Selectivity	Void fraction	Specific ethane yield
La/MgO	4	800	29.3	26.7	32.1	0.734	7.8
SrO/Nd_2O_3	4	850	30.0	21.5	30.5	0.752	6.4
$SnBaTiO_3$	3	750	40.3	12.0	46.5	0.683	4.8

After obtained the model parameters, the models were test at other operating conditions over the same catalyst. The results were plotted in bar chart comparing with experiment at 700, 750, 800, and 850°C. Methane conversion, ethane and ethylene selectivity were the comparing reactor performances. Comparison charts were shown in figure 5.48 to 5.50 for La/MgO, SrO/Nd_2O_3 and $SnBaTiO_3$ respectively.

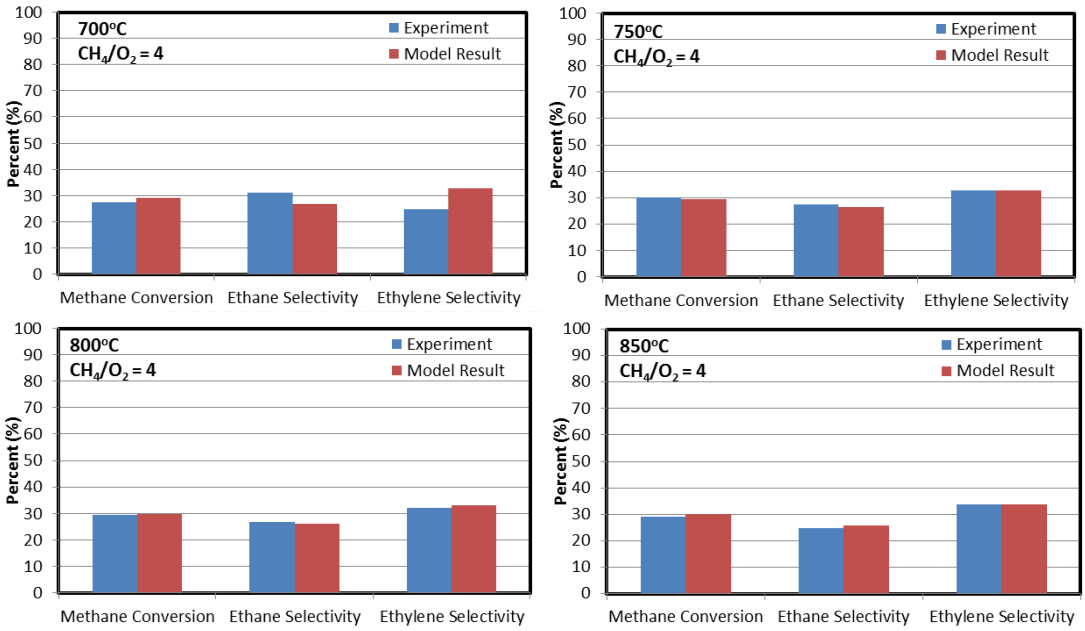

Fig 5.48 Comparative results of experiment and extrapolated results of equilibrium model at variety of operating condition over La/MgO catalyst

The extrapolation results over La/MgO catalyst were very close to the experiment. As seen in figure 5.48, methane conversion and C_2 selectivity results for 750-850°C at feed ratio equal to 4 were very acceptable with slightly deviation. However, at lower temperature than reference point (750°C), methane conversion from extrapolation was higher than experiment. As Choudhary et al [74] studied these operating condition at the same space time, lower temperature system would reach equilibrium slower than higher temperature. Thus, this deviation was attributed to the comparison of the model with experiment that did not reach equilibrium.

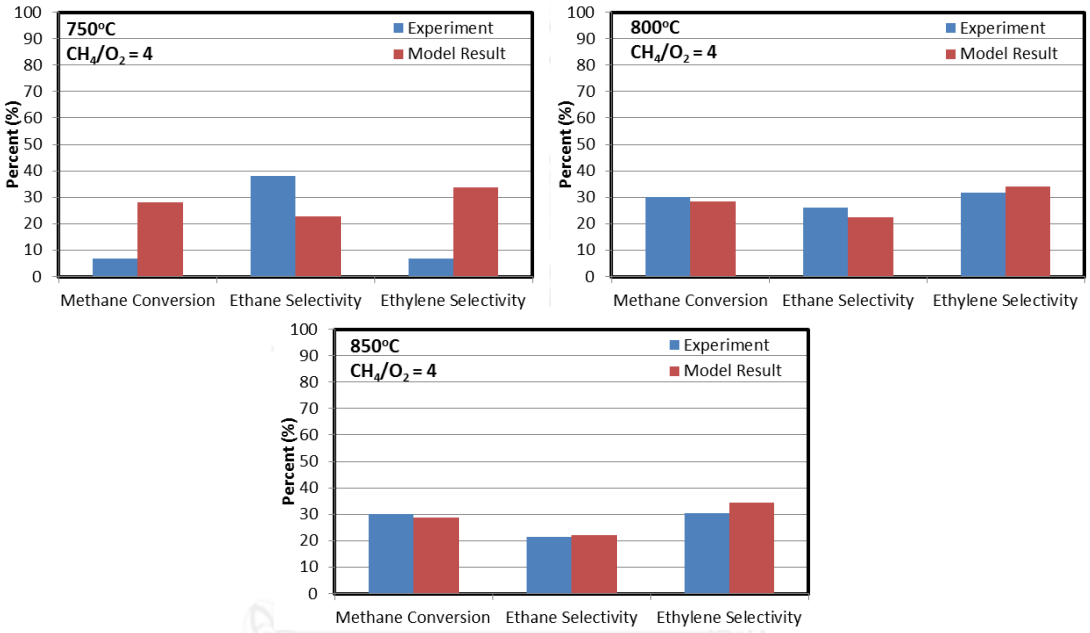

Fig 5.49 Comparative results of experiment and extrapolated results of equilibrium model at variety of operating condition over SrO/Nd_2O_3 catalyst

The results over SrO/Nd_2O_3 were the same tendency with previous catalyst. The model could predict the outcome at operating condition nearby the reference point. However, at the temperature much lower than reference point (850°C), the precision was very low. As seen in the comparison at 750°C and methane to oxygen feed ratio equal to 4, the equilibrium model predicted very higher methane conversion and much deviation of ethane and ethylene selectivity. This deviation was caused by the same reason as previous catalyst. It was attributed to the comparison of the model with experiment that did not reach equilibrium.

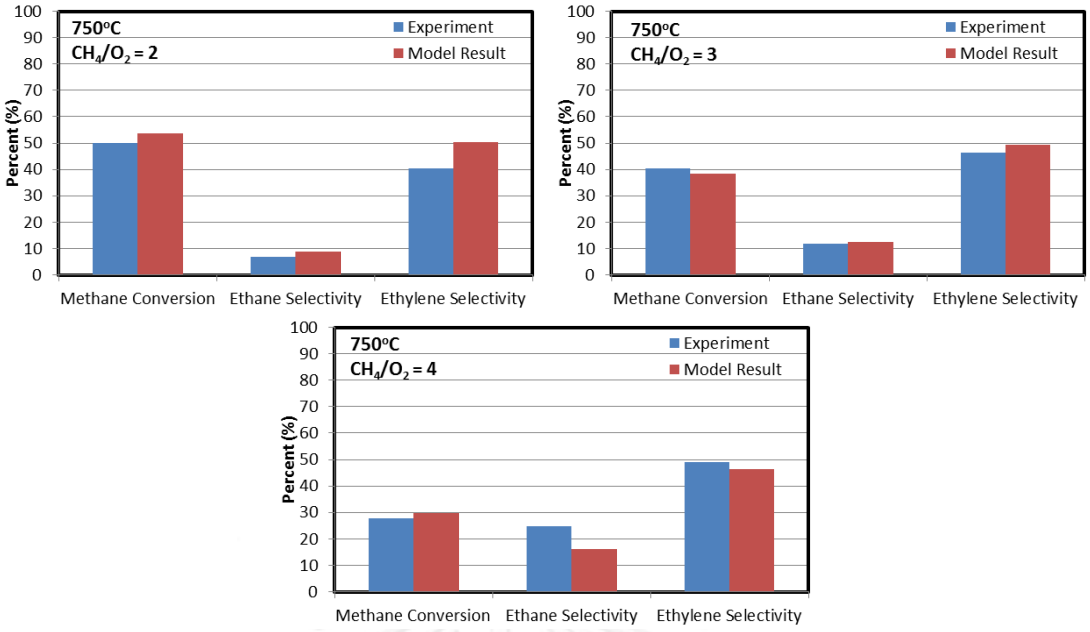

Fig 5.50 Comparative results of experiment and extrapolated results of equilibrium model at variety of operating condition over $SnBaTiO_3$ catalyst

From figure 5.50, it showed that the model could predict the results at the variation of methane to oxygen feed ratio (CH_4/O_2) well. As seen in the figure, there were small deviations occurred in the system.

The comparison chart of experiment and extrapolation results over the three catalysts were then calculated the statistic variable AARD to confirm the accuracy of the models. The AARD of each catalyst at various operating conditions were showed in table 5.15.

Table 5.15 AARD of extrapolation results at various operating conditions.

Catalyst	CH_4/O_2	Temp (^{o}C)	AARD (%)
La/MgO	4	700	15.82
La/MgO	4	750	2.03
La/MgO[a]	4	800	2.24
La/MgO	4	850	3.33
SrO/Nd_2O_3	4	750	283.59
SrO/Nd_2O_3	4	800	8.54
SrO/Nd_2O_3[a]	4	850	6.35
$SnBaTiO_3$	2	750	23.32
$SnBaTiO_3$[a]	3	750	3.85
$SnBaTiO_3$	4	750	13.95

[a] First Information used to find the void fraction and ethane specific yield

In the table, extrapolation results showed good capable of prediction according to the lower than 15% of AARD. It revealed that most of the extrapolated predictions from the proposed model were acceptable with low percent error. It should be noticed that the large deviation was the prediction at low temperature or low methane fraction. This deviation was attributed to the comparison of equilibrium model and experiment that did not reach equilibrium (too short residence time or too high fraction of oxygen which required more space time).

There were 11 more catalysts which were subjected to study the accuracy of extrapolated prediction. Detail for extrapolation results were summarized in Appendix C.

In order to increase extrapolation accuracy, it was suggested to use average split fraction as well as specific ethane yield for each catalyst. However, this research was used one-point extrapolation because the others operating conditions were kept for validation with the results calculated from the reference point.

In summary, equilibrium model had capability in extrapolation prediction of OCM reactions. After determine model parameters from experiment, the model could predict outcome of reactor within AARD less than 20%.

CHAPTER 6

Conclusion

6.1 Conclusion

1. Equilibrium model could predict Oxidative Coupling of Methane reaction model with concept of split calculation between catalytic surface reactions and spontaneous gas phase reactions.

2. Major catalytic reactions were Oxidative coupling of methane (OCM) and Oxidative Dehydrogenation of ethane (ODH) while major gas phase reaction were combustion of methane and water-gas shift reaction.

Oxidative Coupling of methane: $CH_4 + 0.5\ O_2 \longrightarrow C_2H_6 + H_2O$

Oxidative Dehydrogenation of ethane: $C_2H_6 + 0.5\ O_2 \longrightarrow C_2H_4 + H_2O$

Complete Combustion of methane: $CH_4 + 2\ O_2 \longrightarrow CO_2 + 2\ H_2O$

Incomplete Combustion of methane: $CH_4 + 1.5\ O_2 \longrightarrow CO + 2\ H_2O$

Water Gas Shift: $CO + H_2O \leftrightarrow CO_2 + H_2$

3. For catalysts which contained element that supported hydrocracking reaction, for example tungsten (W) and lead (Pb), hydrocracking reaction was also reacted on catalytic surface.

Ethane hydrocracking reaction $C_2H_6 + H_2 \longrightarrow 2\ CH_4$

4. For typical catalyst, the duo-equilibrium reaction model which parallel calculated gas phase and catalytic reaction was appropriate while catalyst contained

metal used in hydrocracking reaction ,for example Lead (Pb) and Tungsten (W), was appropriate for trio-equilibrium reaction model which add hydrocracking reaction following parallel reactors of the duo-equilibrium reaction model.

5. Equilibrium models had two parameters, split fraction and specific ethane yield, which represented catalyst characteristic.

- Split fraction showed maximum capacity of catalyst activity which occurred at high temperature. This value was equal to void fraction in reactor.

- Specific ethane yield represented activity of catalyst to catalyze OCM compared with ODH. This value was almost constant in each catalyst.

5. Equilibrium model had limitation in prediction only at high temperature and oxygen conversion reached almost 100 percent.

6. Advantage of equilibrium model compared to kinetic was its ease in utilization due to much lower amount of parameters and equations in equilibrium model. However, the equilibrium model could not be used to design the reactor.

7. Equilibrium model could extrapolation predict by fitting methane conversion, ethane and ethylene of one experiment that reached equilibrium with the model.

6.2 Recommendation

This model could be further developed to predict outcome of OCM reactor by specified only catalyst type and properties. Unfortunately, without experiment, the data obtained from literature was not sufficed

REFERENCES

1. Lunsford, J.H., *The Catalytic Oxidative Coupling of Methane.* Chem. Int. Ed. Engl, 1995. **34**: p. 970-980.
2. Oosterkamp, P.F.v.d., *Encyclopedia of Catalysis.* I. Horvath (Ed.), 2003. **6**: p. 770.
3. Holmen, A., *Direct conversion of methane to fuels and chemicals.* Catalysis Today, 2009. **142**(1-2): p. 2-8.
4. Al-Shalchi, W., *Gas to Liquid Technology (GTL)*. 2006.
5. G.Ertl, H.K., *Handbook of Heterogeneous Catalysis*. Vol. 1. 2008.
6. Tiemersma, T.P., et al., *A kinetics study for the oxidative coupling of methane on a Mn/Na2WO4/SiO2 catalyst.* Applied Catalysis A: General, 2012. **433-434**: p. 96-108.
7. Arndt, S., et al., *Mn–Na2WO4/SiO2 as catalyst for the oxidative coupling of methane. What is really known?* Applied Catalysis A: General, 2012. **425-426**: p. 53-61.
8. Simon, U., et al., *Fluidized bed processing of sodium tungsten manganese catalysts for the oxidative coupling of methane.* Chemical Engineering Journal, 2011. **168**(3): p. 1352-1359.
9. Sergei Pak, P.Q., and Jack H. Lunsford, *Elementary Reactions in the Oxidative Coupling of Methane over Mn/Na2WO4/SiO2 and Mn/Na2WO4/MgO Catalysts.* Journal of catalysis 1998. **179**: p. 222-230.
10. Z. Stansch, L.M., * and M. Baerns‡, *Comprehensive Kinetics of Oxidative Coupling of Methane over the La2O3/CaO Catalyst.* Ind. Eng. Chem. Res., 1997. **36**: p. 2568-2579.
11. Daneshpayeh, M., et al., *Kinetic modeling of oxidative coupling of methane over Mn/Na2WO4/SiO2 catalyst.* Fuel Processing Technology, 2009. **90**(3): p. 403-410.
12. Hinsen, W.B., W.; Baerns, *Oxidative Dehydrogenation and Coupling of Methane.* Proceedings of the 8th International Congress on Catalysis, 1985: p. 251-283.
13. Olsbye, U., et al., *A kinetic study of the oxidative coupling of methane over a BaCO3 / La2On(CO3)3-n catalyst: I. Determination of a global reaction scheme and the influence of heterogeneous and homogeneous reactions.* Catalysis Today, 1992. **13**(2–3): p. 209-218.
14. J.M. Smith, H.C.V.N., M.M. Abbott, *Introduction to Chemical Engineering Thermodynamics*. 2005: McGraw-Hill Companies, Inc.
15. Keller, G.E. and M.M. Bhasin, *Synthesis of ethylene via oxidative coupling of methane: I. Determination of active catalysts.* Journal of Catalysis, 1982. **73**(1): p. 9-19.

16. Lee, J.Y., et al., *Scaled-up production of C2 hydrocarbons by the oxidative coupling of methane over pelletized Na2WO4/Mn/SiO2 catalysts: Observing hot spots for the selective process.* Fuel, 2013. **106**: p. 851-857.
17. Jašo, S., et al., *Oxidative Coupling of Methane: Reactor Performance and Operating Conditions.* 2010. **28**: p. 781-786.
18. Liu, H., et al., *Scale up and stability test for oxidative coupling of methane over Na2WO4-Mn/SiO2 catalyst in a 200 ml fixed-bed reactor.* Journal of Natural Gas Chemistry, 2008. **17**(1): p. 59-63.
19. Jašo, S., et al., *Experimental investigation of fluidized-bed reactor performance for oxidative coupling of methane.* Journal of Natural Gas Chemistry, 2012. **21**(5): p. 534-543.
20. Klvana, D., *Methane and its derivatives (Chemical Industries Series/70), by Sunggyu Lee, 1996, 424 + viii pages, illustrated, Marcel Dekker inc, Monticello, NY 12701. ISBN#: 0-8247-9754-X. Price: US $165.00.* The Canadian Journal of Chemical Engineering, 1997. **75**(5): p. 990-990.
21. Alvarez-Galvan, M.C., et al., *Direct methane conversion routes to chemicals and fuels.* Catalysis Today, 2011. **171**(1): p. 15-23.
22. Rostrup-Nielsen, J.R., *Production of synthesis gas.* Catalysis Today, 1993. **18**(4): p. 305-324.
23. *Ullmann's Encyclopedia of Industrial Chemistry* 2003. **10**(Cyano Compounds, Inorganic): p. 774.
24. *Oryx GTL plant officially opened.* Focus on Catalysts, 2006. **2006**(9): p. 4.
25. Quanli Zhu, X.Z., Youquan Deng, *Advances in the Partial Oxidation of Methane to Synthesis Gas.* Journal of Natural Gas Chemistry, 2004. **13**: p. 191-203.
26. Lobo, W.E., *Chemical Process Industries, Third Edition, R. Norris Shreve, McGraw-Hill Book Company, New York (1967). $18.50.* AIChE Journal, 1968. **14**(2): p. 210-364.
27. Driscoll, D.J., et al., *Formation of gas-phase methyl radicals over magnesium oxide.* Journal of the American Chemical Society, 1985. **107**(1): p. 58-63.
28. Dissanayake, D., J.H. Lunsford, and M.P. Rosynek, *Site Differentiation in Homolytic vs. Heterolytic Activation of Methane over Ba/MgO Catalysts.* Journal of Catalysis, 1994. **146**(2): p. 613-615.
29. Buyevskaya, O.V., et al., *Transient Studies on Reaction Steps in the Oxidative Coupling of Methane over Catalytic Surfaces of MgO and Sm2O3.* Journal of Catalysis, 1994. **146**(2): p. 346-357.

30. Jones, C.A., J.J. Leonard, and J.A. Sofranko, *The oxidative conversion of methane to higher hydrocarbons over alkali-promoted MnSiO2.* Journal of Catalysis, 1987. **103**(2): p. 311-319.
31. Lin, C.H., et al., *Oxidative dimerization of methane over lanthanum oxide.* The Journal of Physical Chemistry, 1986. **90**(4): p. 534-537.
32. Nelson, P.F., C.A. Lukey, and N.W. Cant, *Isotopic evidence for direct methyl coupling and ethane to ethylene conversion during partial oxidation of methane over lithium/magnesium oxide.* The Journal of Physical Chemistry, 1988. **92**(22): p. 6176-6179.
33. Morales, E. and J.H. Lunsford, *Oxidative dehydrogenation of ethane over a lithium-promoted magnesium oxide catalyst.* Journal of Catalysis, 1989. **118**(1): p. 255-265.
34. M. Kennedy, E. and N. W. Cant, *Comparison of the oxidative dehydrogenation of ethane and oxidative coupling of methane over rare earth oxides.* Applied Catalysis, 1991. **75**(1): p. 321-330.
35. Sun, J., J. Thybaut, and G. Marin, *Microkinetics of methane oxidative coupling.* Catalysis Today, 2008. **137**(1): p. 90-102.
36. Miro, E., J. Santamaria, and E.E. Wolf, *Oxidative coupling of methane on alkali metal-promoted nickel titanate: I. Catalyst characterization and transient studies.* Journal of Catalysis, 1990. **124**(2): p. 451-464.
37. Morteza Sohrabi, B.D., Asghar Eskandari, Rahmatolah D. Golpasha, *Some Aspects of Kinetics and Mechanism of the Oxidative Coupling of Methane.* J. Chem. Tech. Biotechnol, 1996. **67**: p. 15-20.
38. Lacombe, S., et al., *Kinetic modelling of the oxidative coupling of methane over lanthanum oxide in connection with mechanistic studies.* Chemical Engineering & Technology, 1995. **18**(3): p. 216-223.
39. Traykova, M., et al., *Oxidative coupling of methane – the transition from reaction to transport control over La2O3/MgO catalyst.* Applied Catalysis A: General, 1998. **169**(2): p. 237-247.
40. Shahri, S.M.K. and S.M. Alavi, *Kinetic studies of the oxidative coupling of methane over the Mn/Na2WO4/SiO2 catalyst.* Journal of Natural Gas Chemistry, 2009. **18**(1): p. 25-34.
41. Lee, M.R., et al., *A kinetic model for the oxidative coupling of methane over Na2WO4/Mn/SiO2.* Fuel Processing Technology, 2012. **96**: p. 175-182.

42. Sadeghzadeh Ahari, J., S. Zarrinpashne, and M.T. Sadeghi, *Micro-kinetic modeling of OCM reactions over Mn/Na2WO4/SiO2 catalyst.* Fuel Processing Technology, 2013. **115**: p. 79-87.
43. Ahari, J.S., M.T. Sadeghi, and S. Zarrinpashne, *Effects of operating parameters on oxidative coupling of methane over Na-W-Mn/SiO2 catalyst at elevated pressures.* Journal of Natural Gas Chemistry, 2011. **20**(2): p. 204-213.
44. Ghiasi, M., et al., *Kinetic study of oxidative coupling of methane over Mn and/or W promoted Na2SO4/SiO2 catalysts.* Journal of Natural Gas Chemistry, 2011. **20**(4): p. 428-434.
45. Su, Y., *Upper bound on the yield for oxidative coupling of methane.* Journal of Catalysis, 2003. **218**(2): p. 321-333.
46. Yaping Lu, A.G.D., William R. Moser, and Yi Hua Ma, *Analysis and Optimization of Cross-Flow Reactors for Oxidative Coupling of Methane.* Ind. Eng. Chem. Res., 1997. **36**: p. 559-567.
47. Reyes, I.P.A.a.S.C., *Role of Distributed Oxygen Addition and Product Removal in the Oxidative Coupling of Methane.* AIChE Journal, 1999. **45**(4): p. 860-868.
48. Kiatkittipong, W., et al., *Comparative study of oxidative coupling of methane modeling in various types of reactor.* Chemical Engineering Journal, 2005. **115**(1-2): p. 63-71.
49. Kruglov, A.V., M.C. Bjorklund, and R.W. Curr, *Optimization of the simulated countercurrent moving-bed chromatographic reactor for the oxidative coupling of methane.* Chemical Engineering Science, 1996. **51**(11): p. 2945-2950.
50. Mleczko, U.P.a.l., *Comprehensive model of oxidative coupling of methane in a fluidized-bed reactor.* Chemical Engineerin Science, 1996. **51**(14): p. 3575-3590.
51. Pannek, U. and L. Mleczko, *Effect of scale-up on the performance of a fluidized-bed reactor for the oxidative coupling of methane.* Chemical Engineering Science, 1997. **52**(14): p. 2429-2434.
52. Ng, K.S. and J. Sadhukhan, *Process integration and economic analysis of bio-oil platform for the production of methanol and combined heat and power.* Biomass and Bioenergy, 2011. **35**(3): p. 1153-1169.
53. Zhang, Y., et al., *Comparative techno-economic analysis of biohydrogen production via bio-oil gasification and bio-oil reforming.* Biomass and Bioenergy, 2013. **51**: p. 99-108.
54. Freitas, A.C.D. and R. Guirardello, *Oxidative reforming of methane for hydrogen and synthesis gas production: Thermodynamic equilibrium analysis.* Journal of Natural Gas Chemistry, 2012. **21**(5): p. 571-580.

55. Tock, L., M. Gassner, and F. Maréchal, *Thermochemical production of liquid fuels from biomass: Thermo-economic modeling, process design and process integration analysis.* Biomass and Bioenergy, 2010. **34**(12): p. 1838-1854.
56. Gutiérrez Ortiz, F.J., P. Ollero, and A. Serrera, *Thermodynamic analysis of the autothermal reforming of glycerol using supercritical water.* International Journal of Hydrogen Energy, 2011. **36**(19): p. 12186-12199.
57. Zhang, Y., et al., *Process simulation and optimization of methanol production coupled to tri-reforming process.* International Journal of Hydrogen Energy, 2013. **38**(31): p. 13617-13630.
58. Trippe, F., et al., *Comprehensive techno-economic assessment of dimethyl ether (DME) synthesis and Fischer–Tropsch synthesis as alternative process steps within biomass-to-liquid production.* Fuel Processing Technology, 2013. **106**: p. 577-586.
59. Bao, B., M.M. El-Halwagi, and N.O. Elbashir, *Simulation, integration, and economic analysis of gas-to-liquid processes.* Fuel Processing Technology, 2010. **91**(7): p. 703-713.
60. Trippe, F., et al., *Techno-economic assessment of gasification as a process step within biomass-to-liquid (BtL) fuel and chemicals production.* Fuel Processing Technology, 2011. **92**(11): p. 2169-2184.
61. Haro, P., et al., *Bio-syngas to gasoline and olefins via DME – A comprehensive techno-economic assessment.* Applied Energy, 2013. **108**: p. 54-65.
62. Zhou, L., et al., *Study on co-feed and co-production system based on coal and natural gas for producing DME and electricity.* Chemical Engineering Journal, 2008. **136**(1): p. 31-40.
63. Chang S. Hsu, P.R.R., *Practical Advances in Petroleum Processing*. Vol. 1. 2006.
64. Kareem, S.A., *SYNERGIC PROMOTION OF CATALYST BY GROUP VIII B ELEMENTS* Journal of Sciences, Islamic Republic of Iran, 2002. **13**: p. 237-240.
65. Wolf, E., *Methane Conversion by Oxidative Processes - Fundamental and Engineering Aspects.* 1992.
66. Limited, A.P.C., *ASPEN PLUS® User Guide*. 2000.
67. Cavani, F., N. Ballarini, and A. Cericola, *Oxidative dehydrogenation of ethane and propane: How far from commercial implementation?* Catalysis Today, 2007. **127**(1-4): p. 113-131.
68. Christian Enger, B., R. Lødeng, and A. Holmen, *A review of catalytic partial oxidation of methane to synthesis gas with emphasis on reaction mechanisms over transition metal catalysts.* Applied Catalysis A: General, 2008. **346**(1-2): p. 1-27.

69. J, B.S.R., *A Review of the Water Gas Shift Reaction Kinetics.* International Journal of Chemical Reactor Engineering, 2010. **8**.

70. Fogler, H.S., *Elements of Chemical Reaction Engineering, 3rd* 2004.

71. Zhiming Gao, J.Z., RuiyanWang, *Formation of hydrogen in oxidative coupling of methane over BaCO3 andMgO catalysts.* Journal of Natural Gas Chemistry 2008. **17**: p. 238-241.

72. V. H. Rane, S.T.C., V. R. Choudhary, *Influence of alkali metal doping on surface properties and catalytic activity/selectivity of CaO catalysts in oxidative coupling of methane.* Journal of Natural Gas Chemistry 2008. **17**: p. 313-320.

73. Farooji, N.R., A. Vatani, and S. Mokhtari, *Kinetic simulation of oxidative coupling of methane over perovskite catalyst by genetic algorithm: Mechanistic aspects.* Journal of Natural Gas Chemistry, 2010. **19**(4): p. 385-392.

74. V. R. Choudhary, S.A.R.M., B.S. Uphade, *Oxidative coupling of methane over alkaline earth oxides deposited on commercial support precoated with rare earth oxides.* Fuel 1999. **78**: p. 427–437.

75. Cantelo, R.C., *The Thermal Decomposition of Methane.* J. Phys. Chem, 1924. **28**(10): p. 1036–1048.

76. Ching Thian Tye, A.R.M., Subhash Bhatia, *Modeling of catalytic reactor for oxidative coupling of methane using La2O3/CaO catalyst.* Chemical Engineering Journal, 2002. **87**: p. 49-59.

APPENDIX

Appendix A: Kinetic Model Validation

Before invention of equilibrium model, reactor effluent data such as conversion and selectivity was required for verification of the model. Unfortunately, effluent data at equilibrium times (very small amount of oxygen left) was lacked. However, this data could be simulated by kinetic model which also represented the system. Nevertheless, kinetic models need to be validated to ensure their precise and accuracy.

In this research, there were three catalysts being studied, PbO/Al_2O_3 La_2O_3/CaO and $Mn/Na_2WO_4/SiO_2$. Kinetic model for La_2O_3/CaO of Stranch et al [10] was validated with the experiment result from Ching Thian Tye et al [76]. Table A.1 showed the validation for methane conversion, C_2 selectivity and yield which had slightly deviation from experimental.

Table A.1 Kinetic Model Validation for La_2O_3/CaO

	Runs					
	1 (1023K)	2 (1073K)	3 (1103K)	4 (973 K)	5 (1023K)	6 (1103K)
Feed Mole Ratio						
CH_4	0.612	0.612	0.612	0.699	0.699	0.699
O_2	0.051	0.051	0.051	0.095	0.095	0.095
N_2	0.337	0.337	0.337	0.206	0.206	0.206
CH_4 Conversion (%)						
Experiment*	4.9	7.9	9.9	4.1	7.1	14.4
Simulated	7.1	11.4	12.2	4.7	8.9	17.3
C_2 Selectivity (%)						
Experiment*	55.6	69.2	72.5	35.6	53.7	69.6
Simulated	56.5	67.2	68.1	32.2	47.7	62.2
C_2 Yield (%)						
Experiment*	2.7	5.5	7.2	1.5	3.8	10
Simulated	4.0	7.7	8.3	1.5	4.2	10.8

* At m_{cat}/V_{STP} = 3.7 kg s m^{-3}

Validation of $Mn/Na_2WO_4/SiO_2$ catalyst [11] was depicted in figure A.1 which plot the data from experimental at x-axis and then simulated the result at the same condition by kinetic equations and parameters obtained from Daneshpayeh et al[11].

The figure indicated that at range of operations in table 4.2, methane conversion, ethane and ethylene selectivity from simulation were closed to experimental.

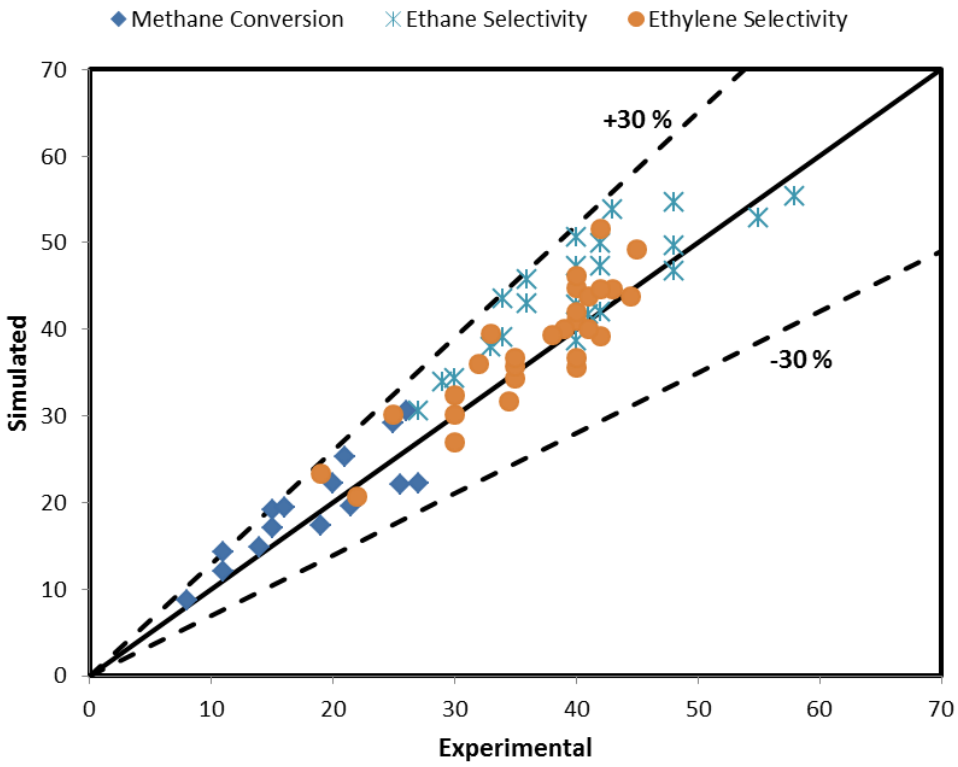

Fig A.1 Kinetic Validation for $Mn/Na_2WO_4/SiO_2$

For PbO/Al_2O_3 catalyst, validation was compared with experiment as showed in table A.2. In the table, conversion and selectivity were compared and found slightly deviation. Thus, kinetic model could be used as representative of experiments.

Table A.2 Kinetic Validation for PbO/Al_2O_3

Runs	CH_4/O_2	CH_4 Conversion (%)		C_2 Selectivity (%)		C_2 Yield (%)	
	Ratio	Experiment	Simulated	Experiment	Simulated	Experiment	Simulated
1 (750°C)	1	66	63.5	20	27.1	13.5	17.2
2 (750°C)	3	25	24.7	37	39.5	9	9.7
3 (750°C)	10	8	8.9	50	52.2	4	4.6

Appendix B: Equilibrium Model Results and Validation

Table B.1 Trio-equilibrium reaction model calculation result for $Mn/Na_2WO_4/SiO_2$ catalyst

Temp (°C)	CH_4/O_2	Effluent Composition								RSS
		H_2	CH_4	C_2H_4	C_2H_6	CO	CO_2	O_2	H_2O	
700	3	0.0005	0.3735	0.1105	0.0016	0.0072	0.0479	0.0000	0.3322	4.88
700	3.5	0.0004	0.4342	0.0987	0.0020	0.0067	0.0431	0.0000	0.2988	4.65
700	4	0.0004	0.4838	0.0892	0.0024	0.0063	0.0393	0.0000	0.2715	4.60
700	4.5	0.0004	0.5251	0.0814	0.0026	0.0058	0.0360	0.0000	0.2487	4.66
700	5	0.0004	0.5601	0.0748	0.0027	0.0055	0.0333	0.0000	0.2294	4.80
700	5.5	0.0003	0.5900	0.0691	0.0028	0.0052	0.0309	0.0000	0.2130	5.04
700	6	0.0003	0.6159	0.0643	0.0029	0.0049	0.0289	0.0000	0.1987	5.35
700	6.5	0.0003	0.6385	0.0600	0.0030	0.0046	0.0271	0.0000	0.1862	5.75
700	7	0.0003	0.6585	0.0563	0.0030	0.0044	0.0255	0.0000	0.1752	6.22
700	7.5	0.0003	0.6762	0.0530	0.0030	0.0042	0.0241	0.0000	0.1654	6.73
700	8	0.0003	0.6921	0.0501	0.0030	0.0040	0.0228	0.0000	0.1566	7.22
700	8.5	0.0003	0.7064	0.0475	0.0030	0.0038	0.0217	0.0000	0.1488	7.82
700	9	0.0002	0.7193	0.0451	0.0030	0.0036	0.0207	0.0000	0.1416	8.50
700	9.5	0.0002	0.7310	0.0429	0.0030	0.0035	0.0197	0.0000	0.1352	9.34
700	10	0.0002	0.7417	0.0410	0.0030	0.0034	0.0189	0.0000	0.1293	10.02
725	3	0.0007	0.3740	0.1100	0.0014	0.0086	0.0471	0.0000	0.3321	2.56
725	3.5	0.0006	0.4345	0.0984	0.0018	0.0079	0.0425	0.0000	0.2988	2.43
725	4	0.0006	0.4840	0.0890	0.0021	0.0073	0.0386	0.0000	0.2715	2.40
725	4.5	0.0006	0.5252	0.0812	0.0023	0.0068	0.0354	0.0000	0.2488	2.43
725	5	0.0005	0.5600	0.0747	0.0024	0.0064	0.0327	0.0000	0.2295	2.52
725	5.5	0.0005	0.5899	0.0691	0.0025	0.0060	0.0304	0.0000	0.2131	2.66
725	6	0.0005	0.6157	0.0643	0.0026	0.0056	0.0284	0.0000	0.1988	2.84
725	6.5	0.0004	0.6384	0.0601	0.0027	0.0053	0.0266	0.0000	0.1863	3.06
725	7	0.0004	0.6583	0.0564	0.0027	0.0050	0.0251	0.0000	0.1753	3.31
725	7.5	0.0004	0.6760	0.0531	0.0027	0.0048	0.0237	0.0000	0.1655	3.62
725	8	0.0004	0.6919	0.0502	0.0027	0.0046	0.0224	0.0000	0.1568	3.97
725	8.5	0.0004	0.7062	0.0476	0.0027	0.0044	0.0213	0.0000	0.1489	4.36
725	9	0.0003	0.7191	0.0452	0.0027	0.0042	0.0203	0.0000	0.1418	4.75
725	9.5	0.0003	0.7308	0.0431	0.0027	0.0040	0.0194	0.0000	0.1353	5.21
725	10	0.0003	0.7415	0.0411	0.0027	0.0038	0.0185	0.0000	0.1294	5.71
750	3	0.0010	0.3738	0.1097	0.0013	0.0099	0.0463	0.0000	0.3322	1.70
750	3.5	0.0009	0.4342	0.0983	0.0017	0.0091	0.0417	0.0000	0.2989	1.61
750	4	0.0008	0.4837	0.0890	0.0019	0.0084	0.0379	0.0000	0.2716	1.57
750	4.5	0.0008	0.5248	0.0813	0.0021	0.0078	0.0348	0.0000	0.2489	1.57

Table B.1 Trio-equilibrium reaction model calculation result for $Mn/Na_2WO_4/SiO_2$ catalyst

Temp (°C)	CH_4/O_2	Effluent Composition								RSS
		H_2	CH_4	C_2H_4	C_2H_6	CO	CO_2	O_2	H_2O	
750	5	0.0007	0.5596	0.0748	0.0022	0.0072	0.0321	0.0000	0.2297	1.61
750	5.5	0.0007	0.5895	0.0692	0.0023	0.0068	0.0298	0.0000	0.2133	1.68
750	6	0.0006	0.6153	0.0644	0.0024	0.0064	0.0278	0.0000	0.1990	1.78
750	6.5	0.0006	0.6379	0.0603	0.0024	0.0060	0.0261	0.0000	0.1865	1.91
750	7	0.0006	0.6579	0.0566	0.0024	0.0057	0.0246	0.0000	0.1755	2.07
750	7.5	0.0005	0.6756	0.0533	0.0025	0.0054	0.0232	0.0000	0.1657	2.26
750	8	0.0005	0.6914	0.0504	0.0025	0.0051	0.0220	0.0000	0.1570	2.47
750	8.5	0.0005	0.7057	0.0478	0.0025	0.0049	0.0209	0.0000	0.1491	2.71
750	9	0.0005	0.7186	0.0454	0.0025	0.0047	0.0199	0.0000	0.1420	2.97
750	9.5	0.0004	0.7303	0.0433	0.0025	0.0045	0.0190	0.0000	0.1355	3.28
750	10	0.0004	0.7410	0.0414	0.0024	0.0043	0.0182	0.0000	0.1296	3.61
775	3	0.0013	0.3732	0.1097	0.0012	0.0112	0.0454	0.0000	0.3324	1.39
775	3.5	0.0012	0.4336	0.0983	0.0015	0.0102	0.0409	0.0000	0.2991	1.30
775	4	0.0011	0.4829	0.0891	0.0017	0.0094	0.0371	0.0000	0.2719	1.25
775	4.5	0.0010	0.5241	0.0814	0.0019	0.0087	0.0341	0.0000	0.2492	1.23
775	5	0.0010	0.5589	0.0750	0.0020	0.0081	0.0314	0.0000	0.2300	1.23
775	5.5	0.0009	0.5887	0.0694	0.0021	0.0075	0.0292	0.0000	0.2135	1.26
775	6	0.0008	0.6146	0.0647	0.0021	0.0071	0.0273	0.0000	0.1993	1.31
775	6.5	0.0008	0.6372	0.0605	0.0022	0.0067	0.0256	0.0000	0.1868	1.38
775	7	0.0007	0.6572	0.0568	0.0022	0.0063	0.0240	0.0000	0.1758	1.48
775	7.5	0.0007	0.6749	0.0536	0.0022	0.0060	0.0227	0.0000	0.1660	1.58
775	8	0.0007	0.6908	0.0507	0.0022	0.0057	0.0215	0.0000	0.1572	1.72
775	8.5	0.0006	0.7051	0.0481	0.0022	0.0054	0.0204	0.0000	0.1494	1.86
775	9	0.0006	0.7180	0.0457	0.0022	0.0051	0.0195	0.0000	0.1422	2.04
775	9.5	0.0006	0.7297	0.0436	0.0022	0.0049	0.0186	0.0000	0.1358	2.22
775	10	0.0006	0.7405	0.0416	0.0022	0.0047	0.0178	0.0000	0.1299	2.45
800	3	0.0017	0.3722	0.1098	0.0011	0.0124	0.0444	0.0000	0.3326	1.28
800	3.5	0.0016	0.4325	0.0985	0.0014	0.0113	0.0400	0.0000	0.2994	1.19
800	4	0.0015	0.4819	0.0893	0.0016	0.0103	0.0364	0.0000	0.2721	1.14
800	4.5	0.0013	0.5231	0.0817	0.0017	0.0095	0.0333	0.0000	0.2495	1.10
800	5	0.0012	0.5579	0.0752	0.0018	0.0088	0.0308	0.0000	0.2303	1.08
800	5.5	0.0012	0.5878	0.0697	0.0019	0.0082	0.0286	0.0000	0.2138	1.08
800	6	0.0011	0.6137	0.0649	0.0020	0.0077	0.0267	0.0000	0.1995	1.09
800	6.5	0.0010	0.6363	0.0608	0.0020	0.0073	0.0250	0.0000	0.1871	1.12
800	7	0.0010	0.6563	0.0571	0.0020	0.0069	0.0235	0.0000	0.1761	1.17
800	7.5	0.0009	0.6741	0.0539	0.0020	0.0065	0.0222	0.0000	0.1663	1.23
800	8	0.0009	0.6900	0.0509	0.0020	0.0062	0.0211	0.0000	0.1575	1.31

Table B.1 Trio-equilibrium reaction model calculation result for $Mn/Na_2WO_4/SiO_2$ catalyst

Temp (°C)	CH_4/O_2	Effluent Composition								RSS
		H_2	CH_4	C_2H_4	C_2H_6	CO	CO_2	O_2	H_2O	
800	8.5	0.0008	0.7043	0.0483	0.0020	0.0059	0.0200	0.0000	0.1496	1.41
800	9	0.0008	0.7172	0.0460	0.0020	0.0056	0.0191	0.0000	0.1425	1.51
800	9.5	0.0008	0.7290	0.0438	0.0020	0.0054	0.0182	0.0000	0.1360	1.64
800	10	0.0007	0.7398	0.0419	0.0020	0.0051	0.0174	0.0000	0.1301	1.77
825	3	0.0023	0.3709	0.1101	0.0010	0.0135	0.0435	0.0000	0.3329	1.29
825	3.5	0.0020	0.4312	0.0988	0.0013	0.0123	0.0391	0.0000	0.2996	1.20
825	4	0.0019	0.4807	0.0896	0.0014	0.0112	0.0356	0.0000	0.2724	1.13
825	4.5	0.0017	0.5219	0.0820	0.0016	0.0103	0.0326	0.0000	0.2498	1.08
825	5	0.0016	0.5568	0.0756	0.0017	0.0096	0.0301	0.0000	0.2306	1.05
825	5.5	0.0015	0.5867	0.0700	0.0017	0.0089	0.0280	0.0000	0.2141	1.02
825	6	0.0014	0.6126	0.0653	0.0018	0.0083	0.0261	0.0000	0.1998	1.01
825	6.5	0.0013	0.6353	0.0611	0.0018	0.0078	0.0245	0.0000	0.1873	1.01
825	7	0.0012	0.6553	0.0574	0.0018	0.0074	0.0230	0.0000	0.1763	1.03
825	7.5	0.0012	0.6731	0.0542	0.0019	0.0070	0.0218	0.0000	0.1665	1.05
825	8	0.0011	0.6891	0.0513	0.0019	0.0066	0.0206	0.0000	0.1578	1.09
825	8.5	0.0011	0.7034	0.0486	0.0019	0.0063	0.0196	0.0000	0.1499	1.14
825	9	0.0010	0.7164	0.0463	0.0019	0.0060	0.0186	0.0000	0.1427	1.21
825	9.5	0.0010	0.7282	0.0441	0.0019	0.0058	0.0178	0.0000	0.1363	1.27
825	10	0.0009	0.7390	0.0422	0.0019	0.0055	0.0170	0.0000	0.1303	1.34
850	3	0.0029	0.3693	0.1105	0.0009	0.0145	0.0425	0.0000	0.3331	1.35
850	3.5	0.0026	0.4297	0.0992	0.0012	0.0132	0.0383	0.0000	0.2999	1.26
850	4	0.0024	0.4792	0.0900	0.0013	0.0120	0.0348	0.0000	0.2727	1.20
850	4.5	0.0022	0.5205	0.0824	0.0014	0.0111	0.0319	0.0000	0.2500	1.14
850	5	0.0020	0.5554	0.0759	0.0015	0.0103	0.0295	0.0000	0.2309	1.09
850	5.5	0.0019	0.5854	0.0704	0.0016	0.0096	0.0274	0.0000	0.2144	1.05
850	6	0.0018	0.6114	0.0656	0.0016	0.0089	0.0255	0.0000	0.2001	1.02
850	6.5	0.0017	0.6341	0.0615	0.0017	0.0084	0.0240	0.0000	0.1876	1.00
850	7	0.0016	0.6542	0.0578	0.0017	0.0079	0.0225	0.0000	0.1766	0.99
850	7.5	0.0015	0.6721	0.0545	0.0017	0.0075	0.0213	0.0000	0.1668	0.99
850	8	0.0014	0.6880	0.0516	0.0017	0.0071	0.0202	0.0000	0.1580	1.00
850	8.5	0.0013	0.7024	0.0490	0.0017	0.0068	0.0192	0.0000	0.1501	1.02
850	9	0.0013	0.7154	0.0466	0.0017	0.0064	0.0183	0.0000	0.1430	1.04
850	9.5	0.0012	0.7273	0.0444	0.0017	0.0062	0.0174	0.0000	0.1365	1.07
850	10	0.0012	0.7381	0.0425	0.0017	0.0059	0.0167	0.0000	0.1306	1.12
875	3	0.0036	0.3675	0.1109	0.0008	0.0155	0.0416	0.0000	0.3334	1.54
875	3.5	0.0032	0.4280	0.0997	0.0011	0.0140	0.0375	0.0000	0.3002	1.45
875	4	0.0029	0.4776	0.0905	0.0012	0.0128	0.0341	0.0000	0.2730	1.38

Table B.1 Trio-equilibrium reaction model calculation result for $Mn/Na_2WO_4/SiO_2$ catalyst

Temp (°C)	CH_4/O_2	Effluent Composition								RSS
		H_2	CH_4	C_2H_4	C_2H_6	CO	CO_2	O_2	H_2O	
875	4.5	0.0027	0.5190	0.0828	0.0013	0.0118	0.0312	0.0000	0.2503	1.30
875	5	0.0025	0.5540	0.0764	0.0014	0.0109	0.0288	0.0000	0.2311	1.22
875	5.5	0.0023	0.5840	0.0708	0.0015	0.0101	0.0268	0.0000	0.2147	1.17
875	6	0.0022	0.6101	0.0660	0.0015	0.0095	0.0250	0.0000	0.2004	1.13
875	6.5	0.0021	0.6329	0.0619	0.0015	0.0089	0.0234	0.0000	0.1879	1.08
875	7	0.0019	0.6530	0.0582	0.0016	0.0084	0.0221	0.0000	0.1769	1.05
875	7.5	0.0018	0.6709	0.0549	0.0016	0.0079	0.0208	0.0000	0.1671	1.03
875	8	0.0017	0.6869	0.0519	0.0016	0.0075	0.0197	0.0000	0.1583	1.01
875	8.5	0.0017	0.7013	0.0493	0.0016	0.0072	0.0188	0.0000	0.1504	1.00
875	9	0.0016	0.7144	0.0469	0.0016	0.0068	0.0179	0.0000	0.1432	1.00
875	9.5	0.0015	0.7263	0.0448	0.0016	0.0065	0.0171	0.0000	0.1367	1.00
875	10	0.0014	0.7371	0.0428	0.0016	0.0062	0.0163	0.0000	0.1308	1.01

Table B.2 Duo-equilibrium reaction model calculation result for La_2O_3/CaO catalyst

Temp (°C)	CH_4/O_2	Effluent Composition								RSS
		H_2	CH_4	C_2H_4	C_2H_6	CO	CO_2	O_2	H_2O	
700	3	0.0785	0.4628	0.0490	0.0006	0.0145	0.0962	0.0000	0.2416	1.94
700	3.5	0.0721	0.5152	0.0439	0.0008	0.0134	0.0864	0.0000	0.2162	1.65
700	4	0.0666	0.5579	0.0397	0.0009	0.0125	0.0785	0.0000	0.1956	1.55
700	4.5	0.0619	0.5936	0.0363	0.0010	0.0117	0.0719	0.0000	0.1786	1.52
700	5	0.0578	0.6237	0.0334	0.0010	0.0109	0.0663	0.0000	0.1644	1.45
700	5.5	0.0542	0.6495	0.0309	0.0011	0.0103	0.0615	0.0000	0.1522	1.49
700	6	0.0510	0.6719	0.0287	0.0011	0.0097	0.0574	0.0000	0.1417	1.50
700	6.5	0.0481	0.6915	0.0269	0.0011	0.0092	0.0538	0.0000	0.1326	1.56
700	7	0.0456	0.7087	0.0252	0.0011	0.0087	0.0506	0.0000	0.1246	1.71
700	7.5	0.0433	0.7241	0.0238	0.0011	0.0083	0.0478	0.0000	0.1175	1.57
700	8	0.0412	0.7378	0.0225	0.0011	0.0079	0.0452	0.0000	0.1112	1.82
700	8.5	0.0393	0.7502	0.0213	0.0011	0.0075	0.0430	0.0000	0.1055	1.70
700	9	0.0376	0.7613	0.0203	0.0011	0.0072	0.0409	0.0000	0.1003	1.83
700	9.5	0.0360	0.7715	0.0193	0.0011	0.0069	0.0391	0.0000	0.0957	2.05
700	10	0.0346	0.7808	0.0184	0.0011	0.0067	0.0373	0.0000	0.0914	1.93
725	3	0.0809	0.4603	0.0489	0.0005	0.0173	0.0945	0.0000	0.2410	1.41
725	3.5	0.0740	0.5129	0.0438	0.0007	0.0159	0.0849	0.0000	0.2159	1.30
725	4	0.0681	0.5559	0.0397	0.0008	0.0147	0.0771	0.0000	0.1955	1.26
725	4.5	0.0630	0.5917	0.0362	0.0009	0.0136	0.0706	0.0000	0.1787	1.22
725	5	0.0587	0.6220	0.0333	0.0009	0.0127	0.0651	0.0000	0.1645	1.24
725	5.5	0.0549	0.6480	0.0309	0.0010	0.0119	0.0604	0.0000	0.1524	1.24
725	6	0.0515	0.6705	0.0288	0.0010	0.0112	0.0563	0.0000	0.1420	1.17
725	6.5	0.0486	0.6901	0.0269	0.0010	0.0106	0.0528	0.0000	0.1329	1.25
725	7	0.0459	0.7075	0.0253	0.0010	0.0100	0.0496	0.0000	0.1249	1.20
725	7.5	0.0435	0.7229	0.0238	0.0010	0.0095	0.0469	0.0000	0.1178	1.34
725	8	0.0414	0.7367	0.0225	0.0010	0.0090	0.0444	0.0000	0.1115	1.30
725	8.5	0.0395	0.7491	0.0214	0.0010	0.0086	0.0421	0.0000	0.1058	1.27
725	9	0.0377	0.7603	0.0203	0.0010	0.0082	0.0401	0.0000	0.1007	1.25
725	9.5	0.0361	0.7705	0.0194	0.0010	0.0079	0.0383	0.0000	0.0960	1.49
725	10	0.0346	0.7798	0.0185	0.0010	0.0076	0.0366	0.0000	0.0918	1.45
750	3	0.0822	0.4582	0.0489	0.0005	0.0199	0.0927	0.0000	0.2411	1.10
750	3.5	0.0749	0.5111	0.0438	0.0006	0.0182	0.0832	0.0000	0.2161	1.08
750	4	0.0687	0.5543	0.0396	0.0007	0.0167	0.0755	0.0000	0.1958	1.06
750	4.5	0.0635	0.5903	0.0362	0.0008	0.0155	0.0692	0.0000	0.1791	1.06
750	5	0.0590	0.6207	0.0333	0.0008	0.0144	0.0638	0.0000	0.1649	1.06
750	5.5	0.0550	0.6468	0.0309	0.0009	0.0135	0.0592	0.0000	0.1529	1.06
750	6	0.0516	0.6693	0.0288	0.0009	0.0126	0.0552	0.0000	0.1425	1.08

Table B.2 Duo-equilibrium reaction model calculation result for La_2O_3/CaO catalyst

Temp (°C)	CH_4/O_2	Effluent Composition								RSS
		H_2	CH_4	C_2H_4	C_2H_6	CO	CO_2	O_2	H_2O	
750	6.5	0.0486	0.6891	0.0269	0.0009	0.0119	0.0517	0.0000	0.1334	1.10
750	7	0.0458	0.7065	0.0253	0.0009	0.0113	0.0486	0.0000	0.1254	1.11
750	7.5	0.0434	0.7219	0.0238	0.0009	0.0107	0.0459	0.0000	0.1183	1.13
750	8	0.0413	0.7357	0.0225	0.0009	0.0101	0.0435	0.0000	0.1120	1.15
750	8.5	0.0393	0.7481	0.0214	0.0009	0.0097	0.0413	0.0000	0.1063	1.15
750	9	0.0375	0.7594	0.0203	0.0009	0.0092	0.0393	0.0000	0.1011	1.18
750	9.5	0.0359	0.7696	0.0194	0.0009	0.0088	0.0375	0.0000	0.0965	1.18
750	10	0.0343	0.7789	0.0185	0.0009	0.0085	0.0359	0.0000	0.0922	1.22
775	3	0.0827	0.4567	0.0488	0.0004	0.0224	0.0908	0.0000	0.2416	1.00
775	3.5	0.0751	0.5097	0.0437	0.0006	0.0204	0.0815	0.0000	0.2167	0.98
775	4	0.0688	0.5531	0.0396	0.0006	0.0187	0.0740	0.0000	0.1965	0.98
775	4.5	0.0634	0.5892	0.0362	0.0007	0.0173	0.0677	0.0000	0.1797	0.97
775	5	0.0588	0.6197	0.0333	0.0007	0.0160	0.0625	0.0000	0.1656	0.99
775	5.5	0.0548	0.6458	0.0309	0.0008	0.0150	0.0579	0.0000	0.1535	1.00
775	6	0.0513	0.6684	0.0288	0.0008	0.0140	0.0540	0.0000	0.1431	1.01
775	6.5	0.0482	0.6881	0.0269	0.0008	0.0132	0.0506	0.0000	0.1340	1.02
775	7	0.0455	0.7055	0.0253	0.0008	0.0124	0.0476	0.0000	0.1260	1.04
775	7.5	0.0431	0.7210	0.0238	0.0008	0.0118	0.0449	0.0000	0.1189	1.06
775	8	0.0409	0.7348	0.0226	0.0008	0.0112	0.0425	0.0000	0.1125	1.08
775	8.5	0.0389	0.7472	0.0214	0.0008	0.0107	0.0404	0.0000	0.1068	1.10
775	9	0.0371	0.7585	0.0203	0.0008	0.0102	0.0385	0.0000	0.1017	1.12
775	9.5	0.0355	0.7687	0.0194	0.0008	0.0097	0.0367	0.0000	0.0970	1.13
775	10	0.0340	0.7780	0.0185	0.0008	0.0093	0.0351	0.0000	0.0927	1.16
800	3	0.0827	0.4555	0.0487	0.0004	0.0248	0.0888	0.0000	0.2425	0.97
800	3.5	0.0749	0.5087	0.0437	0.0005	0.0225	0.0798	0.0000	0.2176	0.97
800	4	0.0684	0.5521	0.0396	0.0006	0.0206	0.0724	0.0000	0.1973	0.97
800	4.5	0.0630	0.5882	0.0362	0.0006	0.0189	0.0663	0.0000	0.1805	0.98
800	5	0.0583	0.6187	0.0333	0.0007	0.0176	0.0611	0.0000	0.1664	0.98
800	5.5	0.0543	0.6449	0.0309	0.0007	0.0164	0.0567	0.0000	0.1543	0.99
800	6	0.0508	0.6675	0.0288	0.0007	0.0153	0.0529	0.0000	0.1438	1.00
800	6.5	0.0477	0.6872	0.0269	0.0007	0.0144	0.0495	0.0000	0.1347	1.02
800	7	0.0450	0.7046	0.0253	0.0007	0.0136	0.0466	0.0000	0.1267	1.04
800	7.5	0.0426	0.7201	0.0239	0.0008	0.0128	0.0440	0.0000	0.1195	1.06
800	8	0.0404	0.7339	0.0226	0.0008	0.0122	0.0416	0.0000	0.1131	1.09
800	8.5	0.0384	0.7463	0.0214	0.0008	0.0116	0.0395	0.0000	0.1074	1.11
800	9	0.0366	0.7575	0.0204	0.0008	0.0111	0.0376	0.0000	0.1022	1.13
800	9.5	0.0350	0.7677	0.0194	0.0008	0.0106	0.0359	0.0000	0.0975	1.16

Table B.2 Duo-equilibrium reaction model calculation result for La_2O_3/CaO catalyst

Temp (°C)	CH_4/O_2	Effluent Composition								RSS
		H_2	CH_4	C_2H_4	C_2H_6	CO	CO_2	O_2	H_2O	
800	10	0.0335	0.7770	0.0185	0.0008	0.0101	0.0343	0.0000	0.0932	1.18
825	3	0.0822	0.4545	0.0487	0.0004	0.0270	0.0869	0.0000	0.2435	0.99
825	3.5	0.0743	0.5078	0.0437	0.0005	0.0244	0.0781	0.0000	0.2186	0.97
825	4	0.0678	0.5512	0.0396	0.0005	0.0223	0.0709	0.0000	0.1983	0.97
825	4.5	0.0623	0.5874	0.0362	0.0006	0.0205	0.0649	0.0000	0.1815	0.96
825	5	0.0577	0.6179	0.0333	0.0006	0.0190	0.0598	0.0000	0.1672	0.97
825	5.5	0.0536	0.6440	0.0309	0.0006	0.0177	0.0555	0.0000	0.1551	0.99
825	6	0.0501	0.6666	0.0288	0.0007	0.0165	0.0517	0.0000	0.1446	1.01
825	6.5	0.0471	0.6864	0.0269	0.0007	0.0155	0.0485	0.0000	0.1354	1.03
825	7	0.0444	0.7038	0.0253	0.0007	0.0146	0.0456	0.0000	0.1273	1.06
825	7.5	0.0419	0.7192	0.0239	0.0007	0.0138	0.0430	0.0000	0.1202	1.08
825	8	0.0398	0.7330	0.0226	0.0007	0.0131	0.0407	0.0000	0.1138	1.12
825	8.5	0.0378	0.7454	0.0214	0.0007	0.0125	0.0387	0.0000	0.1080	1.15
825	9	0.0360	0.7565	0.0204	0.0007	0.0119	0.0368	0.0000	0.1028	1.18
825	9.5	0.0344	0.7667	0.0194	0.0007	0.0114	0.0351	0.0000	0.0981	1.22
825	10	0.0329	0.7760	0.0186	0.0007	0.0109	0.0336	0.0000	0.0938	1.25
850	3	0.0814	0.4538	0.0487	0.0003	0.0291	0.0851	0.0000	0.2447	1.02
850	3.5	0.0735	0.5070	0.0437	0.0004	0.0263	0.0764	0.0000	0.2197	0.98
850	4	0.0670	0.5505	0.0396	0.0005	0.0240	0.0693	0.0000	0.1993	0.99
850	4.5	0.0615	0.5866	0.0362	0.0005	0.0220	0.0635	0.0000	0.1824	0.99
850	5	0.0569	0.6172	0.0333	0.0006	0.0204	0.0585	0.0000	0.1681	1.00
850	5.5	0.0529	0.6432	0.0309	0.0006	0.0189	0.0543	0.0000	0.1559	1.03
850	6	0.0494	0.6658	0.0288	0.0006	0.0177	0.0506	0.0000	0.1454	1.06
850	6.5	0.0463	0.6855	0.0269	0.0006	0.0166	0.0474	0.0000	0.1362	1.10
850	7	0.0436	0.7028	0.0253	0.0006	0.0156	0.0446	0.0000	0.1280	1.12
850	7.5	0.0412	0.7182	0.0239	0.0006	0.0148	0.0421	0.0000	0.1208	1.17
850	8	0.0391	0.7320	0.0226	0.0006	0.0140	0.0398	0.0000	0.1144	1.20
850	8.5	0.0371	0.7443	0.0214	0.0006	0.0133	0.0378	0.0000	0.1086	1.27
850	9	0.0354	0.7555	0.0204	0.0006	0.0127	0.0360	0.0000	0.1034	1.29
850	9.5	0.0338	0.7656	0.0194	0.0006	0.0121	0.0343	0.0000	0.0986	1.32
850	10	0.0323	0.7749	0.0186	0.0006	0.0116	0.0328	0.0000	0.0943	1.41
875	3	0.0804	0.4531	0.0486	0.0003	0.0311	0.0833	0.0000	0.2459	1.25
875	3.5	0.0725	0.5064	0.0436	0.0004	0.0280	0.0748	0.0000	0.2208	1.22
875	4	0.0660	0.5498	0.0396	0.0005	0.0255	0.0679	0.0000	0.2004	1.22
875	4.5	0.0606	0.5859	0.0362	0.0005	0.0234	0.0621	0.0000	0.1834	1.23
875	5	0.0560	0.6164	0.0333	0.0005	0.0217	0.0573	0.0000	0.1690	1.25
875	5.5	0.0520	0.6424	0.0309	0.0005	0.0201	0.0531	0.0000	0.1567	1.28

Table B.2 Duo-equilibrium reaction model calculation result for La_2O_3/CaO catalyst

Temp (°C)	CH_4/O_2	Effluent Composition								RSS
		H_2	CH_4	C_2H_4	C_2H_6	CO	CO_2	O_2	H_2O	
875	6	0.0486	0.6649	0.0288	0.0006	0.0188	0.0495	0.0000	0.1461	1.34
875	6.5	0.0455	0.6846	0.0269	0.0006	0.0176	0.0464	0.0000	0.1369	1.36
875	7	0.0429	0.7019	0.0253	0.0006	0.0166	0.0436	0.0000	0.1287	1.40
875	7.5	0.0405	0.7172	0.0238	0.0006	0.0157	0.0412	0.0000	0.1215	1.44
875	8	0.0384	0.7309	0.0226	0.0006	0.0149	0.0390	0.0000	0.1150	1.50
875	8.5	0.0365	0.7432	0.0214	0.0006	0.0141	0.0370	0.0000	0.1092	1.58
875	9	0.0347	0.7544	0.0204	0.0006	0.0135	0.0352	0.0000	0.1039	1.62
875	9.5	0.0332	0.7644	0.0194	0.0006	0.0128	0.0336	0.0000	0.0991	1.66
875	10	0.0317	0.7736	0.0185	0.0006	0.0123	0.0321	0.0000	0.0948	1.72

Table B.3 Trio-equilibrium reaction model calculation result for PbO/Al_2O_3 catalyst

Temp (°C)	CH_4/O_2	Effluent Composition								RSS
		H_2	CH_4	C_2H_4	C_2H_6	CO	CO_2	O_2	H_2O	
650	5	0.0010	0.7311	0.0077	0.0014	0.0078	0.0732	0.0000	0.1778	1.86
650	5.5	0.0010	0.7521	0.0065	0.0014	0.0074	0.0677	0.0000	0.1638	1.26
650	6	0.0010	0.7701	0.0056	0.0015	0.0070	0.0630	0.0000	0.1518	1.29
650	6.5	0.0009	0.7857	0.0049	0.0015	0.0066	0.0589	0.0000	0.1414	1.41
650	7	0.0009	0.7993	0.0043	0.0015	0.0063	0.0553	0.0000	0.1324	1.50
650	7.5	0.0009	0.8113	0.0038	0.0015	0.0061	0.0521	0.0000	0.1244	1.61
650	8	0.0009	0.8219	0.0033	0.0015	0.0058	0.0493	0.0000	0.1174	1.69
650	8.5	0.0009	0.8313	0.0030	0.0015	0.0056	0.0467	0.0000	0.1110	1.76
650	9	0.0009	0.8399	0.0026	0.0015	0.0053	0.0444	0.0000	0.1054	1.84
650	9.5	0.0009	0.8475	0.0024	0.0015	0.0051	0.0423	0.0000	0.1003	1.85
650	10	0.0009	0.8545	0.0021	0.0015	0.0049	0.0404	0.0000	0.0956	1.92
675	5	0.0017	0.7314	0.0065	0.0012	0.0098	0.0724	0.0000	0.1770	2.20
675	5.5	0.0016	0.7522	0.0056	0.0013	0.0092	0.0669	0.0000	0.1632	2.15
675	6	0.0016	0.7701	0.0049	0.0013	0.0087	0.0622	0.0000	0.1513	2.12
675	6.5	0.0015	0.7855	0.0043	0.0013	0.0082	0.0582	0.0000	0.1410	2.10
675	7	0.0015	0.7990	0.0038	0.0013	0.0078	0.0546	0.0000	0.1321	2.21
675	7.5	0.0014	0.8109	0.0033	0.0013	0.0074	0.0514	0.0000	0.1242	2.22
675	8	0.0014	0.8214	0.0030	0.0013	0.0071	0.0486	0.0000	0.1172	2.24
675	8.5	0.0014	0.8308	0.0027	0.0013	0.0068	0.0461	0.0000	0.1109	2.24
675	9	0.0014	0.8393	0.0024	0.0013	0.0065	0.0438	0.0000	0.1053	2.25
675	9.5	0.0013	0.8470	0.0022	0.0013	0.0062	0.0417	0.0000	0.1002	2.26
675	10	0.0013	0.8539	0.0020	0.0013	0.0060	0.0398	0.0000	0.0956	2.23
700	5	0.0025	0.7305	0.0060	0.0011	0.0117	0.0713	0.0000	0.1768	1.62
700	5.5	0.0024	0.7513	0.0053	0.0011	0.0110	0.0659	0.0000	0.1630	1.65
700	6	0.0023	0.7691	0.0046	0.0012	0.0103	0.0612	0.0000	0.1513	1.70
700	6.5	0.0022	0.7845	0.0041	0.0012	0.0097	0.0572	0.0000	0.1411	1.73
700	7	0.0022	0.7979	0.0037	0.0012	0.0092	0.0537	0.0000	0.1322	1.77
700	7.5	0.0021	0.8098	0.0033	0.0012	0.0088	0.0505	0.0000	0.1243	1.80
700	8	0.0020	0.8204	0.0030	0.0012	0.0083	0.0478	0.0000	0.1173	1.85
700	8.5	0.0020	0.8298	0.0027	0.0012	0.0079	0.0453	0.0000	0.1111	1.88
700	9	0.0019	0.8383	0.0025	0.0012	0.0076	0.0430	0.0000	0.1055	3.06
700	9.5	0.0019	0.8459	0.0023	0.0012	0.0073	0.0410	0.0000	0.1005	2.93
700	10	0.0018	0.8529	0.0021	0.0012	0.0070	0.0391	0.0000	0.0959	2.83
725	5	0.0035	0.7288	0.0061	0.0010	0.0137	0.0700	0.0000	0.1770	1.59
725	5.5	0.0033	0.7496	0.0054	0.0010	0.0127	0.0647	0.0000	0.1633	1.63
725	6	0.0032	0.7674	0.0048	0.0010	0.0119	0.0601	0.0000	0.1515	1.66
725	6.5	0.0030	0.7828	0.0043	0.0011	0.0112	0.0561	0.0000	0.1414	1.70

Table B.3 Trio-equilibrium reaction model calculation result for PbO/Al_2O_3 catalyst

Temp (°C)	CH_4/O_2	Effluent Composition								RSS
		H_2	CH_4	C_2H_4	C_2H_6	CO	CO_2	O_2	H_2O	
725	7	0.0029	0.7963	0.0039	0.0011	0.0106	0.0527	0.0000	0.1325	1.73
725	7.5	0.0028	0.8083	0.0036	0.0011	0.0101	0.0496	0.0000	0.1247	1.76
725	8	0.0027	0.8189	0.0033	0.0011	0.0095	0.0469	0.0000	0.1177	1.79
725	8.5	0.0026	0.8283	0.0030	0.0011	0.0091	0.0444	0.0000	0.1115	1.82
725	9	0.0025	0.8369	0.0028	0.0011	0.0087	0.0422	0.0000	0.1059	1.85
725	9.5	0.0024	0.8446	0.0026	0.0011	0.0083	0.0402	0.0000	0.1008	1.88
725	10	0.0023	0.8516	0.0024	0.0011	0.0079	0.0384	0.0000	0.0962	1.90
750	5	0.0046	0.7265	0.0065	0.0009	0.0155	0.0686	0.0000	0.1774	3.31
750	5.5	0.0043	0.7474	0.0058	0.0009	0.0144	0.0634	0.0000	0.1638	2.25
750	6	0.0041	0.7653	0.0052	0.0009	0.0135	0.0589	0.0000	0.1521	2.14
750	6.5	0.0039	0.7808	0.0048	0.0010	0.0127	0.0550	0.0000	0.1419	2.08
750	7	0.0037	0.7944	0.0044	0.0010	0.0119	0.0516	0.0000	0.1330	2.04
750	7.5	0.0036	0.8064	0.0040	0.0010	0.0113	0.0486	0.0000	0.1252	2.02
750	8	0.0034	0.8171	0.0037	0.0010	0.0107	0.0459	0.0000	0.1182	2.01
750	8.5	0.0033	0.8266	0.0035	0.0010	0.0102	0.0435	0.0000	0.1120	2.00
750	9	0.0031	0.8352	0.0032	0.0010	0.0097	0.0413	0.0000	0.1064	2.00
750	9.5	0.0030	0.8430	0.0030	0.0010	0.0093	0.0394	0.0000	0.1013	2.00
750	10	0.0029	0.8501	0.0029	0.0010	0.0089	0.0376	0.0000	0.0967	2.00

Appendix C: Manipulated Equilibrium Model Results and Validation

Table C.1 Manipulated Trio-equilibrium reaction model calculation result for $Mn/Na_2WO_4/SiO_2$ catalyst

Temp (°C)	CH_4/O_2	Effluent Composition								RSS
		H_2	CH_4	C_2H_4	C_2H_6	CO	CO_2	O_2	H_2O	
700	3	0.0005	0.3495	0.0974	0.0311	0.0073	0.0486	0.0000	0.3371	4.37
700	3.5	0.0005	0.4102	0.0850	0.0327	0.0068	0.0438	0.0000	0.3034	3.81
700	4	0.0005	0.4598	0.0749	0.0340	0.0063	0.0399	0.0000	0.2757	3.52
700	4.5	0.0004	0.5011	0.0665	0.0351	0.0059	0.0366	0.0000	0.2527	3.36
700	5	0.0004	0.5360	0.0594	0.0360	0.0056	0.0338	0.0000	0.2333	3.32
700	5.5	0.0004	0.5660	0.0534	0.0368	0.0052	0.0315	0.0000	0.2166	3.38
700	6	0.0004	0.5919	0.0482	0.0375	0.0050	0.0294	0.0000	0.2021	3.53
700	6.5	0.0004	0.6146	0.0436	0.0381	0.0047	0.0276	0.0000	0.1894	3.77
700	7	0.0004	0.6345	0.0396	0.0386	0.0045	0.0260	0.0000	0.1783	4.09
700	7.5	0.0004	0.6523	0.0360	0.0391	0.0043	0.0245	0.0000	0.1683	4.45
700	8	0.0003	0.6682	0.0328	0.0395	0.0041	0.0233	0.0000	0.1595	4.74
700	8.5	0.0003	0.6825	0.0300	0.0399	0.0039	0.0221	0.0000	0.1515	5.19
700	9	0.0003	0.6954	0.0274	0.0402	0.0037	0.0211	0.0000	0.1443	5.70
700	9.5	0.0003	0.7072	0.0251	0.0405	0.0036	0.0201	0.0000	0.1377	6.42
700	10	0.0003	0.7179	0.0229	0.0408	0.0034	0.0192	0.0000	0.1317	6.88
725	3	0.0008	0.3498	0.0968	0.0311	0.0087	0.0478	0.0000	0.3371	1.73
725	3.5	0.0007	0.4103	0.0845	0.0327	0.0081	0.0431	0.0000	0.3034	1.48
725	4	0.0007	0.4597	0.0745	0.0340	0.0075	0.0392	0.0000	0.2758	1.35
725	4.5	0.0006	0.5009	0.0662	0.0351	0.0069	0.0360	0.0000	0.2528	1.30
725	5	0.0006	0.5358	0.0592	0.0360	0.0065	0.0333	0.0000	0.2334	1.31
725	5.5	0.0006	0.5657	0.0532	0.0368	0.0061	0.0309	0.0000	0.2167	1.38
725	6	0.0006	0.5915	0.0481	0.0375	0.0057	0.0289	0.0000	0.2022	1.50
725	6.5	0.0005	0.6142	0.0435	0.0381	0.0054	0.0271	0.0000	0.1896	1.66
725	7	0.0005	0.6341	0.0395	0.0386	0.0051	0.0255	0.0000	0.1784	1.84
725	7.5	0.0005	0.6519	0.0360	0.0391	0.0049	0.0241	0.0000	0.1685	2.08
725	8	0.0005	0.6677	0.0328	0.0395	0.0047	0.0228	0.0000	0.1597	2.36
725	8.5	0.0005	0.6820	0.0300	0.0398	0.0044	0.0217	0.0000	0.1517	2.69
725	9	0.0005	0.6949	0.0274	0.0402	0.0042	0.0207	0.0000	0.1444	3.01
725	9.5	0.0005	0.7067	0.0251	0.0405	0.0041	0.0197	0.0000	0.1379	3.40
725	10	0.0004	0.7174	0.0230	0.0408	0.0039	0.0189	0.0000	0.1319	3.83
750	3	0.0011	0.3495	0.0965	0.0311	0.0101	0.0470	0.0000	0.3372	0.74
750	3.5	0.0010	0.4099	0.0843	0.0327	0.0092	0.0423	0.0000	0.3035	0.59
750	4	0.0009	0.4592	0.0744	0.0340	0.0085	0.0385	0.0000	0.2760	0.52

Table C.1 Manipulated Trio-equilibrium reaction model calculation result for $Mn/Na_2WO_4/SiO_2$ catalyst

Temp (°C)	CH_4/O_2	Effluent Composition								RSS
		H_2	CH_4	C_2H_4	C_2H_6	CO	CO_2	O_2	H_2O	
750	4.5	0.0009	0.5004	0.0662	0.0351	0.0079	0.0353	0.0000	0.2530	0.50
750	5	0.0008	0.5352	0.0592	0.0360	0.0074	0.0326	0.0000	0.2336	0.51
750	5.5	0.0008	0.5650	0.0533	0.0368	0.0069	0.0303	0.0000	0.2169	0.56
750	6	0.0008	0.5909	0.0481	0.0374	0.0065	0.0283	0.0000	0.2025	0.64
750	6.5	0.0007	0.6135	0.0436	0.0380	0.0061	0.0266	0.0000	0.1898	0.74
750	7	0.0007	0.6335	0.0396	0.0386	0.0058	0.0250	0.0000	0.1787	0.88
750	7.5	0.0007	0.6512	0.0361	0.0390	0.0055	0.0236	0.0000	0.1688	1.04
750	8	0.0007	0.6671	0.0329	0.0395	0.0052	0.0224	0.0000	0.1599	1.22
750	8.5	0.0006	0.6813	0.0301	0.0398	0.0050	0.0213	0.0000	0.1519	1.43
750	9	0.0006	0.6943	0.0275	0.0402	0.0048	0.0203	0.0000	0.1447	1.66
750	9.5	0.0006	0.7060	0.0252	0.0405	0.0046	0.0193	0.0000	0.1381	1.96
750	10	0.0006	0.7167	0.0231	0.0408	0.0044	0.0185	0.0000	0.1321	2.26
775	3	0.0015	0.3488	0.0964	0.0311	0.0114	0.0460	0.0000	0.3373	0.36
775	3.5	0.0013	0.4090	0.0844	0.0327	0.0104	0.0415	0.0000	0.3037	0.25
775	4	0.0013	0.4584	0.0745	0.0340	0.0095	0.0377	0.0000	0.2762	0.20
775	4.5	0.0012	0.4995	0.0663	0.0350	0.0088	0.0346	0.0000	0.2533	0.17
775	5	0.0011	0.5343	0.0593	0.0360	0.0082	0.0320	0.0000	0.2339	0.18
775	5.5	0.0011	0.5641	0.0534	0.0367	0.0077	0.0297	0.0000	0.2172	0.20
775	6	0.0010	0.5900	0.0482	0.0374	0.0072	0.0277	0.0000	0.2028	0.24
775	6.5	0.0010	0.6126	0.0438	0.0380	0.0068	0.0260	0.0000	0.1901	0.31
775	7	0.0009	0.6326	0.0398	0.0385	0.0064	0.0245	0.0000	0.1790	0.40
775	7.5	0.0009	0.6503	0.0363	0.0390	0.0061	0.0231	0.0000	0.1690	0.49
775	8	0.0009	0.6662	0.0331	0.0394	0.0058	0.0219	0.0000	0.1601	0.63
775	8.5	0.0008	0.6805	0.0303	0.0398	0.0055	0.0208	0.0000	0.1522	0.77
775	9	0.0008	0.6934	0.0277	0.0401	0.0052	0.0198	0.0000	0.1449	0.94
775	9.5	0.0008	0.7052	0.0254	0.0405	0.0050	0.0189	0.0000	0.1383	1.11
775	10	0.0008	0.7159	0.0233	0.0407	0.0048	0.0181	0.0000	0.1323	1.33
800	3	0.0019	0.3476	0.0966	0.0310	0.0126	0.0451	0.0000	0.3376	0.23
800	3.5	0.0018	0.4079	0.0845	0.0326	0.0114	0.0406	0.0000	0.3040	0.14
800	4	0.0016	0.4572	0.0747	0.0339	0.0105	0.0370	0.0000	0.2765	0.09
800	4.5	0.0015	0.4983	0.0665	0.0350	0.0097	0.0339	0.0000	0.2536	0.05
800	5	0.0015	0.5331	0.0596	0.0359	0.0090	0.0313	0.0000	0.2342	0.04
800	5.5	0.0014	0.5630	0.0536	0.0367	0.0084	0.0291	0.0000	0.2175	0.04
800	6	0.0013	0.5889	0.0485	0.0374	0.0079	0.0271	0.0000	0.2031	0.07
800	6.5	0.0013	0.6115	0.0440	0.0380	0.0074	0.0255	0.0000	0.1904	0.10
800	7	0.0012	0.6315	0.0400	0.0385	0.0070	0.0240	0.0000	0.1792	0.15

Table C.1 Manipulated Trio-equilibrium reaction model calculation result for $Mn/Na_2WO_4/SiO_2$ catalyst

Temp (°C)	CH_4/O_2	Effluent Composition								RSS
		H_2	CH_4	C_2H_4	C_2H_6	CO	CO_2	O_2	H_2O	
800	7.5	0.0012	0.6493	0.0365	0.0390	0.0066	0.0226	0.0000	0.1693	0.21
800	8	0.0011	0.6652	0.0333	0.0394	0.0063	0.0215	0.0000	0.1604	0.30
800	8.5	0.0011	0.6795	0.0305	0.0398	0.0060	0.0204	0.0000	0.1524	0.40
800	9	0.0011	0.6925	0.0279	0.0401	0.0057	0.0194	0.0000	0.1452	0.50
800	9.5	0.0010	0.7043	0.0256	0.0404	0.0055	0.0185	0.0000	0.1386	0.63
800	10	0.0010	0.7150	0.0235	0.0407	0.0052	0.0177	0.0000	0.1326	0.77
825	3	0.0025	0.3462	0.0968	0.0310	0.0137	0.0441	0.0000	0.3378	0.24
825	3.5	0.0023	0.4064	0.0848	0.0326	0.0124	0.0397	0.0000	0.3043	0.15
825	4	0.0021	0.4558	0.0750	0.0339	0.0114	0.0362	0.0000	0.2768	0.09
825	4.5	0.0020	0.4969	0.0668	0.0350	0.0105	0.0332	0.0000	0.2539	0.05
825	5	0.0019	0.5318	0.0599	0.0359	0.0097	0.0306	0.0000	0.2345	0.02
825	5.5	0.0018	0.5617	0.0539	0.0367	0.0091	0.0285	0.0000	0.2178	0.01
825	6	0.0017	0.5876	0.0488	0.0374	0.0085	0.0266	0.0000	0.2034	0.00
825	6.5	0.0016	0.6103	0.0443	0.0380	0.0080	0.0249	0.0000	0.1907	0.01
825	7	0.0015	0.6303	0.0403	0.0385	0.0075	0.0235	0.0000	0.1795	0.03
825	7.5	0.0015	0.6481	0.0368	0.0390	0.0071	0.0222	0.0000	0.1696	0.06
825	8	0.0014	0.6641	0.0336	0.0394	0.0068	0.0210	0.0000	0.1607	0.11
825	8.5	0.0014	0.6784	0.0308	0.0398	0.0064	0.0199	0.0000	0.1527	0.16
825	9	0.0014	0.6914	0.0282	0.0401	0.0061	0.0190	0.0000	0.1455	0.24
825	9.5	0.0013	0.7032	0.0259	0.0404	0.0059	0.0181	0.0000	0.1389	0.31
825	10	0.0013	0.7140	0.0237	0.0407	0.0056	0.0174	0.0000	0.1328	0.39
850	3	0.0031	0.3445	0.0972	0.0310	0.0148	0.0432	0.0000	0.3381	0.35
850	3.5	0.0029	0.4048	0.0852	0.0325	0.0134	0.0389	0.0000	0.3046	0.25
850	4	0.0027	0.4542	0.0754	0.0338	0.0122	0.0354	0.0000	0.2771	0.19
850	4.5	0.0025	0.4954	0.0672	0.0349	0.0113	0.0325	0.0000	0.2542	0.13
850	5	0.0024	0.5303	0.0602	0.0359	0.0104	0.0300	0.0000	0.2348	0.09
850	5.5	0.0022	0.5602	0.0543	0.0366	0.0097	0.0278	0.0000	0.2181	0.06
850	6	0.0021	0.5862	0.0491	0.0373	0.0091	0.0260	0.0000	0.2037	0.03
850	6.5	0.0020	0.6090	0.0446	0.0379	0.0085	0.0244	0.0000	0.1910	0.02
850	7	0.0019	0.6290	0.0406	0.0385	0.0081	0.0230	0.0000	0.1798	0.01
850	7.5	0.0019	0.6469	0.0371	0.0389	0.0076	0.0217	0.0000	0.1699	0.02
850	8	0.0018	0.6629	0.0339	0.0393	0.0072	0.0205	0.0000	0.1610	0.03
850	8.5	0.0017	0.6773	0.0311	0.0397	0.0069	0.0195	0.0000	0.1530	0.06
850	9	0.0017	0.6903	0.0285	0.0401	0.0066	0.0186	0.0000	0.1457	0.09
850	9.5	0.0017	0.7021	0.0262	0.0404	0.0063	0.0178	0.0000	0.1391	0.14
850	10	0.0016	0.7129	0.0240	0.0407	0.0060	0.0170	0.0000	0.1331	0.19

Table C.1 Manipulated Trio-equilibrium reaction model calculation result for $Mn/Na_2WO_4/SiO_2$ catalyst

Temp (°C)	CH_4/O_2	Effluent Composition								RSS
		H_2	CH_4	C_2H_4	C_2H_6	CO	CO_2	O_2	H_2O	
875	3	0.0039	0.3426	0.0977	0.0309	0.0157	0.0422	0.0000	0.3383	0.67
875	3.5	0.0036	0.4030	0.0857	0.0325	0.0143	0.0380	0.0000	0.3048	0.55
875	4	0.0033	0.4524	0.0758	0.0338	0.0130	0.0346	0.0000	0.2774	0.45
875	4.5	0.0031	0.4937	0.0676	0.0349	0.0120	0.0318	0.0000	0.2545	0.36
875	5	0.0029	0.5287	0.0607	0.0358	0.0111	0.0293	0.0000	0.2351	0.28
875	5.5	0.0027	0.5587	0.0547	0.0366	0.0103	0.0272	0.0000	0.2184	0.22
875	6	0.0026	0.5847	0.0495	0.0373	0.0097	0.0254	0.0000	0.2039	0.18
875	6.5	0.0025	0.6075	0.0450	0.0379	0.0091	0.0239	0.0000	0.1913	0.13
875	7	0.0024	0.6276	0.0410	0.0384	0.0086	0.0225	0.0000	0.1801	0.10
875	7.5	0.0023	0.6455	0.0375	0.0389	0.0081	0.0212	0.0000	0.1701	0.08
875	8	0.0022	0.6616	0.0343	0.0393	0.0077	0.0201	0.0000	0.1612	0.07
875	8.5	0.0021	0.6760	0.0314	0.0397	0.0073	0.0191	0.0000	0.1532	0.07
875	9	0.0021	0.6890	0.0288	0.0400	0.0070	0.0182	0.0000	0.1460	0.07
875	9.5	0.0020	0.7009	0.0265	0.0404	0.0066	0.0174	0.0000	0.1394	0.09
875	10	0.0020	0.7117	0.0243	0.0406	0.0064	0.0166	0.0000	0.1333	0.11

Table C.2 Manipulated Duo-equilibrium reaction model calculation result for La_2O_3/CaO catalyst

Temp (°C)	CH_4/O_2	Effluent Composition								RSS
		H_2	CH_4	C_2H_4	C_2H_6	CO	CO_2	O_2	H_2O	
700	3	0.0762	0.4518	0.0428	0.0142	0.0179	0.0936	0.0000	0.2465	299.26
700	3.5	0.0703	0.5038	0.0375	0.0149	0.0165	0.0840	0.0000	0.2206	113.80
700	4	0.0652	0.5463	0.0332	0.0154	0.0154	0.0762	0.0000	0.1997	50.27
700	4.5	0.0608	0.5816	0.0296	0.0159	0.0144	0.0697	0.0000	0.1825	25.51
700	5	0.0570	0.6115	0.0266	0.0163	0.0135	0.0643	0.0000	0.1680	16.96
700	5.5	0.0537	0.6370	0.0241	0.0166	0.0127	0.0596	0.0000	0.1556	9.90
700	6	0.0508	0.6591	0.0219	0.0169	0.0120	0.0555	0.0000	0.1450	6.88
700	6.5	0.0482	0.6784	0.0200	0.0171	0.0114	0.0520	0.0000	0.1357	4.50
700	7	0.0459	0.6954	0.0183	0.0174	0.0109	0.0489	0.0000	0.1276	2.82
700	7.5	0.0438	0.7105	0.0169	0.0176	0.0104	0.0461	0.0000	0.1204	3.06
700	8	0.0420	0.7240	0.0156	0.0177	0.0099	0.0436	0.0000	0.1139	1.80
700	8.5	0.0403	0.7361	0.0144	0.0179	0.0095	0.0414	0.0000	0.1081	1.90
700	9	0.0388	0.7470	0.0134	0.0180	0.0092	0.0393	0.0000	0.1029	1.46
700	9.5	0.0374	0.7570	0.0124	0.0182	0.0088	0.0375	0.0000	0.0982	1.15
700	10	0.0361	0.7660	0.0116	0.0183	0.0085	0.0358	0.0000	0.0939	1.16
725	3	0.0790	0.4490	0.0427	0.0142	0.0204	0.0921	0.0000	0.2456	31.43
725	3.5	0.0726	0.5012	0.0375	0.0149	0.0188	0.0827	0.0000	0.2201	13.35
725	4	0.0671	0.5438	0.0333	0.0154	0.0174	0.0750	0.0000	0.1994	6.43
725	4.5	0.0625	0.5792	0.0298	0.0159	0.0162	0.0686	0.0000	0.1823	4.06
725	5	0.0585	0.6091	0.0268	0.0162	0.0151	0.0631	0.0000	0.1680	2.28
725	5.5	0.0550	0.6347	0.0243	0.0166	0.0142	0.0585	0.0000	0.1557	1.58
725	6	0.0520	0.6568	0.0222	0.0169	0.0135	0.0545	0.0000	0.1451	1.80
725	6.5	0.0494	0.6761	0.0203	0.0171	0.0128	0.0510	0.0000	0.1359	0.95
725	7	0.0470	0.6931	0.0187	0.0173	0.0121	0.0479	0.0000	0.1278	1.04
725	7.5	0.0449	0.7082	0.0173	0.0175	0.0116	0.0452	0.0000	0.1206	0.52
725	8	0.0430	0.7216	0.0160	0.0177	0.0111	0.0427	0.0000	0.1142	0.55
725	8.5	0.0413	0.7337	0.0149	0.0179	0.0106	0.0405	0.0000	0.1085	0.60
725	9	0.0398	0.7446	0.0138	0.0180	0.0102	0.0385	0.0000	0.1033	0.64
725	9.5	0.0384	0.7544	0.0129	0.0181	0.0098	0.0367	0.0000	0.0985	0.32
725	10	0.0372	0.7634	0.0121	0.0182	0.0095	0.0350	0.0000	0.0943	0.33
750	3	0.0808	0.4467	0.0427	0.0141	0.0228	0.0905	0.0000	0.2454	6.44
750	3.5	0.0741	0.4990	0.0376	0.0148	0.0209	0.0812	0.0000	0.2201	2.32
750	4	0.0684	0.5416	0.0334	0.0154	0.0193	0.0736	0.0000	0.1995	1.12
750	4.5	0.0636	0.5770	0.0300	0.0158	0.0179	0.0673	0.0000	0.1825	0.64
750	5	0.0596	0.6069	0.0271	0.0162	0.0167	0.0620	0.0000	0.1682	0.40
750	5.5	0.0560	0.6324	0.0247	0.0165	0.0157	0.0574	0.0000	0.1560	0.30
750	6	0.0530	0.6545	0.0226	0.0168	0.0148	0.0534	0.0000	0.1455	0.21

Table C.2 Manipulated Duo-equilibrium reaction model calculation result for La_2O_3/CaO catalyst

Temp (°C)	CH_4/O_2	Effluent Composition								RSS
		H_2	CH_4	C_2H_4	C_2H_6	CO	CO_2	O_2	H_2O	
750	6.5	0.0503	0.6737	0.0207	0.0171	0.0141	0.0500	0.0000	0.1363	0.15
750	7	0.0479	0.6907	0.0192	0.0173	0.0134	0.0469	0.0000	0.1282	0.14
750	7.5	0.0458	0.7057	0.0178	0.0175	0.0128	0.0442	0.0000	0.1211	0.13
750	8	0.0440	0.7190	0.0165	0.0177	0.0122	0.0417	0.0000	0.1147	0.12
750	8.5	0.0423	0.7310	0.0154	0.0178	0.0117	0.0395	0.0000	0.1089	0.14
750	9	0.0408	0.7418	0.0145	0.0180	0.0113	0.0376	0.0000	0.1037	0.14
750	9.5	0.0394	0.7516	0.0136	0.0181	0.0109	0.0357	0.0000	0.0990	0.16
750	10	0.0382	0.7605	0.0128	0.0182	0.0105	0.0341	0.0000	0.0947	0.15
775	3	0.0819	0.4448	0.0428	0.0141	0.0249	0.0889	0.0000	0.2455	1.21
775	3.5	0.0750	0.4970	0.0377	0.0148	0.0228	0.0797	0.0000	0.2204	0.56
775	4	0.0692	0.5396	0.0336	0.0153	0.0210	0.0722	0.0000	0.1999	0.31
775	4.5	0.0644	0.5749	0.0303	0.0158	0.0195	0.0660	0.0000	0.1830	0.25
775	5	0.0603	0.6047	0.0275	0.0162	0.0182	0.0607	0.0000	0.1687	0.11
775	5.5	0.0568	0.6302	0.0251	0.0165	0.0171	0.0562	0.0000	0.1565	0.09
775	6	0.0537	0.6521	0.0230	0.0168	0.0162	0.0523	0.0000	0.1460	0.07
775	6.5	0.0511	0.6712	0.0213	0.0171	0.0153	0.0488	0.0000	0.1368	0.08
775	7	0.0488	0.6881	0.0197	0.0173	0.0146	0.0458	0.0000	0.1288	0.08
775	7.5	0.0467	0.7029	0.0184	0.0175	0.0139	0.0431	0.0000	0.1216	0.09
775	8	0.0449	0.7162	0.0172	0.0176	0.0133	0.0407	0.0000	0.1152	0.10
775	8.5	0.0432	0.7281	0.0161	0.0178	0.0128	0.0385	0.0000	0.1095	0.11
775	9	0.0418	0.7388	0.0152	0.0179	0.0123	0.0366	0.0000	0.1043	0.12
775	9.5	0.0405	0.7484	0.0144	0.0181	0.0119	0.0348	0.0000	0.0996	0.14
775	10	0.0393	0.7572	0.0136	0.0182	0.0115	0.0331	0.0000	0.0953	0.15
800	3	0.0825	0.4432	0.0429	0.0141	0.0270	0.0873	0.0000	0.2460	0.51
800	3.5	0.0755	0.4953	0.0379	0.0148	0.0246	0.0783	0.0000	0.2209	0.25
800	4	0.0698	0.5377	0.0339	0.0153	0.0227	0.0708	0.0000	0.2005	0.14
800	4.5	0.0650	0.5728	0.0307	0.0158	0.0211	0.0647	0.0000	0.1836	0.10
800	5	0.0609	0.6025	0.0279	0.0162	0.0197	0.0594	0.0000	0.1693	0.07
800	5.5	0.0574	0.6277	0.0256	0.0165	0.0185	0.0550	0.0000	0.1572	0.07
800	6	0.0545	0.6495	0.0236	0.0168	0.0175	0.0511	0.0000	0.1467	0.07
800	6.5	0.0519	0.6685	0.0219	0.0170	0.0166	0.0477	0.0000	0.1375	0.08
800	7	0.0496	0.6851	0.0204	0.0172	0.0158	0.0447	0.0000	0.1294	0.09
800	7.5	0.0476	0.6999	0.0192	0.0174	0.0151	0.0420	0.0000	0.1223	0.10
800	8	0.0459	0.7130	0.0180	0.0176	0.0144	0.0396	0.0000	0.1159	0.12
800	8.5	0.0443	0.7247	0.0170	0.0178	0.0139	0.0375	0.0000	0.1101	0.13
800	9	0.0429	0.7353	0.0161	0.0179	0.0134	0.0355	0.0000	0.1050	0.15
800	9.5	0.0417	0.7448	0.0153	0.0180	0.0129	0.0337	0.0000	0.1002	0.17

Table C.2 Manipulated Duo-equilibrium reaction model calculation result for La_2O_3/CaO catalyst

Temp (°C)	CH_4/O_2	Effluent Composition								RSS
		H_2	CH_4	C_2H_4	C_2H_6	CO	CO_2	O_2	H_2O	
800	10	0.0405	0.7535	0.0146	0.0181	0.0125	0.0321	0.0000	0.0960	0.18
825	3	0.0828	0.4417	0.0430	0.0141	0.0289	0.0857	0.0000	0.2467	0.25
825	3.5	0.0758	0.4935	0.0382	0.0148	0.0264	0.0768	0.0000	0.2216	0.12
825	4	0.0701	0.5357	0.0343	0.0153	0.0243	0.0694	0.0000	0.2012	0.06
825	4.5	0.0654	0.5706	0.0311	0.0158	0.0226	0.0633	0.0000	0.1843	0.04
825	5	0.0615	0.6000	0.0285	0.0161	0.0211	0.0581	0.0000	0.1701	0.03
825	5.5	0.0581	0.6250	0.0263	0.0165	0.0198	0.0537	0.0000	0.1579	0.03
825	6	0.0552	0.6466	0.0244	0.0167	0.0187	0.0498	0.0000	0.1474	0.04
825	6.5	0.0527	0.6654	0.0227	0.0170	0.0178	0.0465	0.0000	0.1382	0.06
825	7	0.0506	0.6818	0.0213	0.0172	0.0170	0.0435	0.0000	0.1301	0.07
825	7.5	0.0487	0.6964	0.0201	0.0174	0.0162	0.0408	0.0000	0.1230	0.09
825	8	0.0470	0.7093	0.0190	0.0176	0.0156	0.0385	0.0000	0.1166	0.11
825	8.5	0.0455	0.7209	0.0180	0.0177	0.0150	0.0363	0.0000	0.1108	0.14
825	9	0.0442	0.7313	0.0171	0.0179	0.0144	0.0344	0.0000	0.1057	0.16
825	9.5	0.0430	0.7407	0.0164	0.0180	0.0140	0.0327	0.0000	0.1009	0.20
825	10	0.0419	0.7493	0.0157	0.0181	0.0135	0.0311	0.0000	0.0967	0.22
850	3	0.0827	0.4403	0.0433	0.0141	0.0307	0.0842	0.0000	0.2475	0.14
850	3.5	0.0759	0.4918	0.0386	0.0147	0.0280	0.0753	0.0000	0.2224	0.06
850	4	0.0704	0.5336	0.0348	0.0153	0.0258	0.0680	0.0000	0.2020	0.01
850	4.5	0.0658	0.5682	0.0317	0.0157	0.0240	0.0619	0.0000	0.1851	0.00
850	5	0.0620	0.5973	0.0292	0.0161	0.0225	0.0568	0.0000	0.1709	0.01
850	5.5	0.0588	0.6221	0.0270	0.0164	0.0212	0.0524	0.0000	0.1587	0.02
850	6	0.0561	0.6434	0.0252	0.0167	0.0200	0.0485	0.0000	0.1482	0.04
850	6.5	0.0537	0.6619	0.0236	0.0170	0.0190	0.0452	0.0000	0.1390	0.08
850	7	0.0517	0.6781	0.0223	0.0172	0.0182	0.0422	0.0000	0.1309	0.09
850	7.5	0.0499	0.6925	0.0211	0.0174	0.0174	0.0396	0.0000	0.1237	0.14
850	8	0.0483	0.7052	0.0201	0.0175	0.0167	0.0373	0.0000	0.1173	0.16
850	8.5	0.0469	0.7166	0.0192	0.0177	0.0161	0.0352	0.0000	0.1116	0.24
850	9	0.0457	0.7269	0.0183	0.0178	0.0155	0.0332	0.0000	0.1064	0.26
850	9.5	0.0446	0.7361	0.0176	0.0179	0.0150	0.0315	0.0000	0.1017	0.28
850	10	0.0436	0.7446	0.0170	0.0180	0.0146	0.0299	0.0000	0.0974	0.40
875	3	0.0826	0.4389	0.0435	0.0140	0.0324	0.0826	0.0000	0.2484	0.28
875	3.5	0.0760	0.4900	0.0390	0.0147	0.0296	0.0737	0.0000	0.2233	0.19
875	4	0.0707	0.5314	0.0354	0.0153	0.0273	0.0665	0.0000	0.2029	0.17
875	4.5	0.0663	0.5656	0.0324	0.0157	0.0254	0.0605	0.0000	0.1860	0.18
875	5	0.0627	0.5943	0.0300	0.0161	0.0238	0.0554	0.0000	0.1717	0.19
875	5.5	0.0596	0.6188	0.0279	0.0164	0.0225	0.0510	0.0000	0.1595	0.23

Table C.2 Manipulated Duo-equilibrium reaction model calculation result for La_2O_3/CaO catalyst

Temp (°C)	CH_4/O_2	Effluent Composition								RSS
		H_2	CH_4	C_2H_4	C_2H_6	CO	CO_2	O_2	H_2O	
875	6	0.0571	0.6398	0.0262	0.0167	0.0213	0.0472	0.0000	0.1490	0.30
875	6.5	0.0548	0.6580	0.0247	0.0169	0.0203	0.0439	0.0000	0.1398	0.33
875	7	0.0529	0.6740	0.0234	0.0171	0.0194	0.0409	0.0000	0.1317	0.38
875	7.5	0.0512	0.6881	0.0223	0.0173	0.0186	0.0383	0.0000	0.1245	0.44
875	8	0.0498	0.7006	0.0213	0.0175	0.0179	0.0360	0.0000	0.1181	0.51
875	8.5	0.0485	0.7118	0.0205	0.0176	0.0172	0.0339	0.0000	0.1124	0.63
875	9	0.0473	0.7219	0.0197	0.0178	0.0167	0.0320	0.0000	0.1072	0.69
875	9.5	0.0463	0.7310	0.0190	0.0179	0.0161	0.0303	0.0000	0.1025	0.76
875	10	0.0454	0.7393	0.0184	0.0180	0.0157	0.0287	0.0000	0.0981	0.84

Table C.3 Manipulated Trio-equilibrium reaction model calculation result for PbO/Al_2O_3 catalyst

Temp (°C)	CH_4/O_2	Effluent Composition								RSS
		H_2	CH_4	C_2H_4	C_2H_6	CO	CO_2	O_2	H_2O	
650	5	0.0006	0.7006	0.0183	0.0125	0.0070	0.0661	0.0000	0.1948	1.23
650	5.5	0.0006	0.7234	0.0159	0.0127	0.0067	0.0612	0.0000	0.1795	1.12
650	6	0.0006	0.7430	0.0139	0.0129	0.0063	0.0569	0.0000	0.1665	1.05
650	6.5	0.0006	0.7599	0.0122	0.0130	0.0060	0.0532	0.0000	0.1552	1.01
650	7	0.0006	0.7747	0.0107	0.0132	0.0057	0.0499	0.0000	0.1453	1.01
650	7.5	0.0005	0.7877	0.0094	0.0133	0.0055	0.0470	0.0000	0.1366	1.02
650	8	0.0005	0.7992	0.0083	0.0134	0.0052	0.0445	0.0000	0.1289	1.06
650	8.5	0.0005	0.8095	0.0073	0.0135	0.0050	0.0422	0.0000	0.1220	1.12
650	9	0.0005	0.8187	0.0065	0.0136	0.0048	0.0401	0.0000	0.1158	1.20
650	9.5	0.0005	0.8271	0.0057	0.0136	0.0046	0.0382	0.0000	0.1102	1.28
650	10	0.0005	0.8347	0.0050	0.0137	0.0045	0.0365	0.0000	0.1051	1.38
675	5	0.0010	0.7011	0.0171	0.0125	0.0088	0.0654	0.0000	0.1941	0.47
675	5.5	0.0009	0.7238	0.0148	0.0127	0.0083	0.0605	0.0000	0.1790	0.38
675	6	0.0009	0.7431	0.0130	0.0129	0.0078	0.0562	0.0000	0.1660	0.32
675	6.5	0.0009	0.7599	0.0114	0.0130	0.0074	0.0525	0.0000	0.1548	0.29
675	7	0.0009	0.7746	0.0100	0.0132	0.0070	0.0493	0.0000	0.1450	0.27
675	7.5	0.0008	0.7875	0.0089	0.0133	0.0067	0.0464	0.0000	0.1364	0.27
675	8	0.0008	0.7990	0.0078	0.0134	0.0064	0.0439	0.0000	0.1287	0.29
675	8.5	0.0008	0.8092	0.0069	0.0135	0.0061	0.0416	0.0000	0.1219	0.32
675	9	0.0008	0.8184	0.0061	0.0135	0.0058	0.0396	0.0000	0.1157	0.36
675	9.5	0.0008	0.8267	0.0054	0.0136	0.0056	0.0377	0.0000	0.1102	0.42
675	10	0.0008	0.8343	0.0047	0.0137	0.0054	0.0360	0.0000	0.1051	0.48
700	5	0.0014	0.7007	0.0164	0.0125	0.0106	0.0644	0.0000	0.1939	0.27
700	5.5	0.0014	0.7232	0.0143	0.0127	0.0099	0.0595	0.0000	0.1789	0.19
700	6	0.0013	0.7425	0.0126	0.0129	0.0093	0.0553	0.0000	0.1660	0.13
700	6.5	0.0013	0.7593	0.0111	0.0130	0.0088	0.0517	0.0000	0.1549	0.08
700	7	0.0013	0.7739	0.0098	0.0131	0.0083	0.0485	0.0000	0.1451	0.06
700	7.5	0.0012	0.7867	0.0087	0.0133	0.0079	0.0457	0.0000	0.1365	0.05
700	8	0.0012	0.7982	0.0077	0.0134	0.0075	0.0432	0.0000	0.1289	0.05
700	8.5	0.0012	0.8084	0.0068	0.0135	0.0072	0.0409	0.0000	0.1221	0.06
700	9	0.0012	0.8176	0.0060	0.0135	0.0069	0.0389	0.0000	0.1159	0.08
700	9.5	0.0012	0.8259	0.0053	0.0136	0.0066	0.0370	0.0000	0.1104	0.11
700	10	0.0012	0.8334	0.0047	0.0137	0.0063	0.0354	0.0000	0.1053	0.15
725	5	0.0020	0.6995	0.0162	0.0125	0.0123	0.0633	0.0000	0.1941	0.28
725	5.5	0.0020	0.7220	0.0142	0.0127	0.0115	0.0585	0.0000	0.1791	0.20
725	6	0.0019	0.7413	0.0125	0.0129	0.0108	0.0543	0.0000	0.1663	0.14
725	6.5	0.0018	0.7580	0.0111	0.0130	0.0102	0.0507	0.0000	0.1552	0.08

Table C.3 Manipulated Trio-equilibrium reaction model calculation result for PbO/Al_2O_3 catalyst

Temp (°C)	CH_4/O_2	Effluent Composition								RSS
		H_2	CH_4	C_2H_4	C_2H_6	CO	CO_2	O_2	H_2O	
725	7	0.0018	0.7727	0.0098	0.0131	0.0096	0.0476	0.0000	0.1454	0.05
725	7.5	0.0017	0.7855	0.0087	0.0133	0.0091	0.0448	0.0000	0.1369	0.02
725	8	0.0017	0.7970	0.0078	0.0134	0.0086	0.0424	0.0000	0.1292	0.01
725	8.5	0.0016	0.8072	0.0069	0.0134	0.0082	0.0401	0.0000	0.1224	0.00
725	9	0.0016	0.8164	0.0062	0.0135	0.0078	0.0381	0.0000	0.1163	0.01
725	9.5	0.0016	0.8247	0.0055	0.0136	0.0075	0.0363	0.0000	0.1107	0.02
725	10	0.0016	0.8323	0.0049	0.0137	0.0072	0.0347	0.0000	0.1057	0.04
750	5	0.0028	0.6978	0.0164	0.0125	0.0140	0.0620	0.0000	0.1945	0.38
750	5.5	0.0026	0.7203	0.0144	0.0127	0.0130	0.0573	0.0000	0.1796	0.30
750	6	0.0025	0.7397	0.0128	0.0128	0.0122	0.0533	0.0000	0.1667	0.23
750	6.5	0.0024	0.7564	0.0114	0.0130	0.0115	0.0497	0.0000	0.1556	0.17
750	7	0.0023	0.7710	0.0101	0.0131	0.0108	0.0466	0.0000	0.1459	0.13
750	7.5	0.0023	0.7840	0.0091	0.0132	0.0102	0.0439	0.0000	0.1373	0.09
750	8	0.0022	0.7955	0.0081	0.0133	0.0097	0.0415	0.0000	0.1297	0.06
750	8.5	0.0022	0.8057	0.0073	0.0134	0.0092	0.0393	0.0000	0.1229	0.04
750	9	0.0021	0.8150	0.0065	0.0135	0.0088	0.0374	0.0000	0.1167	0.03
750	9.5	0.0021	0.8233	0.0058	0.0136	0.0084	0.0356	0.0000	0.1112	0.03
750	10	0.0021	0.8309	0.0052	0.0137	0.0080	0.0340	0.0000	0.1061	0.03

Appendix D: Experiment Extrapolation Results

Table D.1 Experiment Extrapolations results

Catalyst	CH_4/O_2	Temp ($^{\circ}C$)	Equilibrium Model	Model Result				AARD (%)
				X_{CH4}	S_{C2H6}	S_{C2H4}	Y_{C2}	
La/MgO	4	700	DMSE	29.1	26.8	32.8	17.3	15.82
La/MgO	4	750	DMSE	29.4	26.5	32.8	17.5	2.03
La/MgO[a]	4	800	DMSE	29.7	26.3	33.1	17.6	2.24
La/MgO	4	850	DMSE	30.1	25.9	33.7	17.9	3.33
Li/MgO	4	700	DMSE	24.2	19.0	24.7	10.6	45.69
Li/MgO	4	740	DMSE	24.4	18.8	24.9	10.7	23.31
Li/MgO[a]	4	780	DMSE	24.6	18.7	25.2	10.8	4.68
Li/MgO	4	820	DMSE	24.9	18.5	25.7	11.0	12.74
Li/MgO	4	860	DMSE	25.1	18.3	26.4	11.2	80.68
Sn/BaTiO3	1	775	DMSE	71.5	5.0	26.6	22.6	18.69
Sn/BaTiO3[a]	2	775	DMSE	47.6	7.6	39.9	22.6	5.69
Sn/BaTiO3	4	775	DMSE	26.1	13.8	37.7	13.4	5.99
K/BaCO3	4	780	DMSE	23.0	9.6	29.3	8.9	68.46
K/BaCO3[a]	4	820	DMSE	23.2	9.5	29.8	9.1	14.75
$K/BaCO_3$	4	860	DMSE	23.5	9.4	30.5	9.4	22.38
Li/CaO	4	700	DMSE	26.4	23.5	28.7	13.8	113.30
Li/CaO[a]	4	750	DMSE	26.7	23.2	28.7	13.9	13.96
Li/CaO	8	750	DMSE	15.4	40.3	17.6	8.9	16.14
Na/CaO	4	700	DMSE	24.6	23.6	22.1	11.2	126.43
Na/CaO[a]	4	750	DMSE	24.9	23.3	22.1	11.3	23.64

Table D.1 Experiment Extrapolations results

Catalyst	CH_4/O_2	Temp (^oC)	Equilibrium Model	Model Result				AARD (%)
				X_{CH4}	S_{C2H6}	S_{C2H4}	Y_{C2}	
Na/CaO	8	750	DMSE	14.3	40.5	11.7	7.5	24.54
K/CaO	4	700	DMSE	25.7	22.6	27.6	12.9	190.03
K/CaO[a]	4	750	DMSE	26.0	22.3	27.6	13.0	4.62
K/CaO	8	750	DMSE	14.9	38.8	17.1	8.4	16.46
Rb/CaO	4	700	DMSE	24.8	20.2	27.0	11.7	150.02
Rb/CaO[a]	4	750	DMSE	25.1	19.9	27.0	11.8	5.33
Rb/CaO	8	750	DMSE	14.2	35.1	17.6	7.5	14.39
Cs/CaO	4	700	DMSE	22.0	21.8	13.4	7.7	257.77
Cs/CaO[a]	4	750	DMSE	22.3	21.5	13.4	7.8	51.00
Cs/CaO	8	750	DMSE	12.7	37.7	4.7	5.4	48.36
SrO/La_2O_3	4	750	DMSE	34.4	20.4	52.2	24.9	262.41
SrO/La_2O_3	4	800	DMSE	34.8	20.1	52.5	25.3	38.18
SrO/La_2O_3	4	850	DMSE	35.4	19.8	53.1	25.8	44.24
SrO/La_2O_3[a]	8	850	DMSE	21.5	32.6	45.1	16.7	15.58
SrO/La_2O_3	16	850	DMSE	15.1	46.3	37.8	12.7	29.92
SrO/La_2O_3	20	850	DMSE	13.9	50.2	35.9	12.0	27.44
SrO/Nd_2O_3	4	750	DMSE	28.1	22.8	33.6	15.8	283.59
SrO/Nd_2O_3	4	800	DMSE	28.4	22.5	33.9	16.0	8.54
SrO/Nd_2O_3[a]	4	850	DMSE	28.7	22.3	34.5	16.3	6.35
SrO/Nd_2O_3	8	850	DMSE	17.2	37.1	26.7	11.0	19.66
SrO/Nd_2O_3	16	850	DMSE	11.9	53.6	20.3	8.8	12.33
SrO/Nd_2O_3	20	850	DMSE	11.0	58.4	18.8	8.5	15.01

Table D.1 Experiment Extrapolations results

Catalyst	CH_4/O_2	Temp (^oC)	Equilibrium Model	Model Result				AARD (%)
				X_{CH4}	S_{C2H6}	S_{C2H4}	Y_{C2}	
SrO/La_2O_3-$Nd2O_3$	4	750	DMSE	36.2	23.7	51.6	27.3	528.15
SrO/La_2O_3-$Nd2O_3$	4	800	DMSE	36.7	23.4	52.0	27.7	181.91
SrO/La_2O_3-$Nd2O_3$	4	850	DMSE	37.3	23.1	52.6	28.2	38.65
SrO/La_2O_3-$Nd2O_3$[a]	8	850	DMSE	23.0	37.4	42.9	18.5	17.73
SrO/La_2O_3-$Nd2O_3$	16	850	DMSE	16.5	52.0	34.2	14.3	21.81
SrO/La_2O_3-$Nd2O_3$	20	850	DMSE	15.4	56.0	32.1	13.5	21.35
$SnBaTiO_3$	2	725	DMSE	53.3	9.0	50.5	31.7	48.97
$SnBaTiO_3$	3	725	DMSE	38.3	12.5	49.3	23.7	35.69
$SnBaTiO_3$	4	725	DMSE	29.5	16.3	46.4	18.5	50.87
$SnBaTiO_3$	4.5	725	DMSE	26.6	18.0	45.0	16.8	71.58
$SnBaTiO_3$	2	750	DMSE	53.6	9.0	50.2	31.7	23.32
$SnBaTiO_3$[a]	3	750	DMSE	38.4	12.5	49.2	23.7	3.85
$SnBaTiO_3$	4	750	DMSE	29.7	16.2	46.4	18.6	13.95
$SnBaTiO_3$	4.5	750	DMSE	26.8	17.9	45.1	16.9	18.37
$SnBaTiO_3$	2	775	DMSE	53.8	8.9	50.0	31.7	33.21
$SnBaTiO_3$	3	775	DMSE	38.6	12.4	49.2	23.8	17.63
$SnBaTiO_3$	4	775	DMSE	29.9	16.1	46.5	18.7	23.54
$SnBaTiO_3$	4.5	775	DMSE	27.0	17.8	45.3	17.0	24.43

[a] Reference value for extrapolation

*DMSE = the duo-equilibrium reaction model with specific ethane yield

Appendix E: International Conference

Pure and Applied Chemistry International Conference 2014 (PACCON 2014)

Topic Chemical Equilibrium Of Oxidative Coupling Of Methane

Location Centara Hotel and Convention Centre, Khon Kaen, Thailand

Conference Date 8-10 January 2013

CHEMICAL EQUILIBRIUM OF OXIDATIVE COUPLING OF METHANE

Kritchart Wongwailikhit, Deacha Chatsiriwech*

Department of Chemical Engineering, Faculty of Engineering, Chulalongkorn University, Bangkok, 10330, Thailand

*Author for correspondence; E-mail: cdeacha@chula.ac.th, Tel. +66 2218 6863

Abstract: Oxidative Coupling of Methane (OCM) for production of ethane is now being interested in many research works. It is one of the great challenges for conversion of methane to more useful chemicals and fuels. In this process, methane is oxidized directly by oxygen and coupled up to form ethane and ethylene. In addition, OCM is operated at high temperature (600-1000^{o}C) and formed many side reactions, mainly combustion competing with OCM reaction, making OCM system very complex. Many kinetic studies have been published and described the rate of reaction of OCM which required very short residence time to complete conversion of oxygen. In this work, since the process get in the equilibrium within the milliseconds which suggests that not only kinetic but also chemical equilibrium theory could be explained these complex reactions. With computer simulation at the equilibrium time for parameters of temperature, pressure, gas feed rate, OCM could be modeled with two continuous steps. The first step was the oxidative reaction which methane was oxidized in both heterogeneous (solid fraction) and homogeneous (gas fraction) phases. The prior mixture products such as ethylene, ethane, CO_X and water were then reacted further by the non-oxidative reaction such as the hydrocracking and water gas shift. Comparing the production results with the kinetic simulation, the small deviation of methane conversion (±3.19%), ethane selectivity (±4.44%), and ethylene selectivity (±7.84%), were obtained. Therefore, chemical equilibria can be used to predict the product distribution of multiple reaction model.

1. Introduction

Natural gas production is currently higher than crude oil and expected to compensate in the 21st century [1]. Converting methane, the main component of natural gas, into more economic products is now being interested in many industries. Most processes are converting methane into syngas via steam reforming [2] and consecutively convert into methanol, ammonia [3] and also hydrocarbons [4] but these routes are 2 steps conversion of methane that require more energy than direct method [3].

Directly converting methane into value added C_2 hydrocarbon products has been developed since 1980s via oxidative coupling of methane (OCM) process[5]. The oxidative coupling of methane is

exothermic reaction that coupling two methanes into ethane by oxidizing agent as oxygen (Eq. 1). As OCM is operated at high temperature (600-1000^{o}C) and simultaneously fed methane with oxygen as raw material, side reactions such as combustion, shown in equation (2-3), could not be avoided. Therefore, methane to oxygen feed ratio should be as high as possible for promoting equation (1) rather than equation (2) and (3).

$$CH_4 + 0.5\ O_2 = C_2H_6 + H_2O \quad (1)$$
$$CH_4 + 1.5\ O_2 = CO + 2\ H_2O \quad (2)$$
$$CH_4 + 2\ O_2 = CO_2 + 2\ H_2O \quad (3)$$

In addition, many catalysts have been developed to achieve higher yield of C_2. Summary of catalyst performance shows in table 1. In the table, $Mn/Na_2WO_4/SiO_2$ is one of the best catalysts [6] in OCM reaction. Not only its performance in selectivity (S_{C2}) and methane conversion (X_{CH4}) but also its stability at high temperature is proven. So this catalyst is one of the future catalysts in OCM reaction.

Table 1: OCM Catalyst and their performance [7]

Catalyst	CH_4/O_2	T(^{o}C)	X_{CH4}	S_{C2}	Y_{C2}
Unsupport					
La/CaO	4	800	28	56	16
Ce/MgO	4	800	28	50	14
Sr/La_2O_3	4	800	29	59	17
La_2O_3	5.4	800	24	65	15.6
Support					
Li/MgO	2	750	37.8	50.3	19
Pb/SiO_2	6	750	13	58.2	7.6
$Mn/Na_2WO_4/MgO$	7.4	800	20	80	16
Li/Sn/MgO	9.6	680	14.3	84	12
$Mn/Na_2WO_4/SiO_2$	4	820	30	68	21

** X_{CH4} = Methane Conversion
** S_{C2} = C_2 Selectivity
** Y_{C2} = C_2 Yield

Kinetic literatures were reported OCM reaction in many types of catalyst and suggested their reactions as shown in table 2. Stranch et al [8] model was one of the most accepted models and was further used in Daneshpayeh et al [9] kinetic study over $Mn/Na_2WO_4/SiO_2$. Moreover, literatures indicated that OCM reaction required very short residence time to complete conversion of oxygen. After oxygen conversion reached 100%, methane conversion, selectivity and yield were stable.

Generally, chemical reaction could be explained in two theories, kinetic and chemical equilibrium. Chemical equilibrium can determine equilibrium composition at equilibrium time [10] with only defining initial point and reaction condition. This advantage overcame kinetic model which required many data to identify its parameters.

As mentioned above, most of OCM were studied with kinetics but not chemical equilibrium. In addition, since the OCM process got in the equilibrium within the milliseconds which suggested that not only kinetic but also chemical equilibrium theory could explain these complex reactions. Thus, it was curious to work with the chemical equilibrium to prove the feasibility of reaction equilibrium explanation for these complex reactions with computational simulation.

2. Simulation

2.1 Assumption

All Chemical Equilibrium Modeling assumptions were as follow. $Mn/Na_2WO_4/SiO_2$ was selected as catalyst. Effluent components in this study were H_2, CO, CO_2, H_2O, C_2H_6, C_2H_4 and C_3H_6. Method for thermodynamic property calculation was RK-Soave. Fixed-bed reactor was chosen in this study.

2.2 Calculation of Product Distribution

In mathematic modeling of a reactor, calculation may be split the reactor into many sections. In this research, three types of models were studied and detailed as follow.

Table 2: Stoichiometric equation of reaction models

No.	Reaction	Stansch [8] (La_2O_3/CaO)	Sohrabi [11] ($CaTiO_3$)	Lacombe [12] (La_2O_3)	Olsbye [13] ($BaCO_3$)/ $LaOn(CO_3)_{3-n}$	Traykova [14] (La_2O_3/MgO)	Shahri [15] (Mn/Na_2WO_4/SiO_2)	Hinsen [16] (Pb_2O_3)
Catalytic Reaction								
	Oxidative Coupling							
1	$2CH_4+0.5O_2 \rightarrow C_2H_6+H_2O$	✓	✓	✓	✓	✓	✓	✓
2	$2CH_4+O_2 \rightarrow C_2H_4+2H_2O$		✓					
	Partial Oxidation							
3	$CH_4+ 0.5O_2 \rightarrow CO + 2H_2$							
4	$C_2H_6+O_2 \rightarrow 2CO+3H_2$			✓				
5	$C_2H_4+O_2 \rightarrow 2CO+2H_2$			✓				
	Steam Reforming							
6	$CH_4+H_2O \rightarrow CO + 3H_2$							
7	$C_2H_6 + 2H_2O \rightarrow 2CO + 5H_2$							
8	$C_2H_4 + 2H_2O \rightarrow 2CO + 4H_2$	✓						
	Carbon Dioxide Reforming							
9	$CH_4 + CO_2 \rightarrow 2CO + 2H_2$							
10	$C_2H_6+ 2CO_2 \rightarrow 4CO + 3H_2$							
11	$C_2H_4+2CO_2 \rightarrow 4CO + 2H_2$							
	Oxidative Dehydrogenation							
12	$C_2H_6 + 0.5O_2 \rightarrow C_2H_4 + H_2O$	✓		✓		✓	✓	✓
	Dehydrogenation							
13	$C_2H_6 \rightarrow C_2H_4 + H_2$	✓			✓	✓		
	Water-Gas Shift							
14	$CO_2 + H_2 \leftrightarrow CO + H_2O$	✓				✓	✓	
Non-Catalytic Reaction								
	Combustion							
15	$CH_4 + O_2 \rightarrow CO + H_2O + H_2$	✓			✓			
16	$CH_4+1.5O_2 \rightarrow CO + 2H_2O$		✓			✓	✓	
17	$CH_4+2O_2 \rightarrow CO_2 + H_2O$	✓	✓	✓	✓		✓	✓
18	$CO + 0.5O_2 \rightarrow CO_2$	✓		✓				
19	$C_2H_6+2.5O_2 \rightarrow 2CO+3H_2O$				✓			
20	$C_2H_6+3.5O_2 \rightarrow 2CO_2+H_2O$			✓	✓			
21	$C_2H_4 + 2O_2 \rightarrow 2CO + 2H_2O$	✓			✓		✓	
22	$C_2H_4+3O_2 \rightarrow 2CO_2+2H_2O$				✓			✓

Model I imitated real configuration of reactor by assembled all calculations in one section as shown in figure 1.

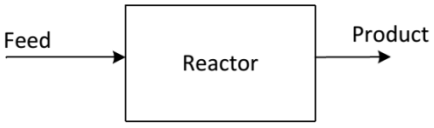

Figure1. Model I.

Model II (Fig. 2) was developed from competitive reactions between main reactions and side reactions occurring in different phases. Main reaction, OCM, reacted on catalytic surface but side reactions, mainly combustions, reacted in gas phase. Calculations in both phases were done with the assumption that void volume in reactor was the volume which allowed gas phase reactions to react while the residue volume allowed catalytic reactions.

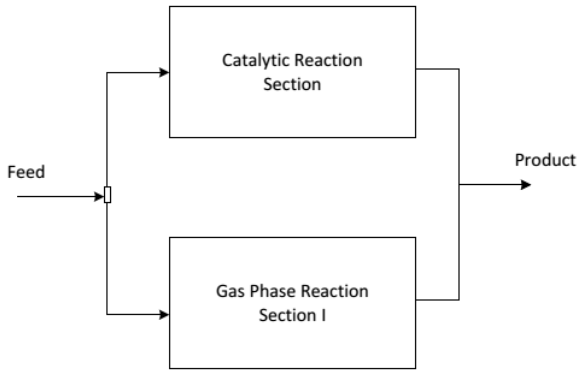

Figure2. Model II.

However, including another calculation section after those two sections in model II might gave better result. Effluent from both sections could further react together via some others gas phase reactions. Therefore, model III (Fig. 3) was then developed to support these consequently reactions by adding another sections after previous sections.

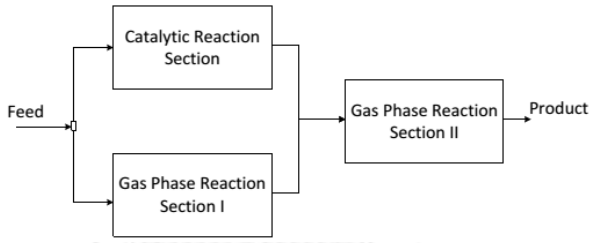

Figure3. Model III.

In those three separately parts of calculations, possible reactions in each part were determined. Arranging different sequence of each reaction yielded dissimilar effluent composition results which were subjected to validate with Residue Sum Square (RSS) method.

2.3 Model Validation

Validation of chemical equilibrium model would utilize Residue Sum Square (RSS) of each component which showed in equation 4. The model which gave lowest RSS would be appropriate model for OCM.

$$RSS = \sum_{i=1}^{N} \left[\frac{(M_{\exp} - M_{model})}{M_{\exp}} \right]^2 \qquad (4)$$

The effluent mole results of chemical equilibrium model (M_{model}) would compare with experiment (M_{exp}). Nevertheless, experimental didn't cover all operating condition at equilibrium time. Simulated results with rate law and parameters from literature were used as supporting data for validation. Ranges of operating conditions to be compared were shown in table 3.

Table 3: Range of Operating Condition Parameters

Parameter	Value
CH_4/O_2 Feed ratio	3-10
Temperature (^oC)	700-875
Pressure (Mpa)	0.1 MPa

Including with RSS, component error and weight average error of each component were also utilized to verify the calculation. Components error was the differential of effluent mole computed by kinetic and chemical equilibrium. The equation was shown in equation (5). Weight average error (WAE) was the summation of mole fraction (y_i) and component error which shown in equation 6. Moreover, yield of component i was calculated based on inlet mole of methane as shown in equation 7.

$$Component\,Error = \frac{(M_{exp} - M_{model})}{M_{exp}} \quad (5)$$

$$WAE = \sum_{i=1}^{N} y_i \left[\frac{(M_{exp} - M_{model})}{M_{exp}} \right] \quad (6)$$

$$Yield = \frac{Effluent\ mole\ of\ component\ i}{inlet\ mole\ of\ methane} \quad (7)$$

3. Results and Discussion

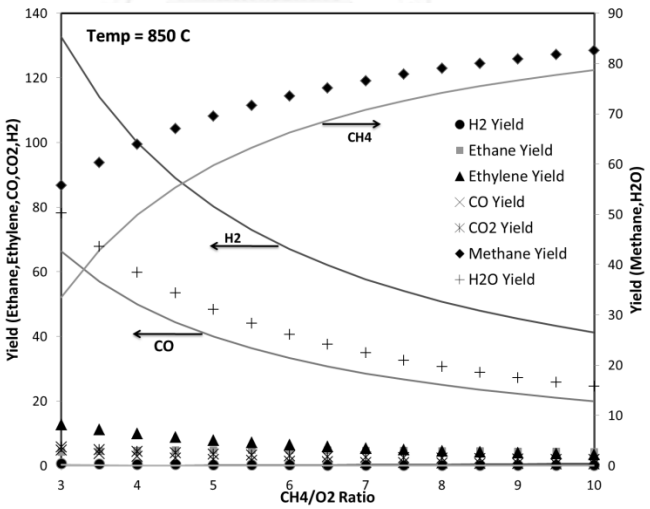

Figure4. Result of Model I calculation.
(Solid Line – Equilibrium Model, Dot – Kinetic Model)

Figure 4 illustrated the yields from model I compared with kinetic simulation. It was clearly shown that there were no matching between those two models for each component particularly H_2 and CO components. The deviations were attributed to the steam reforming reactions (Eq. 6-8 in table 2) which syngas was formed by methane, ethylene and ethane. These suggested that this model could not explain OCM reaction.

With the separately calculation of catalytic phase (Eq. 1-2 in table 2) and gas phase (Eq. 14, 16-17 in table 2), the result for model II, shown in figure 5, was much better than model I. It was found that

ethane yield at equilibrium was 4.7 at all range of operations. This indicated that spilt calculations into two parts were appropriate for OCM reaction. It should be noticed that the higher the methane ratio, the closer expected results to that of kinetic model. However, H_2 component showed significantly deviate for every ratio of methane. This implied that some other reactions were simultaneously occurred in system. Then, some corrections were developed in model III.

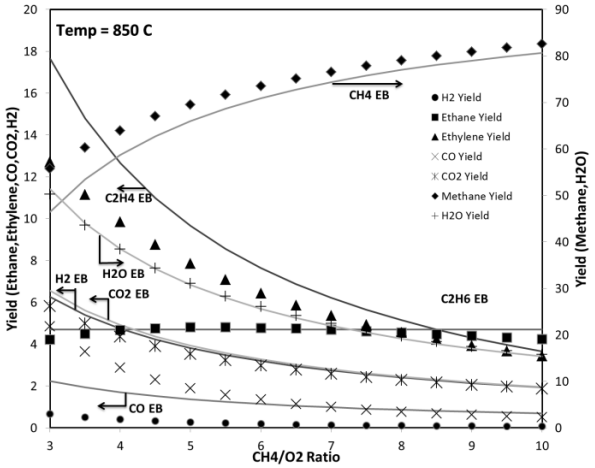

Figure5. Result of Model II calculation.
(Solid Line – Equilibrium Model, Dot – Kinetic Model)

In model III, correction for the previous deviation was applied. Combining H_2 with two other deviation components, CH_4 and C_2H_4, the reaction was found to be ethylene cracking (Eq. 8).

$$C_2H_4 + H_2 \rightarrow 2CH_4 \qquad (8)$$

It was also clarified that the cracking reacted after the catalytic and gas section in model II. This calculation result, similar to model III, was depicted in figure 6 which indicated the best fit in prediction for OCM reaction than model I and II.

Table 4 and 5 showed all deviations for all models at 700-775^{o}C and 775-875^{o}C, respectively. Both tables revealed that the errors decreased from model I through model III. However, at the temperature lower than 775^{o}C showed in table 4, the limitation for utilizing model III in OCM was found because the errors were higher than 10%.

Table 4: Deviation of each Model at 700-775^{o}C

Model	RSS	X_{CH4}	S_{C2H6}	S_{C2H4}	S_{COX}	WAE
1	3,708,311	57.73	99.72	99.37	288.44	127.88
2	9,372	40.49	15.33	49.42	42.56	18.60
3	3.54	25.12	6.74	31.56	35.54	11.52

Table 5: Deviation of each Model at 775-875^{o}C

Model	RSS	X_{CH4}	S_{C2H6}	S_{C2H4}	S_{COX}	WAE
1	280,179	31.49	99.39	95.85	475.04	129.36
2	612	13.78	9.17	10.41	13.13	8.77
3	1.03	3.19	4.44	7.87	9.57	2.86

** X_{CH4} =Methane Conversion, S_i = Component i Selectivity

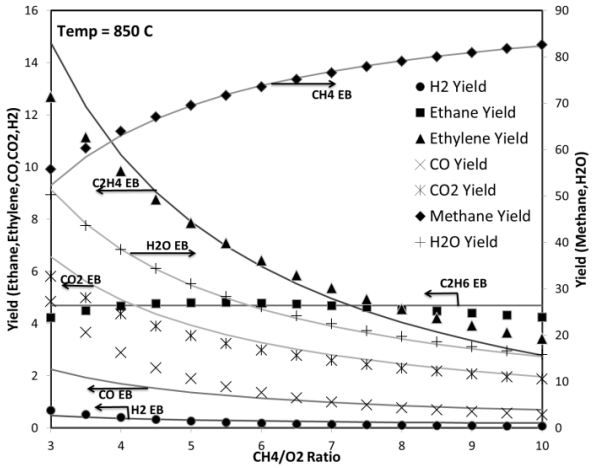

Figure6. Result of Model III calculation.
(Solid Line – Equilibrium Model, Dot – Kinetic Model)

4. Conclusions

Chemical equilibrium model was studied to explain the OCM reaction with respected to kinetic model. Simulation was run in fixed bed reactor and $Mn/Na_2WO_4/SiO_2$ catalyst. The studies were tested with three different models. It was found that model III which was run under the assumption that OCM reaction occurred at the surface of catalyst and the combustion side reaction occur at the gas phase. Cracking reaction was simultaneous reacted just after the previous OCM reaction. The results showed the best fit with kinetic model with less than 10% error for each component error with 1.03 and 2.86 in RSS and WAE, respectively. Therefore, chemical equilibrium model could describe OCM reaction as well as kinetic model. Furthermore, this work proposed an alternative methodology to explain chemical reactions and exposed the usage of chemical equilibrium in another point of view.

Acknowledgements

This work would like to thank Chulalongkorn University for Master Degree Scholarship.

Reference

[1] J. H. Lunsford, *Chem. Int. Ed. Engl*. **34** (1995) 970-980.
[2] P. F. v. d. Oosterkamp, *I. Horvath (Ed.)*. **6** (2003) 770.
[3] Holmen, *Catal. Today*. **142** (2009) 2-8.
[4] Al-Shalchi, *Gas to Liquid Technology (GTL)*. (2006)
[5] Ertl, Handbook of Heterogeneous Catalysis,**Vol. 1**, (2008)
[6] S. Arndt., *Appl. Catal. A.* **425-426** (2012) 53-61.
[7] Tiemersma, *Appl. Catal. A.* **433-434** (2012) 96-108.
[8] Stansch, *Ind. Eng. Chem. Res.* **36** (1997) 2568-2579.
[9] Daneshpayeh, *Fuel Process. Technol*.**90** (2009) 403-410.
[10] Sohrabi, *J. Chem. Tech. Biotechnol*. **67** (1996) 15-20.
[11] Lacombe, *Chem. Eng. Technol*. **18** (1995) 216-223.
[12] Olsbye, *Catal. Today*. **13** (1992) 209-218.
[13] M. Traykova., *Appl. Catal. A.* **169** (1998) 237-247.
[14] Shahri, et al., *J. Nat. Gas Chem*. **18** (2009) 25-34.
[15] Hinsen, *Proceedings of the 8th International Congress on Catalysis*. (1985) 251-283.
[16] Smith, M.M. Abbott, *Introduction to Chemical Engineering Thermodynamics*, McGraw-Hill, Inc., (2005)

VITA

Kritchart Wongwailikhit graduated Chemical Engineering from Chulalongkorn University at 2011 and entered Master Degree of Chemical Engineering at 2012.